Distance Considerations and Coding Techniques for Bandlimited Channels

by

R.M.A.P.Rajatheva

A Thesis

Presented to the University of Manitoba

in Partial Fulfilment of the Requirements for the Degree of the Doctor of Philosophy

in

the Department of Electrical and Computer Engineering

Winnipeg, Manitoba

April 1995

ISBN 0-612-13467-9

Name _____

Dissertation Abstracts International is arranged by broad, general subject categories. Please select the one subject which most nearly describes the content of your dissertation. Enter the corresponding four-digit code in the spaces provided.

Electronics and Electrical Engineering — SUBJECT TERM

0544 — SUBJECT CODE

U·M·I

Subject Categories

THE HUMANITIES AND SOCIAL SCIENCES

COMMUNICATIONS AND THE ARTS
- Architecture 0729
- Art History 0377
- Cinema 0900
- Dance 0378
- Fine Arts 0357
- Information Science 0723
- Journalism 0391
- Library Science 0399
- Mass Communications 0708
- Music 0413
- Speech Communication 0459
- Theater 0465

EDUCATION
- General 0515
- Administration 0514
- Adult and Continuing 0516
- Agricultural 0517
- Art 0273
- Bilingual and Multicultural 0282
- Business 0688
- Community College 0275
- Curriculum and Instruction 0727
- Early Childhood 0518
- Elementary 0524
- Finance 0277
- Guidance and Counseling 0519
- Health 0680
- Higher 0745
- History of 0520
- Home Economics 0278
- Industrial 0521
- Language and Literature 0279
- Mathematics 0280
- Music 0522
- Philosophy of 0998
- Physical 0523
- Psychology 0525
- Reading 0535
- Religious 0527
- Sciences 0714
- Secondary 0533
- Social Sciences 0534
- Sociology of 0340
- Special 0529
- Teacher Training 0530
- Technology 0710
- Tests and Measurements 0288
- Vocational 0747

LANGUAGE, LITERATURE AND LINGUISTICS
- Language
  - General 0679
  - Ancient 0289
  - Linguistics 0290
  - Modern 0291
- Literature
  - General 0401
  - Classical 0294
  - Comparative 0295
  - Medieval 0297
  - Modern 0298
  - African 0316
  - American 0591
  - Asian 0305
  - Canadian (English) 0352
  - Canadian (French) 0355
  - English 0593
  - Germanic 0311
  - Latin American 0312
  - Middle Eastern 0315
  - Romance 0313
  - Slavic and East European 0314

PHILOSOPHY, RELIGION AND THEOLOGY
- Philosophy 0422
- Religion
  - General 0318
  - Biblical Studies 0321
  - Clergy 0319
  - History of 0320
  - Philosophy of 0322
- Theology 0469

SOCIAL SCIENCES
- American Studies 0323
- Anthropology
  - Archaeology 0324
  - Cultural 0326
  - Physical 0327
- Business Administration
  - General 0310
  - Accounting 0272
  - Banking 0770
  - Management 0454
  - Marketing 0338
- Canadian Studies 0385
- Economics
  - General 0501
  - Agricultural 0503
  - Commerce-Business 0505
  - Finance 0508
  - History 0509
  - Labor 0510
  - Theory 0511
- Folklore 0358
- Geography 0366
- Gerontology 0351
- History
  - General 0578
  - Ancient 0579
  - Medieval 0581
  - Modern 0582
  - Black 0328
  - African 0331
  - Asia, Australia and Oceania 0332
  - Canadian 0334
  - European 0335
  - Latin American 0336
  - Middle Eastern 0333
  - United States 0337
- History of Science 0585
- Law 0398
- Political Science
  - General 0615
  - International Law and Relations 0616
  - Public Administration 0617
- Recreation 0814
- Social Work 0452
- Sociology
  - General 0626
  - Criminology and Penology 0627
  - Demography 0938
  - Ethnic and Racial Studies 0631
  - Individual and Family Studies 0628
  - Industrial and Labor Relations 0629
  - Public and Social Welfare 0630
  - Social Structure and Development 0700
  - Theory and Methods 0344
- Transportation 0709
- Urban and Regional Planning 0999
- Women's Studies 0453

THE SCIENCES AND ENGINEERING

BIOLOGICAL SCIENCES
- Agriculture
  - General 0473
  - Agronomy 0285
  - Animal Culture and Nutrition 0475
  - Animal Pathology 0476
  - Food Science and Technology 0359
  - Forestry and Wildlife 0478
  - Plant Culture 0479
  - Plant Pathology 0480
  - Plant Physiology 0817
  - Range Management 0777
  - Wood Technology 0746
- Biology
  - General 0306
  - Anatomy 0287
  - Biostatistics 0308
  - Botany 0309
  - Cell 0379
  - Ecology 0329
  - Entomology 0353
  - Genetics 0369
  - Limnology 0793
  - Microbiology 0410
  - Molecular 0307
  - Neuroscience 0317
  - Oceanography 0416
  - Physiology 0433
  - Radiation 0821
  - Veterinary Science 0778
  - Zoology 0472
- Biophysics
  - General 0786
  - Medical 0760

EARTH SCIENCES
- Biogeochemistry 0425
- Geochemistry 0996
- Geodesy 0370
- Geology 0372
- Geophysics 0373
- Hydrology 0388
- Mineralogy 0411
- Paleobotany 0345
- Paleoecology 0426
- Paleontology 0418
- Paleozoology 0985
- Palynology 0427
- Physical Geography 0368
- Physical Oceanography 0415

HEALTH AND ENVIRONMENTAL SCIENCES
- Environmental Sciences 0768
- Health Sciences
  - General 0566
  - Audiology 0300
  - Chemotherapy 0992
  - Dentistry 0567
  - Education 0350
  - Hospital Management 0769
  - Human Development 0758
  - Immunology 0982
  - Medicine and Surgery 0564
  - Mental Health 0347
  - Nursing 0569
  - Nutrition 0570
  - Obstetrics and Gynecology 0380
  - Occupational Health and Therapy 0354
  - Ophthalmology 0381
  - Pathology 0571
  - Pharmacology 0419
  - Pharmacy 0572
  - Physical Therapy 0382
  - Public Health 0573
  - Radiology 0574
  - Recreation 0575
  - Speech Pathology 0460
  - Toxicology 0383
- Home Economics 0386

PHYSICAL SCIENCES

Pure Sciences
- Chemistry
  - General 0485
  - Agricultural 0749
  - Analytical 0486
  - Biochemistry 0487
  - Inorganic 0488
  - Nuclear 0738
  - Organic 0490
  - Pharmaceutical 0491
  - Physical 0494
  - Polymer 0495
  - Radiation 0754
- Mathematics 0405
- Physics
  - General 0605
  - Acoustics 0986
  - Astronomy and Astrophysics 0606
  - Atmospheric Science 0608
  - Atomic 0748
  - Electronics and Electricity 0607
  - Elementary Particles and High Energy 0798
  - Fluid and Plasma 0759
  - Molecular 0609
  - Nuclear 0610
  - Optics 0752
  - Radiation 0756
  - Solid State 0611
- Statistics 0463

Applied Sciences
- Applied Mechanics 0346
- Computer Science 0984
- Engineering
  - General 0537
  - Aerospace 0538
  - Agricultural 0539
  - Automotive 0540
  - Biomedical 0541
  - Chemical 0542
  - Civil 0543
  - Electronics and Electrical 0544
  - Heat and Thermodynamics 0348
  - Hydraulic 0545
  - Industrial 0546
  - Marine 0547
  - Materials Science 0794
  - Mechanical 0548
  - Metallurgy 0743
  - Mining 0551
  - Nuclear 0552
  - Packaging 0549
  - Petroleum 0765
  - Sanitary and Municipal 0554
  - System Science 0790
- Geotechnology 0428
- Operations Research 0796
- Plastics Technology 0795
- Textile Technology 0994

PSYCHOLOGY
- General 0621
- Behavioral 0384
- Clinical 0622
- Developmental 0620
- Experimental 0623
- Industrial 0624
- Personality 0625
- Physiological 0989
- Psychobiology 0349
- Psychometrics 0632
- Social 0451

Nom _____

Dissertation Abstracts International est organisé en catégories de sujets. Veuillez s.v.p. choisir le sujet qui décrit le mieux votre thèse et inscrivez le code numérique approprié dans l'espace réservé ci-dessous.

_____ ☐☐☐ U·M·I

SUJET — CODE DE SUJET

Catégories par sujets

HUMANITÉS ET SCIENCES SOCIALES

COMMUNICATIONS ET LES ARTS
Architecture 0729
Beaux-arts 0357
Bibliothéconomie 0399
Cinéma 0900
Communication verbale 0459
Communications 0708
Danse 0378
Histoire de l'art 0377
Journalisme 0391
Musique 0413
Sciences de l'information 0723
Théâtre 0465

ÉDUCATION
Généralités 515
Administration 0514
Art 0273
Collèges communautaires 0275
Commerce 0688
Économie domestique 0278
Éducation permanente 0516
Éducation préscolaire 0518
Éducation sanitaire 0680
Enseignement agricole 0517
Enseignement bilingue et multiculturel 0282
Enseignement industriel 0521
Enseignement primaire. 0524
Enseignement professionnel 0747
Enseignement religieux 0527
Enseignement secondaire 0533
Enseignement spécial 0529
Enseignement supérieur 0745
Évaluation 0288
Finances 0277
Formation des enseignants 0530
Histoire de l'éducation 0520
Langues et littérature 0279
Lecture 0535
Mathématiques 0280
Musique 0522
Orientation et consultation 0519
Philosophie de l'éducation 0998
Physique 0523
Programmes d'études et enseignement 0727
Psychologie 0525
Sciences 0714
Sciences sociales 0534
Sociologie de l'éducation 0340
Technologie 0710

LANGUE, LITTÉRATURE ET LINGUISTIQUE
Langues
- Généralités 0679
- Anciennes 0289
- Linguistique 0290
- Modernes 0291

Littérature
- Généralités 0401
- Anciennes 0294
- Comparée 0295
- Médiévale 0297
- Moderne 0298
- Africaine 0316
- Américaine 0591
- Anglaise 0593
- Asiatique 0305
- Canadienne (Anglaise) 0352
- Canadienne (Française) 0355
- Germanique 0311
- Latino-américaine 0312
- Moyen-orientale 0315
- Romane 0313
- Slave et est-européenne 0314

PHILOSOPHIE, RELIGION ET THÉOLOGIE
Philosophie 0422
Religion
- Généralités 0318
- Clergé 0319
- Études bibliques 0321
- Histoire des religions 0320
- Philosophie de la religion 0322

Théologie 0469

SCIENCES SOCIALES
Anthropologie
- Archéologie 0324
- Culturelle 0326
- Physique 0327

Droit 0398
Économie
- Généralités 0501
- Commerce-Affaires 0505
- Économie agricole 0503
- Économie du travail 0510
- Finances 0508
- Histoire 0509
- Théorie 0511

Études américaines 0323
Études canadiennes 0385
Études féministes 0453
Folklore 0358
Géographie 0366
Gérontologie 0351
Gestion des affaires
- Généralités 0310
- Administration 0454
- Banques 0770
- Comptabilité 0272
- Marketing 0338

Histoire
- Histoire générale 0578
- Ancienne 0579
- Médiévale 0581
- Moderne 0582
- Histoire des noirs 0328
- Africaine 0331
- Canadienne 0334
- États-Unis 0337
- Européenne 0335
- Moyen-orientale 0333
- Latino-américaine 0336
- Asie, Australie et Océanie 0332

Histoire des sciences 0585
Loisirs 0814
Planification urbaine et régionale 0999
Science politique
- Généralités 0615
- Administration publique 0617
- Droit et relations internationales 0616

Sociologie
- Généralités 0626
- Aide et bien-être social 0630
- Criminologie et établissements pénitentiaires 0627
- Démographie 0938
- Études de l' individu et de la famille 0628
- Études des relations interethniques et des relations raciales 0631
- Structure et développement social 0700
- Théorie et méthodes. 0344
- Travail et relations industrielles 0629

Transports 0709
Travail social 0452

SCIENCES ET INGÉNIERIE

SCIENCES BIOLOGIQUES
Agriculture
- Généralités 0473
- Agronomie. 0285
- Alimentation et technologie alimentaire 0359
- Culture 0479
- Élevage et alimentation 0475
- Exploitation des pâturages 0777
- Pathologie animale 0476
- Pathologie végétale 0480
- Physiologie végétale 0817
- Sylviculture et faune 0478
- Technologie du bois 0746

Biologie
- Généralités 0306
- Anatomie 0287
- Biologie (Statistiques) 0308
- Biologie moléculaire 0307
- Botanique 0309
- Cellule 0379
- Écologie 0329
- Entomologie 0353
- Génétique 0369
- Limnologie 0793
- Microbiologie 0410
- Neurologie 0317
- Océanographie 0416
- Physiologie 0433
- Radiation 0821
- Science vétérinaire 0778
- Zoologie 0472

Biophysique
- Généralités 0786
- Medicale 0760

SCIENCES DE LA TERRE
Biogéochimie 0425
Géochimie 0996
Géodésie 0370
Géographie physique 0368
Géologie 0372
Géophysique 0373
Hydrologie 0388
Minéralogie 0411
Océanographie physique 0415
Paléobotanique 0345
Paléoécologie 0426
Paléontologie 0418
Paléozoologie 0985
Palynologie 0427

SCIENCES DE LA SANTÉ ET DE L'ENVIRONNEMENT
Économie domestique 0386
Sciences de l'environnement 0768
Sciences de la santé
- Généralités 0566
- Administration des hôpitaux 0769
- Alimentation et nutrition 0570
- Audiologie 0300
- Chimiothérapie 0992
- Dentisterie 0567
- Développement humain 0758
- Enseignement 0350
- Immunologie 0982
- Loisirs 0575
- Médecine du travail et thérapie 0354
- Médecine et chirurgie 0564
- Obstétrique et gynécologie 0380
- Ophtalmologie 0381
- Orthophonie 0460
- Pathologie 0571
- Pharmacie 0572
- Pharmacologie 0419
- Physiothérapie 0382
- Radiologie 0574
- Santé mentale 0347
- Santé publique 0573
- Soins infirmiers 0569
- Toxicologie 0383

SCIENCES PHYSIQUES
Sciences Pures
Chimie
- Généralités 0485
- Biochimie 487
- Chimie agricole 0749
- Chimie analytique 0486
- Chimie minérale 0488
- Chimie nucléaire 0738
- Chimie organique 0490
- Chimie pharmaceutique 0491
- Physique 0494
- PolymÈres 0495
- Radiation 0754

Mathématiques 0405
Physique
- Généralités 0605
- Acoustique 0986
- Astronomie et astrophysique 0606
- Électronique et électricité 0607
- Fluides et plasma 0759
- Météorologie 0608
- Optique 0752
- Particules (Physique nucléaire) 0798
- Physique atomique 0748
- Physique de l'état solide 0611
- Physique moléculaire 0609
- Physique nucléaire 0610
- Radiation 0756

Statistiques 0463

Sciences Appliqués Et Technologie
Informatique 0984
Ingénierie
- Généralités 0537
- Agricole 0539
- Automobile 0540
- Biomédicale 0541
- Chaleur et thermodynamique 0348
- Conditionnement (Emballage) 0549
- Génie aérospatial 0538
- Génie chimique 0542
- Génie civil 0543
- Génie électronique et électrique 0544
- Génie industriel 0546
- Génie mécanique 0548
- Génie nucléaire 0552
- Ingénierie des systèmes 0790
- Mécanique navale 0547
- Métallurgie 0743
- Science des matériaux 0794
- Technique du pétrole 0765
- Technique minière 0551
- Techniques sanitaires et municipales 0554
- Technologie hydraulique 0545

Mécanique appliquée 0346
Géotechnologie 0428
Matières plastiques (Technologie) 0795
Recherche opérationnelle 0796
Textiles et tissus (Technologie) 0794

PSYCHOLOGIE
Généralités 0621
Personnalité 0625
Psychobiologie 0349
Psychologie clinique 0622
Psychologie du comportement 0384
Psychologie du développement 0620
Psychologie expérimentale 0623
Psychologie industrielle 0624
Psychologie physiologique 0989
Psychologie sociale 0451
Psychométrie 0632

DISTANCE CONSIDERATIONS AND CODING TECHNIQUES FOR BANDLIMITED CHANNELS

BY

R.M.A.P. RAJATHEVA

A Thesis submitted to the Faculty of Graduate Studies of the University of Manitoba in partial fulfillment of the requirements of the degree of

DOCTOR OF PHILOSOPHY

ACKNOWLEDGEMENT

The author wishes to express his sincere thanks to Professor Ed. Shwedyk for constant guidance, support and encouragement throughout the Ph.D. program. Grateful acknowledgement is also due the Canadian commonwealth scholarship program and University of Manitoba for the NSERC operating grant. Special thanks also go to University of Moratuwa, Sri Lanka for providing the study leave necessary to continue graduate studies. This thesis is dedicated to my family; my wife Chandana, kids - Namal and Hansini and our parents, whose understanding and encouragement have always been a source of inspiration.

ABSTRACT

High speed data communication over channels with limited bandwidth results in intersymbol interference (ISI) at the receiver. This results in a poor receiver error performance. An important parameter that determines the receiver error performance is the minimum Euclidean distance between two received sequences.

Properties of the minimum Euclidean distance for ISI channels are considered in detail in this thesis. Channel properties for worst distance properties and for maximum distance are investigated. A condition is established if the zeros of worst distance channels are to lie on the unit circle. Also a theorem is given that proves the existence of maximal distance channels for any length of interference.

The Euclidean distance can be increased using a convolutional encoder at the transmitter to improve the receiver performance. The addition of an encoder results in several problems such as increased channel signaling rate which produces more ISI terms. It is seen from the results that by selecting an appropriate encoder matched to the channel, coding gain can be improved significantly compared to the uncoded situation. Another important aspect is that encoders with best free Hamming distance, d_{free} , do not always give the best overall Euclidean distance. A proposition is made to show that the maximum distance channels usually give higher coded distances than the rest of the channels. A search is carried out to find the best encoder of different rates for length two and three ISI channels. Results indicate that while the encoder with the best Hamming distance doesn't always give the best coded distance, it generally gives the highest distance achievable for encoders of given constraint length.

As an alternative to using convolutional coders application of trellis coded modulation (TCM) is also considered for ISI channels. Euclidean distance is found for best encoders for given modulation schemes where the channel considered has one interference term. Although TCM is generally used with ISI free channels results show that these can be applied with the ISI present to obtain moderate coding gains. A particular class of encoders known as quasiregular encoders are considered to simplify the finding of Euclidean distance. As an alternative to binary convolutional encoders, ring convolutional encoders working directly with the modulation alphabet are briefly looked at. A maximum of 2 dB coding gain can be expected over the regular TCM using PAM (pulse amplitude modulation) for this kind of encoders.

I hereby declare that I am the sole author of this thesis. I authorize the University of Manitoba to lend this thesis to other institutions or individuals for the purpose of scholarly research.

R. M. A. P. Rajatheva

I further authorize the University of Manitoba to reproduce this thesis by photocopying or by other means, in whole or in part, at the request of other institutions or individuals for the purpose of scholarly research.

R. M. A. P. Rajatheva

CONTENTS

LIST OF FIGURES

LIST OF TABLES

Chapter 1

Introduction

As technology advances it is essential to exchange information at increasingly higher rates around the globe to various places. This in terms of digital communication systems gives rise to the need for transmission of digital data at very high speed. If the channel used in this case is bandlimited the transmitted pulse overlaps with other transmission pulses causing intersymbol interference (ISI), with the number of overlapping pulses known as the memory of the channel or length of ISI. The simplest communication system to exhibit ISI is a pulse amplitude modulation (PAM) communication system. The telephone channel can be considered as a real world example of a bandlimited medium with ISI. The presence of ISI degrades the receiver performance.

Various techniques have been developed for combating ISI. Among these the Viterbi algorithm is well known. Originally developed by Viterbi for decoding convolutional codes, it can be applied to ISI channels with a finite memory for maximum likelihood sequence estimation (MLSE) as shown by Forney [12]. The receiver consists of a whitened matched filter and a sampler. The detection problem is modelled as a graph search through a trellis. The Euclidean distance between two channel output sequences which diverge from a common state in the trellis and later merge into one state, is an important parameter in MLSE. More important, for the determination of error probability at high signal to noise ratios, however, is the minimum Euclidean distance which is the minimum of all distances. Assuming an additive white Gaussian noise (AWGN) channel, the error probability can be approximated by a Q-function with the ratio of minimum distance to noise variance as the argument. It is therefore clear that at high

signal to noise ratios the error probability decreases with an increase of the minimum distance.

A finite memory channel can be represented by the discrete spectral factorization of its impulse response [12]. The channel coefficients obtained from the factorization completely describe the ISI characteristics of the channel. In light of the discussion in the previous paragraph it is worthwhile to investigate the dependence of the minimum distance on the channel coefficients.

Therefore one of the objectives in the research was to find out which channel coefficients give rise to the maximum value of the minimum distance and also which attain the minimum value of the minimum distance for different ISI lengths. This is considered in detail in chapter 2. In [8,13,19] the problem of worst ISI channels has been addressed. Channel characteristics which give worst ISI channels for different lengths and location of zeros of the channel spectrum have been studied. Zero locations are important if equalization techniques are to be used at the receiver. It can be shown that worst ISI channels are obtained when the distance correlation matrix corresponding to an error event attains its minimum eigenvalue [19]. In fact the smallest of all minimum eigenvalues for different distance correlation matrices is the worst minimum distance for a channel of given ISI length, subject to a channel energy constraint. For these channels Larsson [19] has shown that if the minimum eigenvalue of the distance correlation matrix is unique then the roots of the channel spectrum lie on the unit circle. Thus finding a method to show the uniqueness of that eigenvalue is certainly of interest.

Of equal importance is to maximize the distance to obtain better error performance. Recently Said [29], among other authors [39,27] considered this problem . He gives a search procedure by computer to find optimal partial response channels subject to distance and bandwidth constraints. In this thesis it is shown that for any ISI length it is possible to find maximum distance channels which in effect give the ISI free

performance in terms of minimum distance at high signal to noise ratios.

Another issue related to this is the signaling scheme. To increase the free Euclidean distance between permitted channel output sequences which results in a better noise margin than found in the baseband system, coding techniques can be used. Typically a convolutional encoder is used at the transmitter which has the original data sequence as its input. As a result of adding an encoder, the memory of the entire system is generally increased. It was shown in [35] that the total ISI length is less than the sum of the memories of the encoder and the channel separately. If a good encoder is used a better noise margin can be obtained at the expense of slightly increasing the ISI length. There have been several papers [7,16] that address this problem for a class of channels. The class considered arises from the magnetic recording channel or a variation of it. Wolf et. al. [38] sought a class of convolutional codes for combatting both noise and ISI which lead to easily implementable Viterbi decoders.

Another objective of the research was therefore to extend these results or to find good codes for the general ISI channel. Since the channel coefficients are real, for a given ISI length there are an infinite number of combinations of channel coefficients. Therefore some constraints, to be discussed in chapter 3, are necessary so that the search for good codes can be conducted with reasonable complexity. Studies of convolutional codes for continuous phase modulation (CPM) schemes [2, 15, 28] provide some clues in this regard. A related issue is to find which convolutional encoder, whether it is the one with the best free distance , gives the best distance when combined with an ISI channel of given memory length. In this respect lower and upper bounds for the overall minimum distance are given to estimate the performance given an encoded input. Once the encoder is placed signaling may be done at a higher rate which maintains the original data rate or keeps at the same signaling rate but reduces the original data rate. If the output signaling rate is increased then number of ISI terms

should change. Bergmans [4] studied this problem for the channels whose forms are variations of the magnetic recording channel. In this research several ISI channels are compared in terms of the coding gain with different signaling rates to discuss the relative merits of each method.

A brief outline of the thesis is as follows. Properties of the minimum Euclidean distance for ISI channels are considered in detail in chapter 2. Channels which give worst distance properties and those with maximum distance properties are investigated. Then in chapter 3, the use of convolutional encoded inputs for ISI is discussed. A search is carried out to find the best encoder of different rates for several ISI channels. As a natural extension to the work in chapter 3 in binary schemes, application of trellis coded modulation (TCM) schemes to ISI is examined next to get a more complete understanding of how ISI channels behave under different coding schemes with different alphabets. This is given in chapter 4, which essentially is a study of TCM with ISI channels. This serves as a comparison to the convolutional codes studied in chapter 3. Several authors [9,10,14,18,33,37] have done some work in this area. They compare different modulation methods according to minimum distance. Another motivation to use TCM is the fact that both TCM and ISI use the Euclidean space for distance calculations whereas with convolutional codes we have to work in GF(2). Because of the involvement of two different fields, the complexity is higher when a convolutional encoder is combined with an ISI channel. A particular class of encoders known as quasiregular encoders are considered to simplify the finding of Euclidean distance. As an alternative to binary convolutional encoders, ring convolutional encoders working directly with the modulation alphabet are briefly considered [3,23,41]. Chapter 5 presents conclusions and suggestions for further research.

Chapter 2
Distance Considerations

Distance properties of bandlimited channels are considered in this chapter. A binary PAM system is typically assumed and throughout only channels of finite intersymbol interference length (ISI) are considered. First the necessary background is given along with the details regarding the free Euclidean distance measure denoted by d_{free}. Then some properties of the worst ISI channels are presented.

Worst case channels are those that for a given ISI length have the smallest d_{free}. In particular it is known that the roots of the transfer function polynomial for these channels lie on the unit circle provided that the minimum eigenvalue of the error correlation matrix is unique [19]. Methods to show this uniqueness are detailed here.

The converse to the worst case channel is(are) the channel(s) that has(have) the maximum d_{free}. Here it is shown that a maximum distance channel exists for any finite length of ISI and a set of sufficient conditions for the channel response coefficients are presented. The chapter concludes with a brief discussion of equalization to obtain a maximum distance channels for a given channel response.

2.1 Background:

A block diagram of the binary PAM communication system considered in the research is shown in Figure 2.1. The channel impulse response is finite of duration LT. The length of interference is then

$$v \equiv L - 1 \text{ symbols.} \tag{2.1}$$

Forney [12] showed that the input can be estimated using MLSE with the receiver as

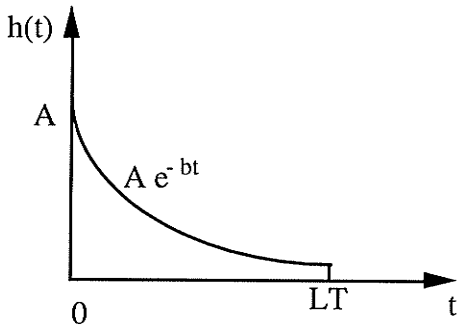

Channel impulse response : e.g.
Truncated exponential channel

Figure 2.1(a)

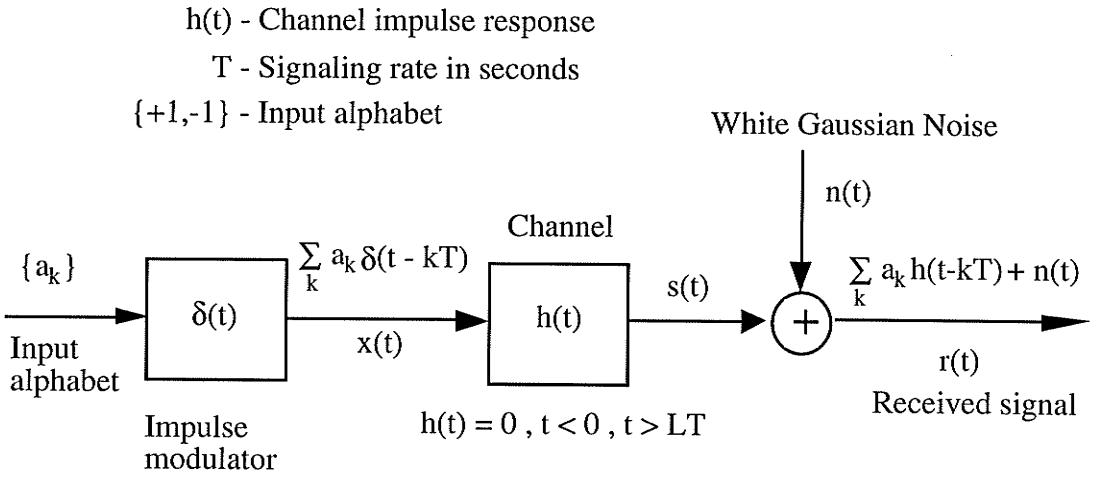

Figure 2.1(b). The digital communication system: Channel and noise

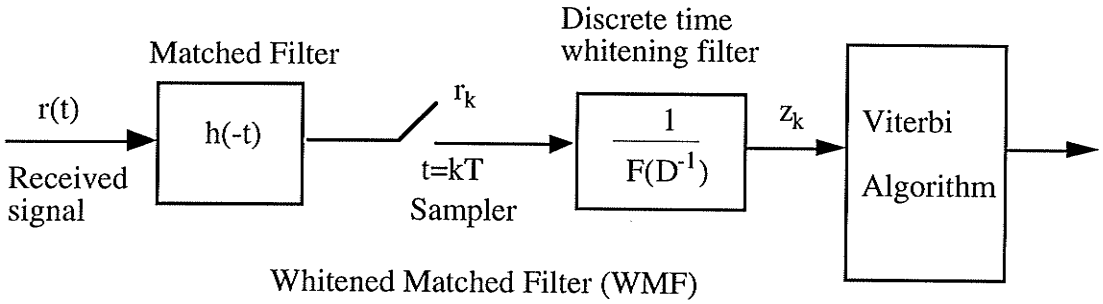

Figure 2.2. Receiver of the digital communication system

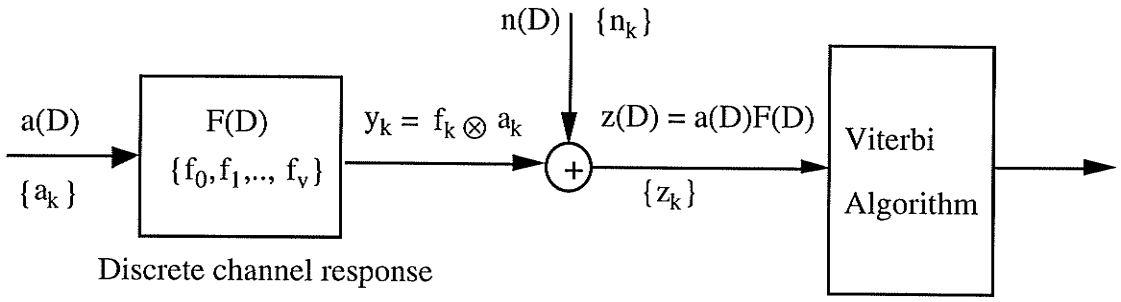

Figure 2.3. Discrete Equivalent model of the communication system

shown in Figure 2.2. The output of the matched filter sampled at t=kT is

$$r_k = \int_{-\infty}^{\infty} r(t)h(t - kT)\, dt \tag{2.2}$$

$$= \sum_{j=k-v}^{k+v} \int_{-\infty}^{\infty} a_j h(t - jT)h(t - kT)\, dt + \int_{-\infty}^{\infty} n(t)h(t - kT)\, dt \tag{2.3}$$

$$= \sum_{j=k-v}^{k+v} a_j h_{j-k} + n'_k \tag{2.4a}$$

where $$h_{j-k} = \int_{-\infty}^{\infty} h(t - jT)h(t - kT)\, dt \tag{2.4b}$$

Using the D transform where $D \equiv z^{-1}$, (2.4) can be written as

$$r(D) = a(D)h(D) + n'(D) \tag{2.5}$$

R(D) is the discrete autocorrelation function of the channel. Using spectral factorization

$$h(D) = F(D)F(D^{-1}) \tag{2.6}$$

where $$F(D) = \sum_{i=0}^{v} f_i D^i \tag{2.7}$$

and f_i's are the channel coefficients of the discrete impulse response.

Therefore

$$r(D) = a(D)F(D)F(D^{-1}) + n(D)F(D^{-1}) \tag{2.8}$$

Dividing by $F(D^{-1})$

$$z(D) = \frac{r(D)}{F(D^{-1})} = a(D)F(D) + n(D) \tag{2.9}$$

The noise n(D) is white. The discrete time equivalent system for the communication system is given in Figure 2.3. As shown in Figure 2.2 $\frac{1}{F(D^{-1})}$ is called the whitening filter. The cascade with the matched filter is usually referred to as the whitened matched filter.

Hence
$$z_k = \sum_{i=0}^{v} f_i a_{k-i} + n_k = y_k + n_k \tag{2.10}$$

$$y_k \equiv \sum_{i=0}^{v} f_i a_{k-i} \tag{2.11}$$

As seen from (2.11), y_k can be represented by a trellis of memory v where for binary inputs the number of trellis states is 2^v. An example of a trellis is shown in Figure 2.4.

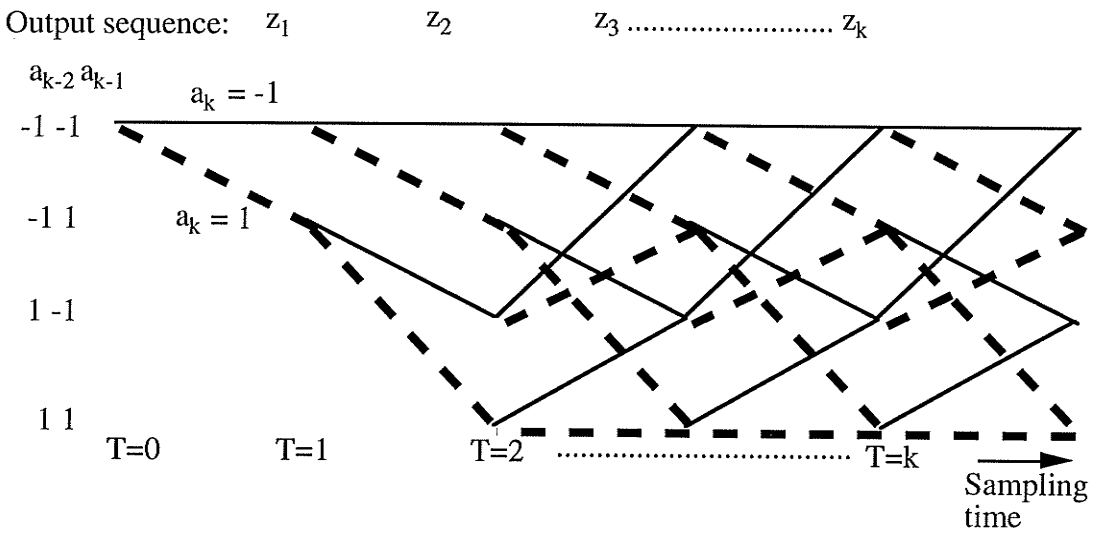

Figure 2.4 : Channel trellis for v=2

The Viterbi algorithm searches the channel trellis and determines the most likely transmitted sequence $\{a_k\}$ based on the received sequence $\{z_k\}$. The parameter that is

important in the receiver performance is the Euclidean distance between any two output sequences, particularly those that diverge from a common trellis state and later merge at a common state. The Euclidean distance between any two sequences in the trellis which diverge from a common state at time step j=k and merge to a common state at time step $j=k+\ell-1$ can be expressed in the form

$$d^2 = \sum_{j=k}^{k+\ell-1} (z_j - z'_j)^2 \tag{2.12}$$

$$= \sum_{j=k}^{k+\ell-1} \left(\sum_{i=0}^{v} f_i a_{j-i} - \sum_{i=0}^{v} f_i a'_{j-i} \right)^2 \tag{2.13}$$

$$= \sum_{j=k}^{k+\ell-1} \left[\sum_{i=0}^{v} f_i (a_{j-i} - a'_{j-i}) \right]^2 \tag{2.14}$$

$$= \sum_{j=k}^{k+\ell-1} \left[\sum_{i=0}^{v} f_i \varepsilon_{j-i} \right]^2 \tag{2.15}$$

where $\varepsilon_j \in \{0, 2, -2\}$ is called an error or difference symbol and ℓ is the length of the error event.

The squared free Euclidean distance is defined as

$$d^2_{free} \equiv \min_{\varepsilon} (d^2) \tag{2.16}$$

where ε is the set of all error sequences. In essence d_{free} is the minimum Euclidean

distance between two received sequences. At high signal to noise ratios this distance dominates the error probability of the communication system which can be approximated by

$$\Pr(\text{error}) \rightarrow Q\left(\frac{d_{free}}{\sigma}\right) \tag{2.17}$$

where

$$Q(x) \cong \frac{1}{\sqrt{2\pi}} \int_x^{\infty} e^{-\frac{\lambda^2}{2}} d\lambda \tag{2.18}$$

and σ^2 is the variance of white noise. Variation of the error probability with $\frac{d_{free}}{\sigma}$ is shown in Figure 2.5.

Thus d_{free} is an important parameter closely related to the error performance of a bandlimited channel. The next section considers the relationship of d_{free} to the channel characteristics, h(t), in terms of $\mathbf{f} = (f_0, f_1, f_2, \ldots, f_v)$ the channel coefficient vector, i.e., the discrete impulse response of the discrete equivalent system.

2.1.1 Channel distance function:

The material of this section is primarily from [26]. The distance from time j=k to j=k+ℓ-1 in the trellis of the discrete equivalent system, i.e. a segment of length ℓ is, from (2.15)

$$d^2 = \sum_{j=k}^{k+\ell-1} \left[\sum_{i=0}^{v} f_i \varepsilon_{j-i} \right]^2 \tag{2.19}$$

which can be expressed in matrix form as

$$= \mathbf{f}^T \mathbf{A} \mathbf{f} \tag{2.20}$$

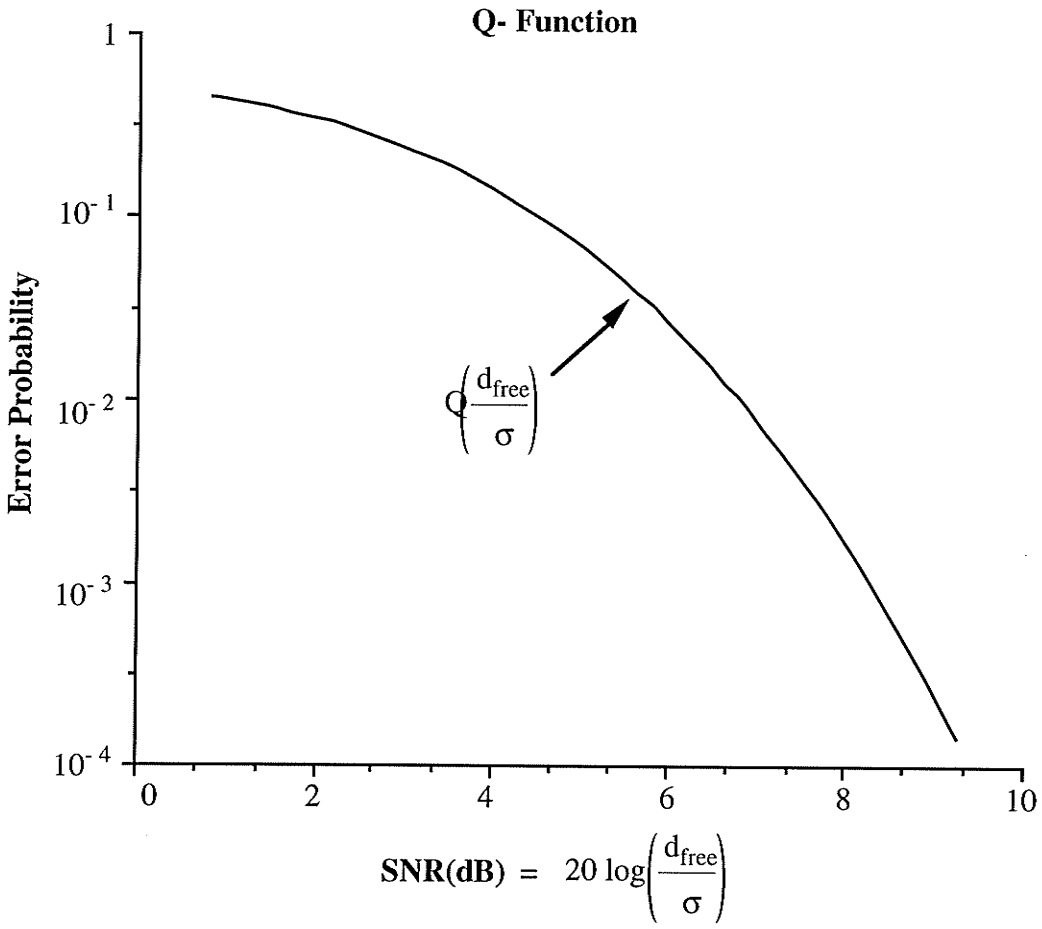
Q- Function
Error Probability
1
10^{-1}
10^{-2}
10^{-3}
10^{-4}
0
2
4
6
8
10
$Q\left(\frac{d_{free}}{\sigma}\right)$
SNR(dB) = $20 \log\left(\frac{d_{free}}{\sigma}\right)$

Figure 2.5

where

$$\mathbf{f} = \begin{bmatrix} f_0 \\ f_1 \\ . \\ . \\ f_v \end{bmatrix} \qquad \mathbf{A} = \begin{bmatrix} \beta_0 & \beta_1 & . & . & \beta_v \\ \beta_1 & \beta_0 & \beta_1 & . & \beta_{v-1} \\ \beta_2 & \beta_1 & . & . & \beta_{v-2} \\ . & & & & \\ \beta_v & . & . & . & \beta_0 \end{bmatrix} \tag{2.21}$$

The entries of matrix A are given by

$$\beta_m = \sum_{i=k}^{k+\ell-1-m} \varepsilon_i \varepsilon_{i+m} \tag{2.22}$$

Matrix **A** is a correlation matrix and hence positive definite. Therefore all the eigenvalues of **A** are positive and hence the quadratic form given in (2.20) can be minimized by considering the eigenvalues of

$$\mathbf{Af} = \mu\mathbf{f}\,, \quad \mu > 0 \tag{2.23}$$

From the above it follows that

$$(d^2_{free})_{min} = \min_{\mathbf{A}} (d^2) \tag{2.24}$$

$$= (\mathbf{f^T} \mu \mathbf{f})_{min} \tag{2.25}$$

$$= \left[\mu(\mathbf{f^T f})\right]_{min} \tag{2.26}$$

But $$\mathbf{f}^T\mathbf{f} = \int_{-\infty}^{\infty} h^2(t)dt = E \quad \text{is fixed.} \tag{2.27}$$

Therefore

$$(d_{free}^2)_{min} = E\mu_{min} \tag{2.28}$$

In this case $\mathbf{f}$ is the eigenvector of $\mathbf{A}$ corresponding to the minimum eigenvalue μ_{min}. Denote it by $\mathbf{f}_{min}$. $\mathbf{f}_{min}$ defines the channel that exhibits the worst ISI characteristics for the given length. Also it is important to note that the matrix $\mathbf{A}$ depends on the error event ε which implies that $(d_{free})_{min}$ depends on ε as well. Further without any loss of generality an error event can start at time 0, i.e., $k = 0$.

An upperbound on d_{free}^2 can be established readily by considering the shortest error event where

$$k=0 \text{ and } \ell=L \ (L=v+1) \ ; \ \varepsilon_0 = 2 \ , \ \varepsilon_j = 0 \text{ for } j > 0$$

Using (2.19)

$$d^2 = 4(f_0^2 + f_1^2 + \ldots\ldots + f_v^2) = 4\,\mathbf{f}^T\mathbf{f} \tag{2.29}$$

In general for M-ary modulation

$$d_{free}^2 \le |\varepsilon_{min}|^2 \, \mathbf{f}^T\mathbf{f} \quad \text{for any L} \tag{2.30}$$

where ε_{min} is the error symbol with the least magnitude.

Further it is easily shown that for L=2

$$d_{free}^2 = 4\,\mathbf{f}^T\mathbf{f} = 4(f_0^2 + f_1^2) \tag{2.31}$$

Thus there is no loss in signal to noise ratio (SNR) in MLSE of the information symbols when the channel dispersion has a length of 2.

2.2 Worst ISI channels:

In the previous section some properties of d_{free} have been discussed. Since d_{free} is a measure of the error performance of the communication system it is of interest to determine the worst possible performance which can be expected over a channel with a fixed energy, finite duration pulse response. Worst case channels for carrier modulated systems and complex symbol alphabets were studied by Larsson [19]. He showed that the zeros of the worst ISI channels lie on the unit circle provided that the minimum eigenvalue of the distance correlation matrix **A** is unique. The main objective of this section is to discuss the methods to show the uniqueness of that eigenvalue. First some examples of ISI channels for which the minimum Euclidean distance is the smallest possible, are given along with an investigation of their characteristics.

Consider the L=3 channel.

$$F(D) = f_0 + f_1 D + f_2 D^2 \tag{2.32}$$

where the channel coefficients are the components of the eigenvector corresponding to the minimum eigenvalue of **A**. The error event of the form

$$\varepsilon(D) = 1 + D \tag{2.33}$$

is the error event that results in the smallest d_{free} for the above channel. All other error events give larger minimum eigenvalues. It results in a matrix

$$\mathbf{A} = \begin{bmatrix} 2 & 1 & 0 \\ 1 & 2 & 1 \\ 0 & 1 & 2 \end{bmatrix} \tag{2.34}$$

and the eigenvector corresponding to the minimum eigenvalue is

$$\mathbf{f}^{T}_{min} = \begin{bmatrix} \frac{1}{2} & \frac{1}{\sqrt{2}} & \frac{1}{2} \end{bmatrix} \tag{2.35}$$

$$\mathbf{f}^{T}\mathbf{f} = 1 \tag{2.36}$$

This is the worst channel for L=3. Extension for other lengths is straightforward by eliminating the error events which give larger eigenvalues. An algorithm to find the worst channel is given in [19] and some examples are given in Table 2.1. It is seen that the zeros of the channel spectra lie on the unit circle (shown for the above examples in Figure 2.6). The following lemma establishes a condition for the uniqueness of the minimum eigenvalue of **A**.

Lemma 2.2.1:

The minimum eigenvalue of the correlation matrix corresponding to the error event of the worst ISI channel is unique if the corresponding worst distance strictly decreases with the length of interference.

Proof:

Consider a channel of length L with a correlation matrix that has multiple eigenvalues. From matrix theory [36] the eigenvalues of the principal submatrix of **A** (obtained by excluding the last row and the last column of **A**) separate the eigenvalues of **A**. This relationship can be given as follows assuming **A** to be a matrix of dimension n×n.

Channel Length L	Performance Loss dB	Minimum distance channel
3	2.3	0.50, 0.71, 0.50
4	4.2	0.38, 0.60, 0.60, 0.38
5	5.7	0.29, 0.50, 0.58, 0.50, 0.29
6	7.0	0.23, 0.42, 0.52, 0.52, 0.42, 0.23

Table 2.1: Maximum performance loss and channel characteristics

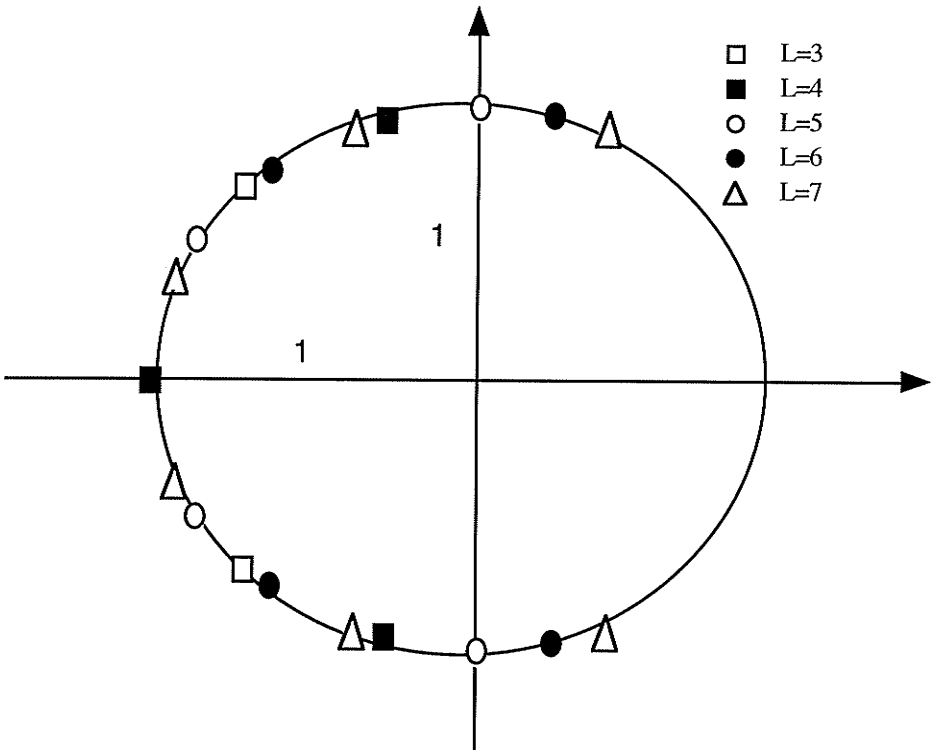

Figure 2.6: Zero locations which result in the Euclidean distance for the channels with length L=3,4,...7

$$\lambda_{i+1} \leq \lambda_{is} \leq \lambda_i \quad ; \; i=n-1,n-2,...,2,1 \tag{2.38}$$

where $\lambda_1,\lambda_2,.....\ \lambda_n$ are eigenvalues of **A** and $\lambda_{1s},\lambda_{2s},.....\ \lambda_{(n-1)s}$ are eigenvalues of its principal submatrix $\mathbf{A}_s$. For multiple eigenvalues of **A** when i=n-1 and i=n,

$$\lambda_n \leq \lambda_{(n-1)s} \leq \lambda_{n-1} \text{ where } \lambda_n = \lambda_{n-1} \tag{2.39}$$

Therefore $$\lambda_{(n-1)s} = \lambda_n \tag{2.40}$$

i.e., the minimum eigenvalue of the principal submatrix is equal to the minimum eigenvalue of **A**.

Now consider a channel of length L-1 and an error event of length L identical to the one that defined **A**. Its correlation matrix is $\mathbf{A}_s$. Hence the minimum eigenvalue in L-1 is the same as that obtained for L which means that the worst distances for L-1 and L are equal. This is a contradiction to the condition given in the lemma. Thus if the condition holds then the minimum eigenvalue of **A** corresponding to the worst channel is unique. QED.

From the above proof since $\lambda_n \leq \lambda_{(n-1)s}$ it follows that

$$(d_{worst})_L \leq (d_{worst})_{L-1} \tag{2.41}$$

To see the effect on distance when going from a length of interference of L-1 to L consider an error correlation matrix $\mathbf{A}_{L-1}$ in L-1. Then

$$d^2_{L-1} = \mathbf{f}^T_{L-1}\mathbf{A}_{L-1}\mathbf{f}_{L-1} \tag{2.42}$$

Assume for example that L-1=3 and that

$$\mathbf{A}_3 = \begin{bmatrix} c_1 & c_2 & c_3 \\ c_2 & c_1 & c_2 \\ c_3 & c_2 & c_1 \end{bmatrix}, \quad \mathbf{f}_3^T = [f_0\ f_1\ f_2] \tag{2.43}$$

where $\mathbf{A}_3$ is the correlation matrix corresponding to the error event that gives the minimum distance.

Since the channel energy is fixed

$$E = f_0^2 + f_1^2 + f_2^2. \tag{2.44}$$

Now consider an incremental change in coefficients so that the channel is in L=4.

Thus $$\mathbf{f}_4^T = [f_0+\delta f_0\ \ f_1+\delta f_1\ \ f_2+\delta f_2\ \ \delta f_3]. \tag{2.45}$$

For fixed energy $$E = \mathbf{f}_4^T\mathbf{f}_4. \tag{2.46}$$

Approximating the 2nd order terms to zero the following relationship can be obtained.

$$f_0\delta f_0 + f_1\delta f_1 + f_2\delta f_2 = 0. \tag{2.47}$$

The error correlation matrix in L=4 is

$$\mathbf{A}_4 = \begin{bmatrix} c_1 & c_2 & c_3 & c_4 \\ c_2 & c_1 & c_2 & c_3 \\ c_3 & c_2 & c_1 & c_2 \\ c_4 & c_3 & c_2 & c_1 \end{bmatrix}. \tag{2.48}$$

$$d_4^2 = \mathbf{f}_4^T \mathbf{A}_4 \mathbf{f}_4 \tag{2.49}$$

Comparing with d_3^2 this can be written as

$$d_4^2 = d_3^2 + 2\delta f_0(c_1 f_0 + c_2 f_1 + c_3 f_2) + 2\delta f_1(c_2 f_0 + c_1 f_1 + c_2 f_2) + 2\delta f_2(c_3 f_0 + c_2 f_1 + c_1 f_2) + 2\delta f_3(c_4 f_0 + c_3 f_1 + c_2 f_2). \tag{2.50}$$

Now consider $\mathbf{A}_3$ corresponding to the error event that results in the worst distance for L=3 with $\mathbf{f}_3$ as the corresponding eigenvector of $\mathbf{A}_3$.

i.e., $c_1 f_0 + c_2 f_1 + c_3 f_2 = \lambda f_0, c_2 f_0 + c_1 f_1 + c_2 f_2 = \lambda f_1, c_3 f_0 + c_2 f_1 + c_1 f_2 = \lambda f_2.$ (2.51)

Hence $d_4^2 = d_3^2 + 2\lambda(f_0\delta f_0 + f_1\delta f_1 + f_2\delta f_2) + 2\delta f_3(c_4 f_0 + c_3 f_1 + c_2 f_2).$ (2.52)

Using (2.47) $d_4^2 = d_3^2 + 2\delta f_3(c_4 f_0 + c_3 f_1 + c_2 f_2).$ (2.53)

Therefore if δf_3 is appropriately selected then d_4^2 can be made smaller than d_3^2.

If $c_4 f_0 + c_3 f_1 + c_2 f_2 = 0$ then

$$d_4^2 = d_3^2. \tag{2.54}$$

This implies that $\mathbf{A}_4$, the matrix in L has multiple eigenvalues according to Lemma 2.2.1. Consider the eigenvectors of the matrix $\mathbf{A}_4$ and consider $\mathbf{f}_4^T = [f_0 \;\; f_1 \;\; f_2 \;\; 0]$. Then

$$\mathbf{A}_4 \mathbf{f}_4 = \lambda \mathbf{f}_4 \tag{2.55}$$

will hold if

$$c_1 f_0 + c_2 f_1 + c_3 f_2 = \lambda f_0$$

$$c_2f_0+c_1f_1+c_2f_2 = \lambda f_1 \qquad (2.56)$$
$$c_3f_0+c_2f_1+c_1f_2 = \lambda f_2$$
$$c_4f_0+c_3f_1+c_2f_2 = \lambda \times 0$$

i.e., if $c_4f_0+c_3f_1+c_2f_2 = 0$ then $\mathbf{f}_4$ is an eigenvector of $\mathbf{A}_4$. By the symmetry of $\mathbf{A}_4$ it can easily be shown that $\mathbf{f}_{4b}^T = [0\ f_2\ f_1\ f_0]$, i.e., $\mathbf{f}_4^T$ taken backwards, is also an eigenvector with the same eigenvalue. The procedure given above can be applied for any length of ISI in a similar manner. Thus the result of the calculations given above can be generalized in the following lemma.

Lemma 2.2.2: Whenever the error correlation matrix in L has multiple minimum eigenvalues the corresponding eigenvectors can be expressed as a combination of $\mathbf{f}_{L-1}$ with a zero added, and $\mathbf{f}_{(L-1)b}$ where $\mathbf{f}_{L-1}$ is the eigenvector corresponding to the minimum eigenvalue in L-1, with respect to the same error event. Note further that in this case minimum eigenvalues in L and L-1 are the same.

The roots of worst ISI channels lie on the unit circle if the corresponding worst distance decreases with the length of ISI as given in Lemma 2.2.1. The worst distance is obtained by the smallest eigenvalue of all the distance correlation matrices possible for a certain length of inteference(L). If for any reason this eigenvalue is multiple it implies that the worst distance for the length L-1 is the same as well. This is given in Lemma 2.2.2. Also in this case the zeros of the channel may not necessarily lie on the unit circle.

The opposite to the worst distance channel is the maximum distance channel where the minimum squared Euclidean distance is equal to the channel energy. In this case there is asymptotically no loss in error performance due to ISI. This is considered next.

2.3 Maximization of Free Euclidean Distance:

Maximization of the free distance can be viewed as an effort to reduce the loss of performance or in other words a loss in the signal to noise ratio, due to intersymbol interference. Here a method to maximize d_{free}, for general bandlimited channels but having finite impulse response with an energy constraint is considered. For the maximization of d_{free} the set of possible free distance paths is important. This can be obtained using signal flow graph theory [35] which is illustrated by an example.

2.3.1 Transfer function approach

To find the shortest path from the all zero state back to the all zero state one needs an error state diagram as shown in Figure 2.7 for a channel with L = 3. Considering a "unit impulse" as an input the following state equations can be written.

$$T_2 = x_1 + x_7 T_5 \tag{2.57}$$

$$T_3 = x_2 T_2 + x_4 T_3 + x_8 T_4 \tag{2.58}$$

$$T_4 = x_3 T_2 + x_9 T_3 + x_5 T_4 \tag{2.59}$$

$$T_5 = x_6 T_2 + x_{10} T_3 + x_{11} T_4 \tag{2.60}$$

$$T(\mathbf{x}) = x_{12} T_5 \tag{2.61}$$

where the "gain" of an edge is $x_i = D^{d_i^2}$ and d_i^2 represents the distance between corresponding error states in the error state diagram as shown. d_i^2 is a quadratic f

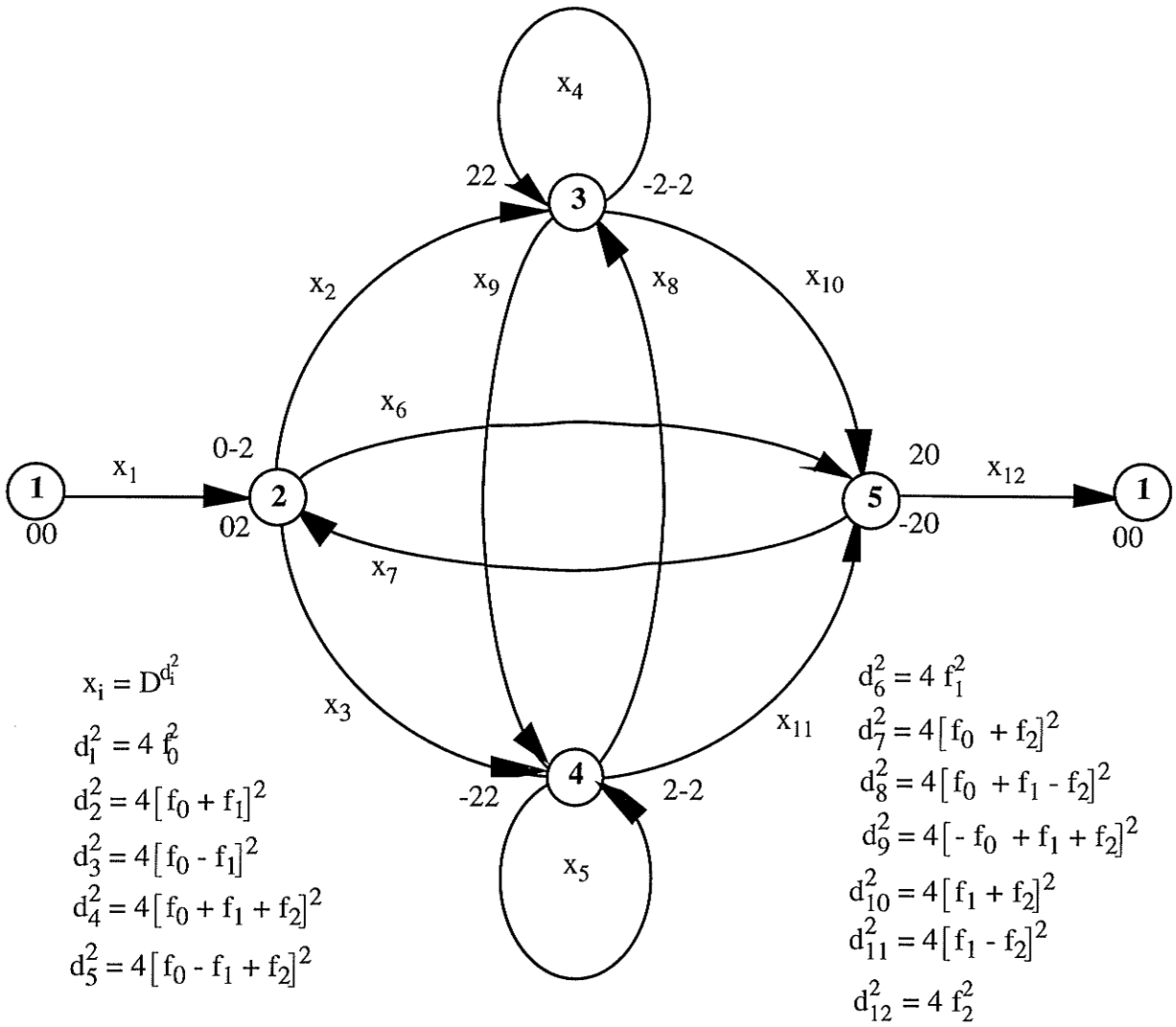

Figure 2.7: Reduced Error State Diagram for L=3

unction of the channel coefficients and is the weight of x_i.

To find the free distance express T(**x**) in the form

$$T(\mathbf{x}) = \frac{g(\mathbf{x})}{1 - \phi(\mathbf{x})} \tag{2.62}$$

where g(**x**) and $\phi(\mathbf{x})$ are functions of x_i obtained by solving the equations given above.

Expand T(x) in a power series

$$= g(\mathbf{x})\left[1 + \phi(\mathbf{x}) + \phi^2(\mathbf{x}) + ...\right] \tag{2.63}$$

which can be written as a summation of products of x_i where $x_i = D^{d_i^2}$. By comparing each term in the sum the ones with the lowest weight terms contributing to T(**x**) can be found. The minimum of these gives the free distance.

For the example, these terms are

$$x_1x_6x_{12} \ , \ x_1x_2x_{10}x_{12} \ , \ x_1x_3\,x_8x_{10}x_{12} \ , \ x_1x_3\,x_{11}x_{12} \ , \ x_1x_2x_9x_{11}x_{12} \tag{2.64}$$

with distances of

$$d_1^2 = 4.\left(f_0^2 + f_1^2 + f_2^2\right) \tag{2.65}$$

$$d_2^2 = 4.\left(f_0^2 + [f_0 + f_1]^2 + [f_1 + f_2]^2 + f_2^2\right) \tag{2.66}$$

$$d_3^2 = 4.\left(f_0^2 + [f_0 - f_1]^2 + [f_2 - f_1 - f_0]^2 + [f_1 + f_2]^2 + f_2^2\right) \tag{2.67}$$

$$d_4^2 = 4.\left(f_0^2 + [f_0 - f_1]^2 + [f_1 - f_2]^2 + f_2^2\right) \tag{2.68}$$

$$d_5^2 = 4.\left(f_0^2 + [f_0 + f_1]^2 + [f_1 + f_2 - f_0]^2 + [f_1 - f_2]^2 + f_2^2\right) \tag{2.69}$$

$$d^2_{free} = \min \left[d_1^2 , d_2^2 , d_3^2 , d_4^2 , d_5^2 \right] \tag{2.70}$$

Other ISI lengths can be handled in the same way. The number of equations from the error state diagram grows exponentially with the channel memory. In addition the lowest weight terms from the expansion of T(**x**) have to be considered as the set of possible free distance paths. Algebraically the problem rapidly becomes very computationally intensive and therefore symbolic processing has to be used to find d^2_{free} for long interference lengths.

2.3.2 Maximum distance channels:

The main result of this section is that for any L, the coefficients of the channel $(f_0, f_1, \cdots, f_{L-1})$ can always be chosen to attain a d_{free} equal to the non ISI case. Before presenting this the case L=3 is described using the set of paths found above. From the previous section the free distance is the minimum of $\left[d_1^2 , d_2^2 , d_3^2 , d_4^2 , d_5^2 \right]$. The maximum value of the d^2_{free} is d_1^2 and is achieved if

$$d_2^2 , d_3^2 , d_4^2 , d_5^2 \geq d_1^2 \tag{2.71}$$

By comparing each distance with d_1^2 the following inequalities are found for the channel coefficients, f_i.

$$-\frac{E}{2} \leq f_1(f_0 + f_2) \leq \frac{E}{2} \tag{2.72}$$

$$f_0 f_2 \leq E = f_0^2 + f_1^2 + f_2^2 \tag{2.73}$$

The condition given in (2.73) is always satisfied as can be seen by noticing that

$$f_0^2 + f_1^2 + f_2^2 = E \geq f_0 f_2, \tag{2.74}$$

where only the case $f_0 f_2 \geq 0$ needs to be considered, since

$$(f_0 - f_2)^2 + f_1^2 \geq 0 \tag{2.75}$$

i.e.,

$$f_0^2 + f_1^2 + f_2^2 \geq 2f_0 f_2 \geq f_0 f_2 \tag{2.76}$$

Thus if the condition in (2.72) is satisfied then the channel (L=3) is a maximum distance channel. Fix one variable by using the energy constraint

$$f_0^2 + f_1^2 = E - f_2^2 \tag{2.77}$$

where f_2 is the variable that is fixed. The above describes a circle of radius $\sqrt{E - f_2^2}$. Thus if the conditions given by (2.72) are satisfied by some segments of the circle, those channel coefficient combinations will have maximum distance. The solution region is sketched approximately in Figure 2.8. From the figure it is clear that the solution is not unique.

These inequalities are derived using the set of possible free distance paths. Therefore once this set of paths is found a series of inequalities can be found to obtain the maximum d^2_{free} channels. In [1] the above set is found for binary, three level and four level signals for channel memories up to four. It is clear that this set is finite because only those paths in the error state diagram which start from all zero state and end in that state without touching the same state twice in between, have the chance of becoming candidates for the free distance path. As seen in (2.70) only a subset of these paths would actually be in the potential free distance path set. Therefore the channel coefficient

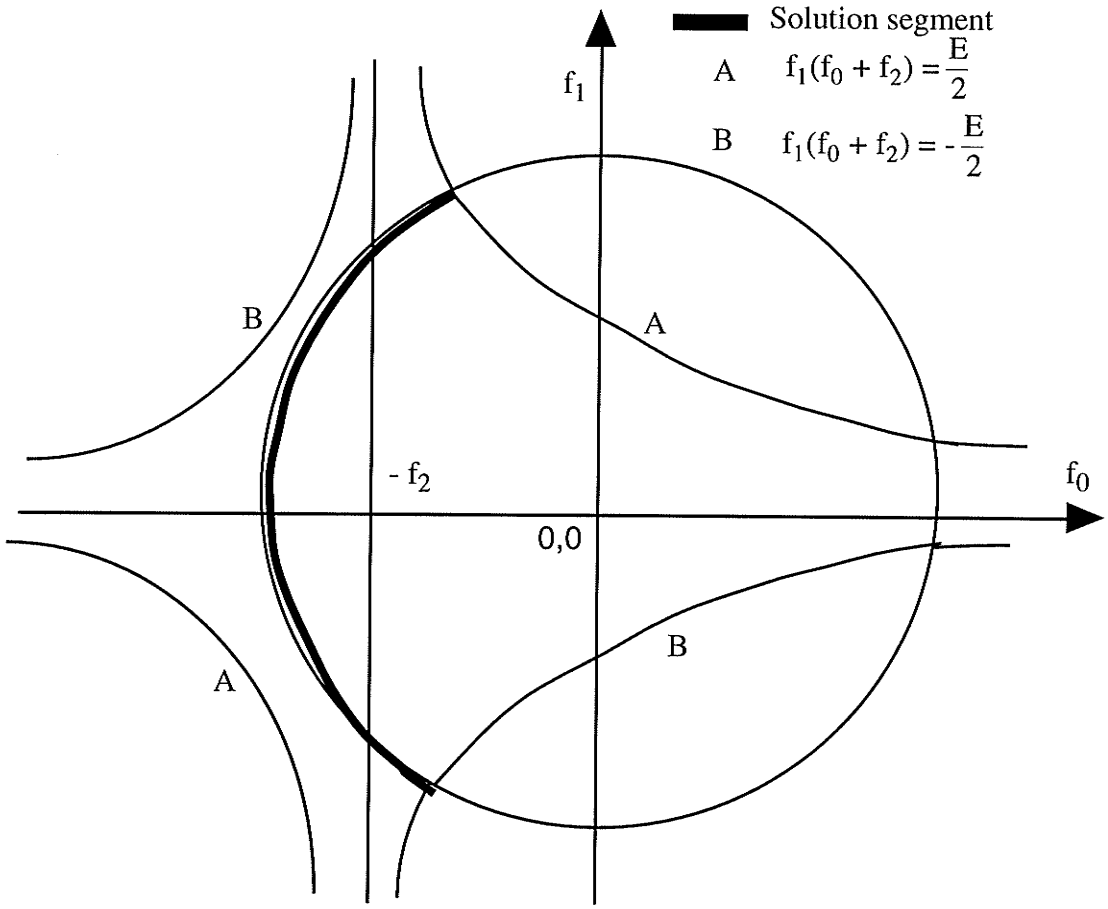

Figure 2.8 : Maximum Distance Channel Coefficient Region for L=3

space is partitioned into regions where in a particular region only one path always gives the free distance. This fact was also shown in [32] where the optimum transmitter filter for ISI channels was found using the eigenvalue technique.

For L=3 this set of paths are

$$\mathbf{S} = \{ (2,0,0),(2,2,0,0),(2,-2,0,0) \}. \qquad (2.78)$$

In general the following theorem can be stated for any finite ISI channel.

Theorem:

For any finite ISI length there exists a maximum distance channel. Specifically if the coefficients of the channel have the relationships given below then that channel is a maximum distance channel for a binary signaling scheme,

$$\forall\ i,\ f_i \geq 0\ \&\ f_i \geq 2f_{i+1} + 2f_{i+2} + ...+ 2f_{L-1}\ ,\ i=0,1,...,L-2 \qquad (2.79)$$

Proof:

The distance of an error event of length ℓ is given by

$$d^2 = \sum_{n=0}^{\ell-1} \left[\sum_{k=0}^{L-1} f_k \varepsilon_{n-k} \right]^2 \qquad \ell \geq L \qquad (2.80)$$

where $\varepsilon_i \in \{0,2,-2\}$ and since there is a merge at $n=\ell - 1$

$$\varepsilon_{\ell-1} = \varepsilon_{\ell-2} = ...= \varepsilon_{\ell-(L-1)} = 0 \qquad (2.81)$$

Also $\varepsilon_0 \neq 0$ to start the error event.

To use an inductive proof first consider $\ell = L$ which establishes the starting conditions.

i) $\ell = L$.

A merge at ℓ=L means that

$$\varepsilon_{L-1} = \varepsilon_{L-2} = \ldots = \varepsilon_{L-(L-1)} = 0 \tag{2.82}$$

and therefore $$d^2 = (f_0\varepsilon_0)^2 + (f_1\varepsilon_0)^2 + \ldots + (f_{L-1}\varepsilon_0)^2 = \varepsilon_0^2\left[\sum_{k=0}^{L-1} f_k^2\right] \tag{2.83}$$

Thus all error events of length L have a distance equal to the maximum free distance.

ii) Assume now that this is true for error events of length $\ell = m > L$

$$d_m^2 = \sum_{n=0}^{m-1}\left[\sum_{k=0}^{L-1} f_k\varepsilon_{n-k}\right]^2 \geq \varepsilon_0^2\left[\sum_{k=0}^{L-1} f_k^2\right] \tag{2.84}$$

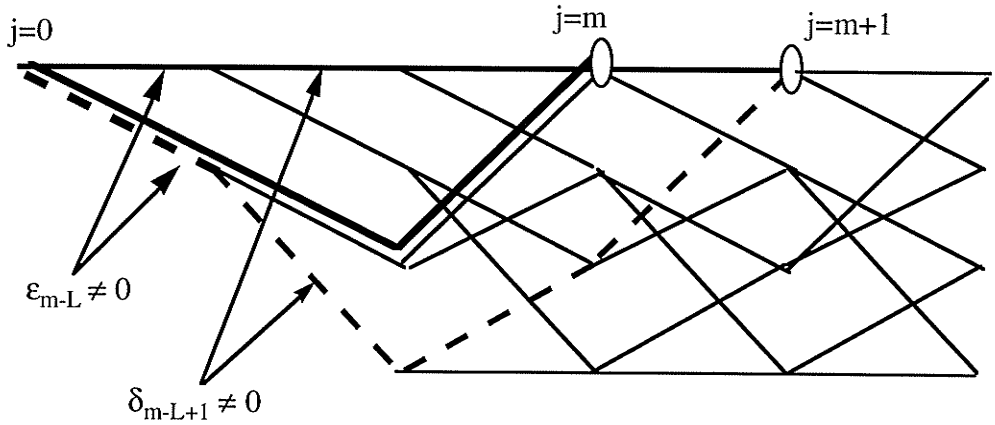

Figure 2.9 j=m + 1 as an Extension of j=m

Consider $\ell = m+1$. If it can be shown that (2.84) implies

$$d_{m+1}^2 \geq \varepsilon_0^2 \left[\sum_{k=0}^{L-1} f_k^2 \right] \tag{2.85}$$

then the proof is complete.

The error event of $\ell = m+1$ can be considered as an extension of the error event $\ell = m$ as shown in Figure 2.9.

Now the distance of this error event is

$$d_{m+1}^2 = \sum_{n=0}^{m} \left[\sum_{k=0}^{L-1} f_k \delta_{n-k} \right]^2 \tag{2.86}$$

where $$\delta_i = \varepsilon_i \quad i=0,1,....,m-L \; ; \; \delta_{m-L+1} \neq 0 \tag{2.87}$$

and the merge conditions mean that

$$\varepsilon_{m-L+i} = 0 \; , \; i=1,....,L-1 \tag{2.88}$$

$$\delta_{m-L+i} = 0 \; , \; i=2,....., \; L \tag{2.89}$$

$$d_m^2 = \sum_{n=0}^{m-L} \left[\sum_{k=0}^{L-1} f_k \varepsilon_{n-k} \right]^2 + \sum_{n=m-L+1}^{m-1} \left[\sum_{k=0}^{L-1} f_k \varepsilon_{n-k} \right]^2 \tag{2.90}$$

$$d_{m+1}^2 = \sum_{n=0}^{m-L} \left[\sum_{k=0}^{L-1} f_k \varepsilon_{n-k} \right]^2 + \sum_{n=m-L+1}^{m-1} \left[\sum_{k=0}^{L-1} f_k \delta_{n-k} \right]^2 + \left(f_{L-1} \delta_{m-L+1} \right)^2 \tag{2.91}$$

From the above if

$$\sum_{n=m-L+1}^{m-1} \left\{ \left[\sum_{k=0}^{L-1} f_k \delta_{n-k} \right]^2 - \left[\sum_{k=0}^{L-1} f_k \varepsilon_{n-k} \right]^2 \right\} \geq 0 \tag{2.92}$$

then the desired result is obtained. The left hand side is a series of L-1 differences. Name these differences Δ_1 , Δ_2 , ..., Δ_{L-1}. Consider the last difference, i.e. Δ_{L-1} (when

n=m-1).

Using equations (2.88) & (2.89) for zero error symbols it can be seen that

$$\Delta_{L-1} = (f_{L-2}\delta_{m-L+1} + f_{L-1}\varepsilon_{m-L})^2 - (f_{L-1}\varepsilon_{m-L})^2 \quad (2.93)$$

$$= f_{L-2}^2\delta_{m-L+1}^2 + 2f_{L-2}f_{L-1}\delta_{m-L+1}\varepsilon_{m-L} \quad (2.94)$$

if $f_i > 0$ then the maximum possible negative value for Δ_{L-1}, which gives the worst case in contributing to possible failure of (2.92), is

$$\Delta_{L-1} = 4(f_{L-2}^2 - 2f_{L-2}f_{L-1}) \quad (2.95)$$

However if $$f_{L-2} \geq 2f_{L-1} \quad (2.96)$$

then Δ_{L-1} in fact contributes a positive amount to left hand side of (2.92).

Now consider the difference when n=m-2. Proceeding as above,

$$\Delta_{L-2} = (f_{L-3}\delta_{m-L+1} + f_{L-2}\varepsilon_{m-L} + f_{L-1}\varepsilon_{m-L-1})^2 - (f_{L-2}\varepsilon_{m-L} + f_{L-1}\varepsilon_{m-L-1})^2 \quad (2.97)$$

Cancelling common terms the maximum possible negative value for Δ_{L-2} is

$$\Delta_{L-2} = f_{L-3}^2 - 2f_{L-3}f_{L-2} - 2f_{L-3}f_{L-1} \quad (2.98)$$

Again if

$$f_{L-3} \geq 2f_{L-2} + 2f_{L-1}. \quad (2.99)$$

then Δ_{L-2} contributes a positive amount to left hand side of (2.92).

Continuing in the same manner for other n a similar set of required inequalities are

obtained to ensure (2.92). In general

$$f_i \geq 2f_{i+1} + 2f_{i+2} + ...+ 2f_{L-1} \ , \ i=0,1,...,L-2 \qquad (2.100)$$

Therefore by induction if the above relationships are satisfied by the channel coefficients it follows that

$$d_\ell^2 \geq \varepsilon_0^2 \left[\sum_{k=0}^{L-1} f_k^2 \right] \quad , \ \forall \ \ell \geq L. \qquad (2.101)$$

and hence the channel is a maximum distance channel.

QED.

The main point behind this proof is to consider the error event of length m+1 as an extension of an event of length m. All the possibilities that could arise are given in Figure 2.10. However, the strongest conditions for the channel coefficients are always obtained by the case considered in the proof. The theorem only gives an existence proof and the conditions on the channel coefficients are only sufficient. There could always be maximum distance channels whose coefficients violate the given conditions. The conditions can be easily extended to M-ary PAM. Extension to complex signal alphabets (QAM) is possible with necessary modifications. For a discussion of these see Appendix A.

2.4 Obtaining the maximum distance by modifying the overall response:

There are clearly two methods of achieving this. A prefilter can be used at the transmitter so that the combination of that filter and the channel response would give a maximum distance channel. The other method is to use an equalizer at the receiver for

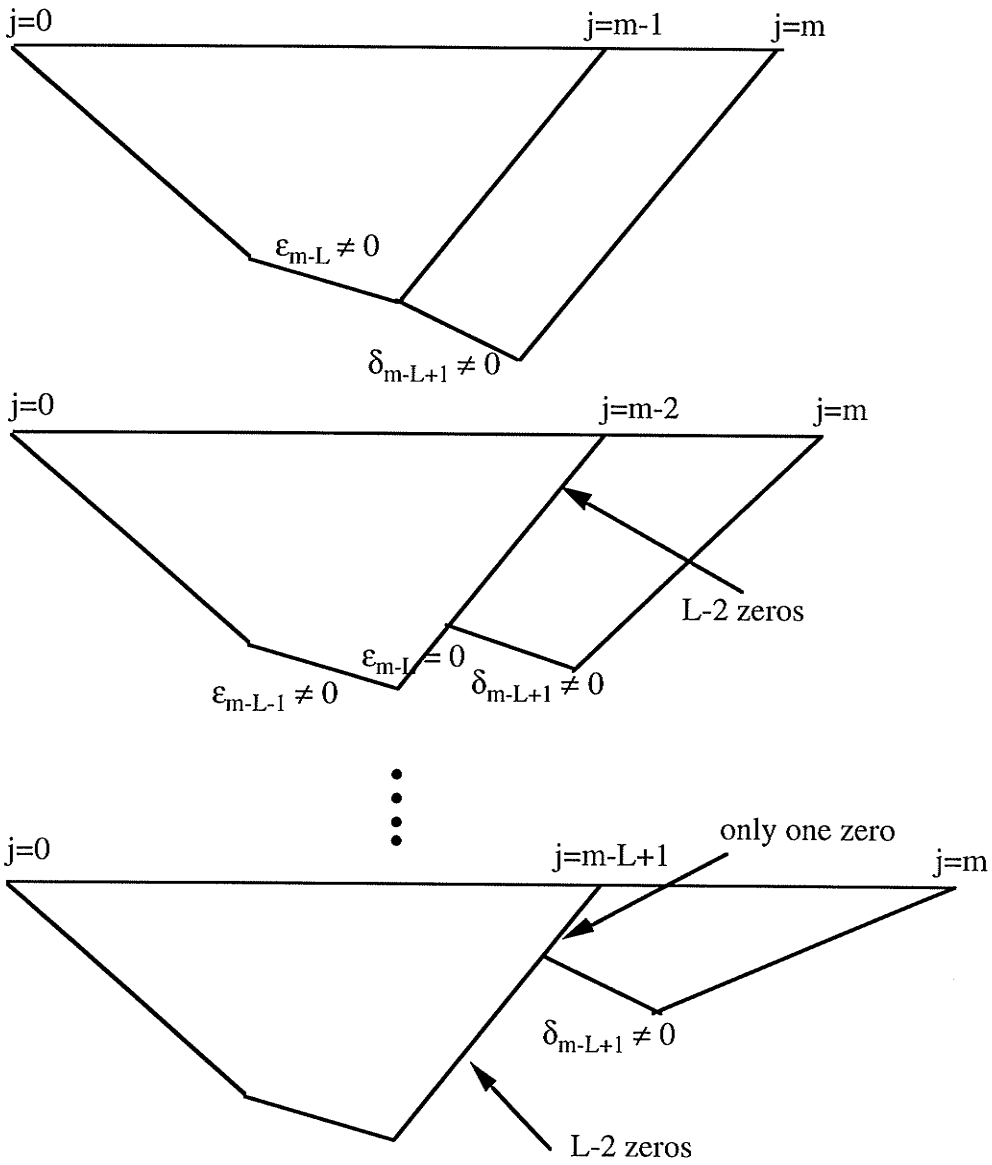

Figure 2.10 All possibilities of extension

the same purpose. When a prefilter is employed at the transmitter the channel response H(f) and discrete response $F_m(Z)$ for the maximum distance case are assumed known. From $F_m(Z)$ the analog response $H_m(f)$ can be found. Thus the response of the prefilter $H_p(f)$ is given by;

$$H_p(f)\, H(f) = H_m(f) \tag{2.102}$$

$$H_p(f) = \frac{H_m(f)}{H(f)} \tag{2.103}$$

If H(f) is stable and does not have spectral nulls then $H_p(f)$, the prefilter, can be realized. This results in an overall response of $H_m(f)$ which will achieve maximum distance. Since this is done at the transmitter there is no noise enhancement.

The other option is to use a equalizer at the receiver end for the same purpose as shown in Fig. 2.11. If the known maximum distance response is $F_m(Z)$ then

$$F_m(Z) = C(Z)\, F(Z) \tag{2.104}$$

$$C(Z) = \frac{F_m(Z)}{F(Z)} \tag{2.105}$$

The equalizer output signal to noise ratio is

$$SNR = \frac{\sigma_x^{\,2} |F_m|^2}{\sigma^2 |C|^2} \tag{2.106}$$

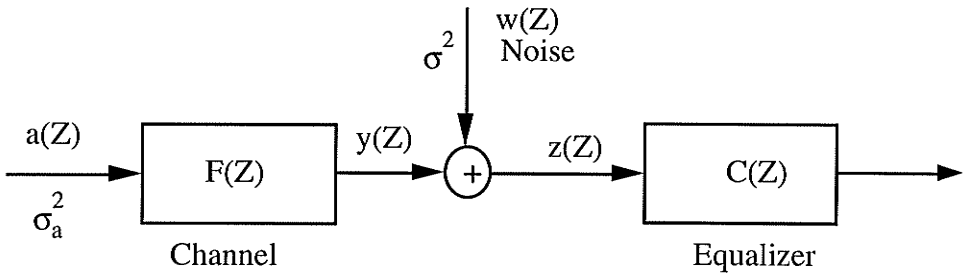

Figure 2.11

As a more sophisticated method, the equalizer for the mean square error (MSE) criterion is described below following the procedure given in [26]. In the MSE criterion the tap coefficients $\{c_j\}$ of the equalizer are adjusted to minimize the mean-square value of the error

$$\varepsilon_k = [y_k]_{max} - [\widehat{y_k}]_{max} \tag{2.107}$$

$[y_k]_{max}$ is the channel output without noise for the maximum distance channel and $[\widehat{y_k}]_{max}$ is the estimated output by the equalizer. These can be expressed as

$$[y_k]_{max} = \sum_{m=0}^{L-1} q_m a_{k-m} \tag{2.108}$$

where Q(Z) is the known maximum distance response.

and

$$[\widehat{y_k}]_{max} = \sum_{m=-\infty}^{\infty} c_m y_{k-m} \tag{2.109}$$

The performance index for the MSE criterion, denoted by J is defined as

$$J = E|\varepsilon_k|^2 \tag{2.110}$$

A set of linear equations can be obtained by invoking the orthogonality principle in the mean-square estimation. That is, the coefficients $\{c_j\}$ are selected to make the error ε_k orthogonal to $\{y^*_{k-m}\}$ for $-\infty < m < \infty$. Thus

$$E(\varepsilon_k y^*_{k-m}) = 0 \quad -\infty < m < \infty \tag{2.111}$$

substitution for ε_k and y^*_{k-m} yields

$$E([y_k]_{max} y^*_{k-m}) = E([\widehat{y_k}]_{max} y^*_{k-m}) \tag{2.112}$$

By simplifying the expectation from MSE it can be shown that

$$F^*(Z^{-1})Q(Z) = C(Z)\left[F(Z)F^*(Z^{-1}) + \sigma^2\right] \tag{2.113}$$

i.e.,
$$C(Z) = \frac{F^*(Z^{-1})Q(Z)}{\left[F(Z)F^*(Z^{-1}) + \sigma^2\right]} \tag{2.114}$$

with the noise whitening filter

$$C'(Z) = \frac{Q(Z)}{\left[F(Z)F^*(Z^{-1}) + \sigma^2\right]} \tag{2.115}$$

The difference in this case is Q(Z) which for zero ISI would be 1.

In the above calculations Q(Z) (maximum distance response) is not unique. There are many maximum distance channels for a given length of interference as shown in section 2.4. Hence one can select Q(Z) subject to the condition that the signal to noise

ratio (SNR) be maximized at the output of the channel. Thus the equalization can be done subject to two constraints; one is the minimizing the error in approximating the maximum distance response, the other is maximizing the SNR. The brute force method of doing this is to go through all the maximum distance channels and select the one which gives the highest SNR. It is also important to realize the fact that if the approximation is close enough one would still end up with a maximum distance channel as they span over a range of coefficients. The main concern is therefore SNR as what is gained by the maximum distance channel can be diminished by the enhancement of noise.

Chapter 3
Convolutional Codes for ISI

The previous chapter considered distance properties of ISI channels. In particular it was shown that any finite ISI channel can achieve the same error performance as the non ISI channel though depending on the specific channel the transmitter power may increase. This is in the sense that the minimum Euclidean distance, d_{min}, between two channel output signals is the same. To further increase d_{min}, block, convolutional or trellis, coding could be used. Though all three techniques have a trellis representation, the trellis structure of convolutional or trellis codes, being regular, is more closely related to that of ISI channels. Thus convolutional codes for ISI channels are considered in this chapter while trellis coding is discussed in the next chapter.

The literature on convolutional coding for ISI channels is sparse. Historically, perhaps Viterbi [35] first discussed the application of convolutional codes to ISI channels. He was primarily concerned with the decoder/demodulator structure and did not consider the interaction between code and channel. Wolf and Ungerboeck [37], motivated by the magnetic recording channel derived several lemmas which show that if convolutional codes with a good d_{free} (Hamming) are used then the resulting minimum Euclidean distance is increased. They considered specifically a (1 - D) channel as shown in Figure 3.1 and used a configuration of a coder followed by a channel precoder (Figure 3.2). Lee [7] considered a slightly more general channel of the form $1 - D^N$ (N = 1,2,3). An algebraic procedure is given to obtain codes with desirable properties such as run length limited codewords.

In this chapter convolutional codes for ISI channels with real coefficients are

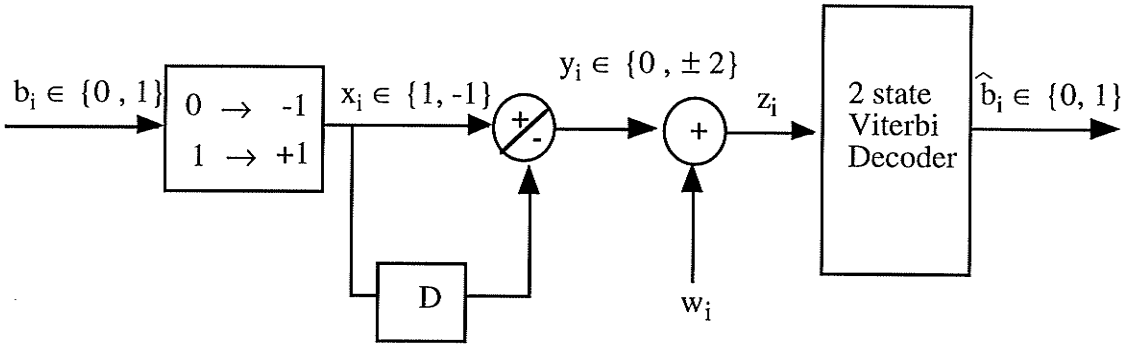

Figure 3.1(a). (1 - D) Baseline Communication System

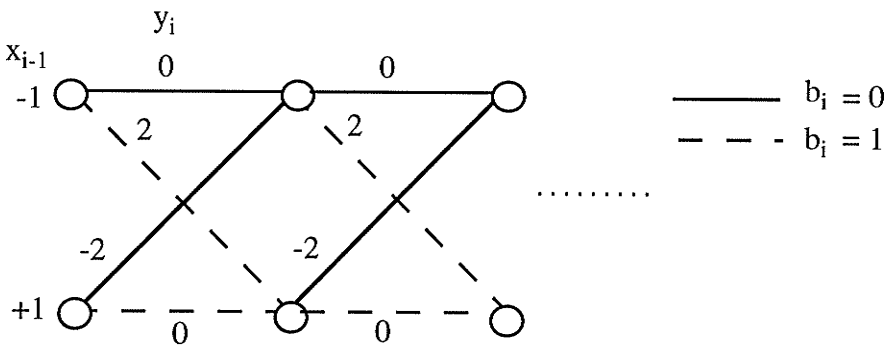

Figure 3.1(b). Trellis Diagram

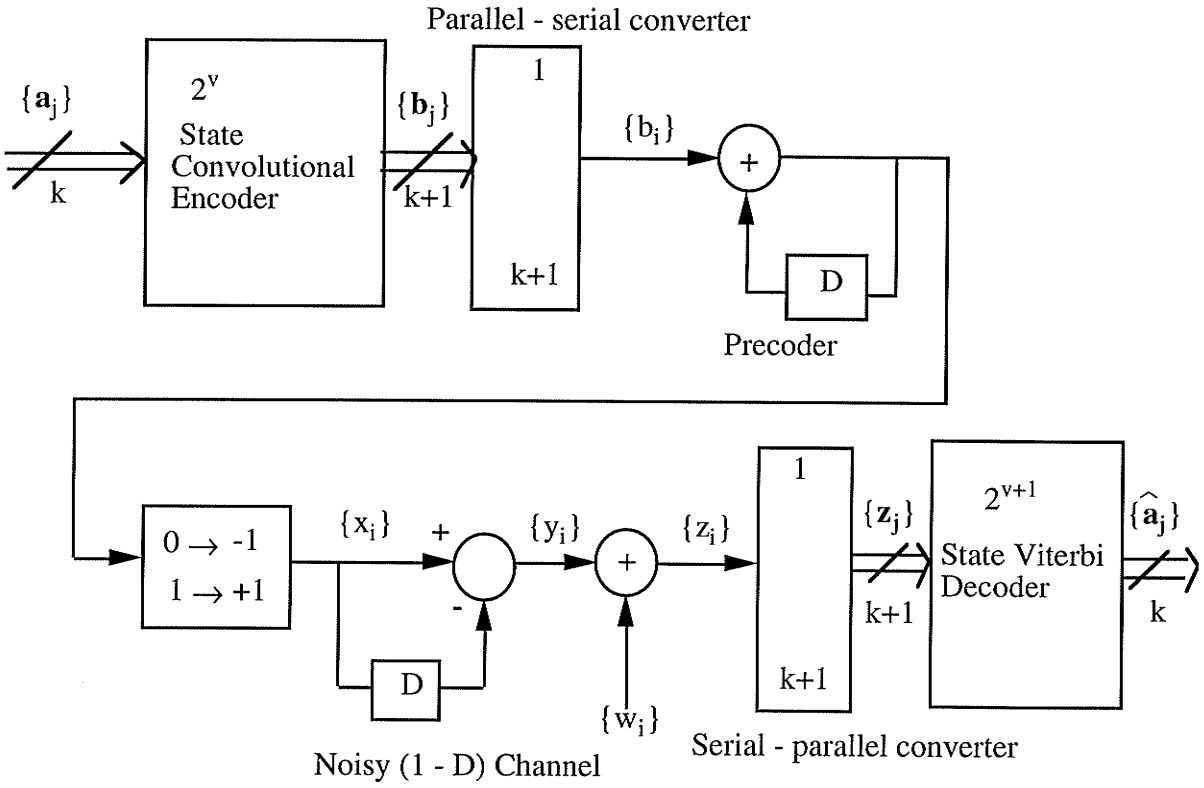

Figure 3.2. Convolutional codes with a precoded (1 - D) channel

investigated. The criterion is to optimize the encoder/channel combination to maximize d_{min}, i.e., the code is "matched" to the bandlimited channel. To do this d_{min} must be determined for the coder/channel cascade. Thus the methods of Chapter 2 are extended and presented in the next section. Following this there is a discussion of the general properties of convolutionally coded ISI channels. Of these, the changes such as signaling rate and change in ISI that should be taken into account when an encoder is placed at the transmitter, are considered first. If the encoder is catastrophic then the coder/channel cascade is also catastrophic. Proof of this is given next followed by bounds on the coded distance of the ISI channel. The chapter concludes by developing search procedures to find the best combination of convolutional encoder and ISI channel. These are illustrated by examples.

3.1 Error state diagram:

A crucial step in determining the minimum distance for the combined system of a convolutional encoder followed by a finite real ISI channel (coded ISI system) is the construction of an error state diagram. Once an error state diagram is constructed, well known graph search techniques such as Dijkstra's algorithm [17,19] can be readily applied to find d_{min}. These methods are essentially those of the uncoded case except for an increase in computational complexity.

To illustrate the construction of an error state diagram consider the system of Figure 3.3. Here PAM with (0,1) signaling instead of (-1,1) is used. For the purpose of distance calculations the difference would be a factor of four. The Euclidean distance between two sequences (i.e. k , k') of length 2ℓ in the channel trellis (ℓ is the length of the input bit sequence u_i and thus 2ℓ is the channel input sequence length) is given by

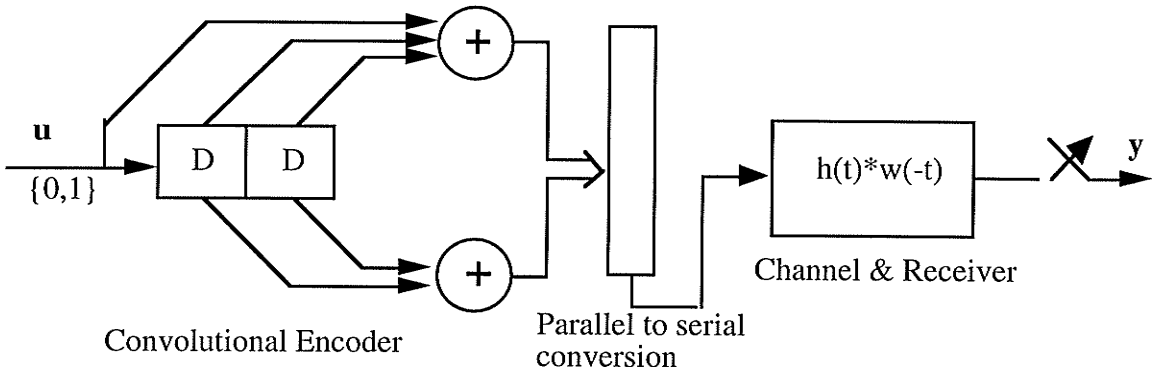

* Convolutional code: R = 1/2 ; Generators $g^{(1)}(D) = 1 + D + D^2$, $g^{(2)}(D) = D + D^2$

* ISI Channel: Impulse response length L=3 ; Coefficients (f_0 , f_1 , f_2)

Figure 3.3. Communication system with convolutionally encoded input

$$d^2 = \sum_{m=1}^{\ell} \left[y_m^{(1)}(k) - y_m^{(1)}(k')\right]^2 + \left[y_m^{(2)}(k) - y_m^{(2)}(k')\right]^2 \qquad (3.1)$$

where

$$y_m^{(1)}(k) = f_0.\left[u_m(k) \oplus u_{m-1}(k) \oplus u_{m-2}(k)\right] + f_1.\left[u_{m-2}(k) \oplus u_{m-3}(k)\right] + f_2.\left[u_{m-1}(k) \oplus u_{m-2}(k) \oplus u_{m-3}(k)\right] \qquad (3.2)$$

$$y_m^{(2)}(k) = f_0.\left[u_{m-1}(k) \oplus u_{m-2}(k)\right] + f_1.\left[u_m(k) \oplus u_{m-1}(k) \oplus u_{m-2}(k)\right] + f_2.\left[u_{m-2}(k) \oplus u_{m-3}(k)\right] \qquad (3.3)$$

$\oplus$ represents modulo 2 addition and '.' ordinary real multiplication ;

$y_m^{(1)}(k)$ is the channel output corresponding to first output of the encoder ;

$y_m^{(2)}(k)$ the channel output corresponding to second output of the encoder ;

each m considers two ISI trellis steps due to the rate of the code (see Figure 3.4).

Thus to calculate d^2, $\left[y_m^{(1)}(k) - y_m^{(1)}(k')\right]$ and $\left[y_m^{(2)}(k) - y_m^{(2)}(k')\right]$ have to be found. If an error state diagram is to be drawn then these differences must be found using error symbols. In addition it is necessary to find the memory of the coded ISI system. From equations (3.2) and (3.3) it can be seen that the memory is 3, (since the present output depends on three previous inputs, u_{m-1}, u_{m-2}, u_{m-3}). Calculation of the memory for a given system is detailed in the next section. For a binary alphabet the error symbols are 0, 1, -1. Thus there are $3^3 = 27$ error states. With the modulo operations present in equations (3.2) and (3.3) values for $u_m(k)$ and $u_m(k')$ should be found given the values of the error symbols. Consider the case where the error symbol is zero.

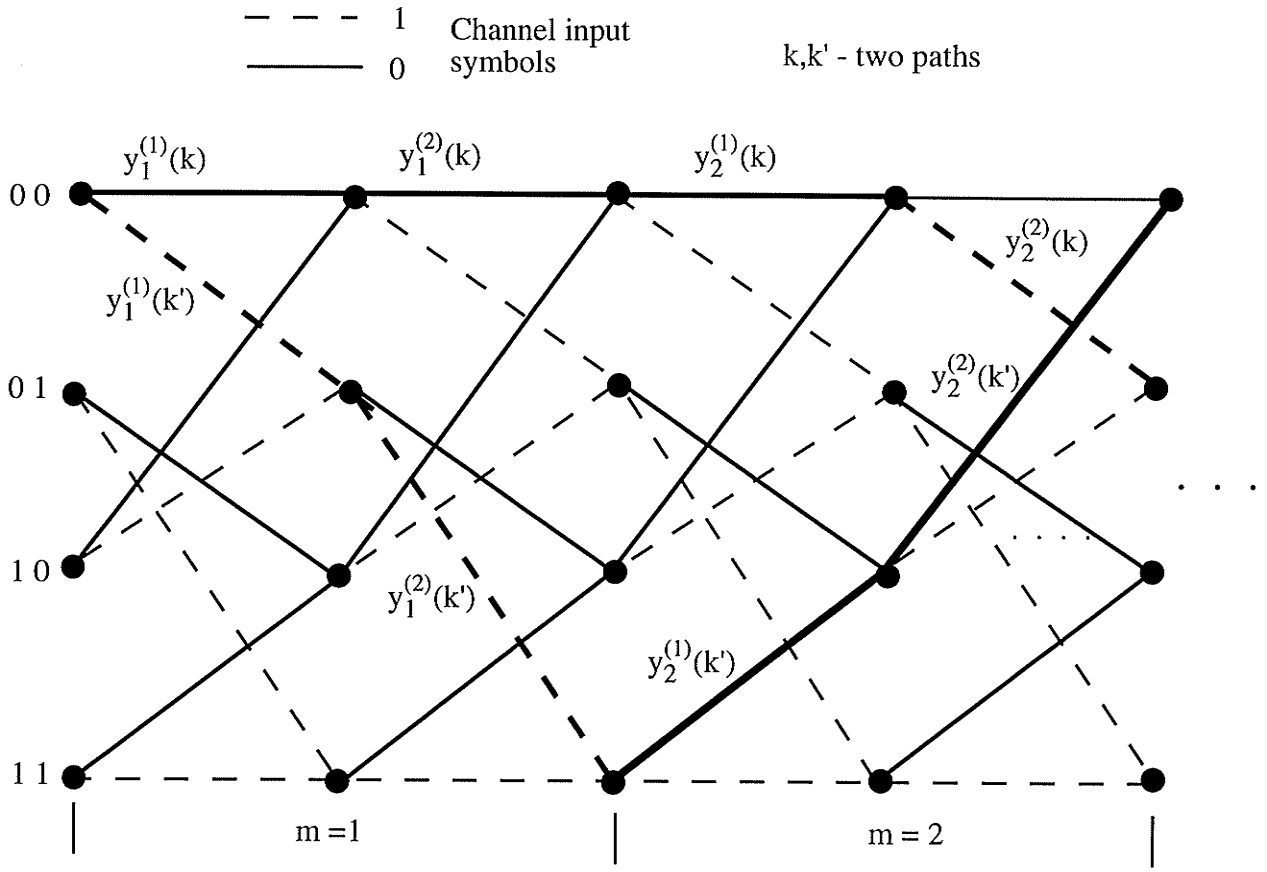

Figure 3.4. Channel trellis for the coded input

$$\varepsilon_m = u_m(k) - u_m(k') \Rightarrow u_m(k) = 1 \, , \, u_m(k') = 1 \text{ or } u_m(k) = 0 \, , \, u_m(k') = 0 \qquad (3.4)$$

For a given error state a set of state pairs for the two sequences are possible. For example

$$\varepsilon = (0,0,0) \Rightarrow \mathbf{u} = (0,0,0) \, , \, \tilde{\mathbf{u}} = (0,0,0) \text{ or } \mathbf{u} = (0,0,1) \, , \tilde{\mathbf{u}} = (0,0,1)$$

etc. Thus for a given error state there can be many state pairs.

A portion of the error state diagram is shown in Figure 3.5 with the state pairs. Distances for each and every set of encoder state pairs need to be calculated in order to obtain the minimum distance. Extensions for the other constraint lengths of the convolutional encoders and ISI can be carried out in a similar manner. Another way to find the distance is to directly use a state pair diagram. Here a state is given by $(\mathbf{u}, \tilde{\mathbf{u}})$. All possibilities for $\mathbf{u}$ and $\tilde{\mathbf{u}}$ have to be considered to construct this state pair diagram.

3.1.1 Memory of the coded ISI system:

An important thing to note is that the combined memory of the coder/channel system is less than the sum of the memories of the ISI channel and the convolutional encoder [35]. In general the n output symbols from the coder that are input to the channel have a memory given by the constraint length (K) of the coder. Since the ISI channel also has a memory of v (= L - 1) there are at most $\left\lceil \frac{v}{n} \right\rceil$ ($\lceil . \rceil$ is the ceiling function.) groups of n symbols in memory length v. Hence in terms of the encoder inputs, if the present time at the encoder is k, then the $k - \left(\left\lceil \frac{v}{n} \right\rceil + K \right)$ previous input is the last to affect the present channel output. Therefore the total combined memory is

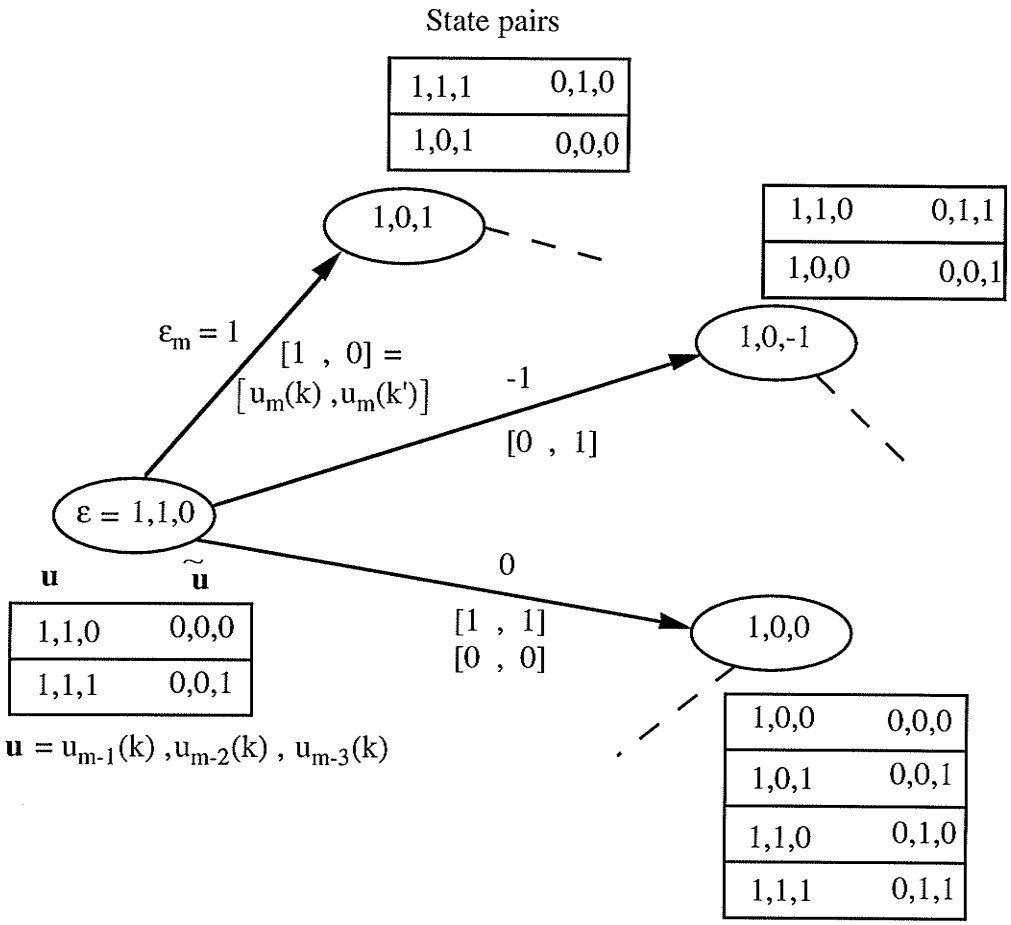

Figure 3.5. Portion of the error state diagram showing state pair needed for distance calculation

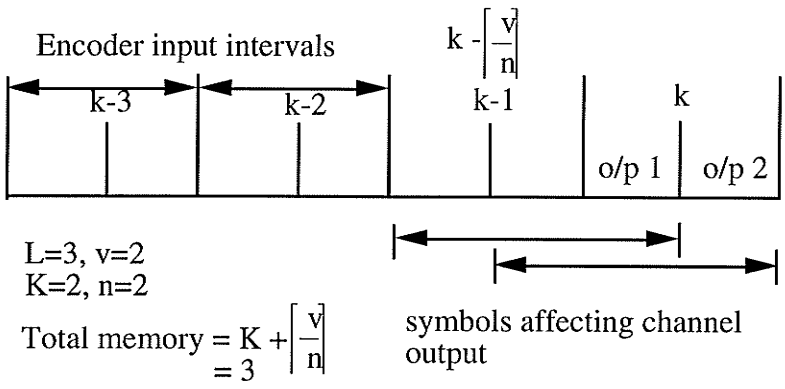

Figure 3.6

$\left\lceil \frac{v}{n} \right\rceil$ + K. This is illustrated in Figure 3.6 for the example.

3.2 Change in ISI due to coding:

The addition of an encoder at the transmitter poses a problem for the data transmission due to the increased rate. Either the source rate, or the channel rate, has to be kept the same. If the source rate is kept constant then the channel rate has to be increased and hence the ISI changes.

Consider the example of a rate 1/n convolutional encoder used with an ISI channel. For every information(source) symbol the encoder produces n channel symbols. Therefore either the channel rate is increased n times if the source rate is maintained or the source rate is reduced by the factor n. If the channel rate is kept constant the reduction of the source rate has to be taken into account when the coding gain is defined. On the other hand, if the channel rate is increased which is the usual situation where one has a fixed source rate, then the number of ISI terms generally increase due to the fixed bandwidth. This is shown in Figure 3.7. In this case the loss of signal to

noise ratio due to additional ISI terms should be taken into account. In the literature the coding gain is defined as follows:

$$G = \frac{Rd^2_{min}(\text{coded})}{d^2_{min}(\text{uncoded})} \quad ; \text{R is the rate of the code.} \qquad (3.5)$$

where R is supposed to take the change in signaling rate into consideration. The above does not account for the change in ISI terms should the channel rate increase. This problem was addressed by Bergmans [4] who incorporated the change of ISI into the coding gain for rate 1/n codes for some integer coefficient channels with response of the form $(1 + D)^N$ or $(1-D)(1 + D)^N$ (N=0,1,2).

Here codes of rate 1/n and b/n are considered for channels with real coefficients with the source rate kept constant. Thus a new set of ISI coefficients have to be found in each case due to the increased channel signaling rate. Consider the autocorrelation function $R(\tau)$ of the channel impulse response. If the code rate is b/n then the new sampling rate at the receiver is bT/n where T is the sampling interval before coding. Thus the sampled autocorrelation function is R(kbT/n). It is straightforward to find the coded channel response $F_c(D)$ using spectral factorization and hence the new set of ISI coefficients. On the other hand if one starts from the coded response $F_c(D)$ and the uncoded F(D) is required this can be found exactly only for the case of rate 1/n. This is done by undersampling $R_c(D)$ by a factor of n as illustrated in Figure 3.8 for a rate 1/2 code. In general if

$$R_c(D) = \sum_i R_i D^i \qquad (3.6)$$

then

$$R(D) = \sum_i R_{ni} D^i \qquad (3.7)$$

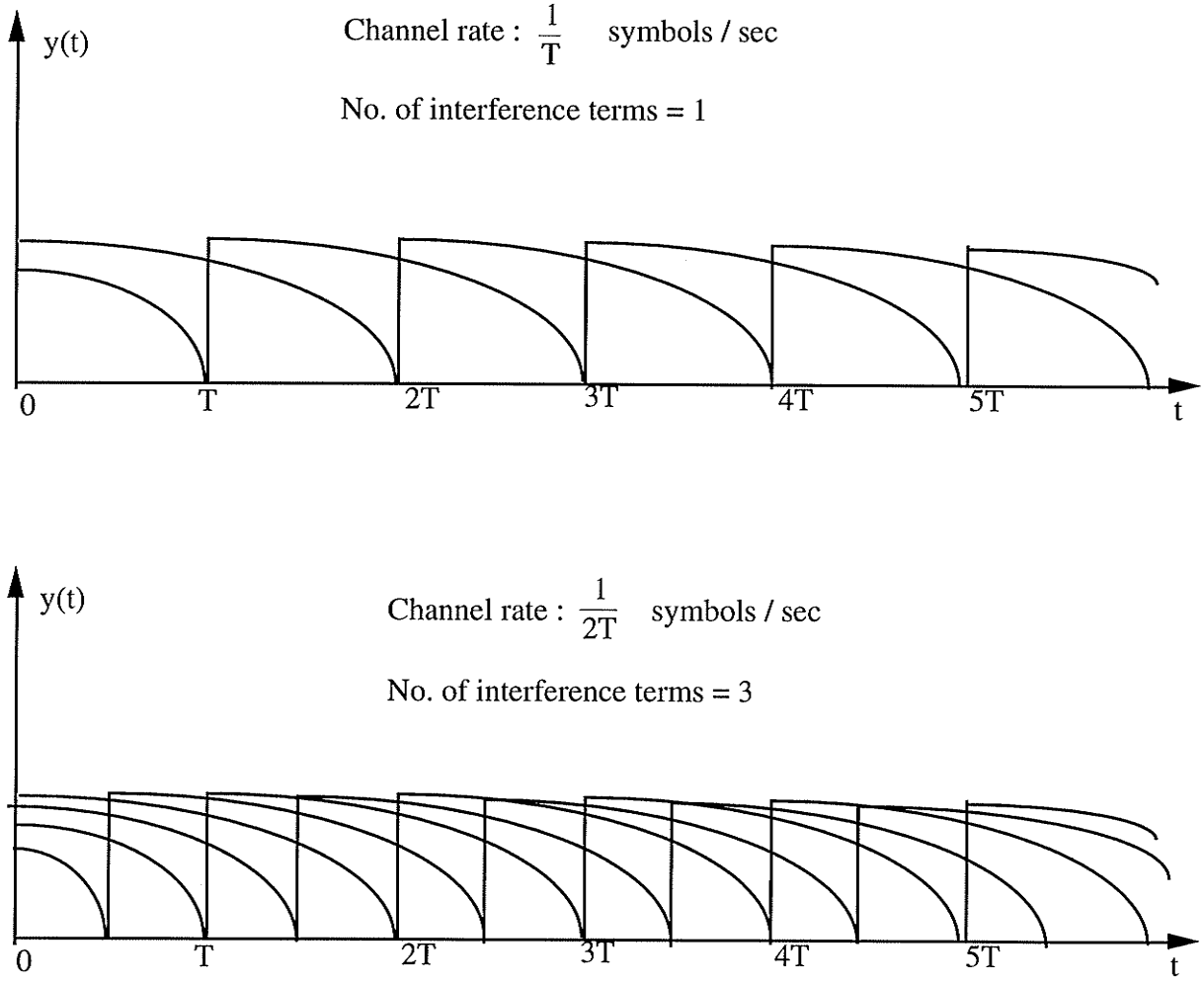

Figure 3.7. Effect on ISI due to a doubling of rate ; Length of channel impulse response = 2T

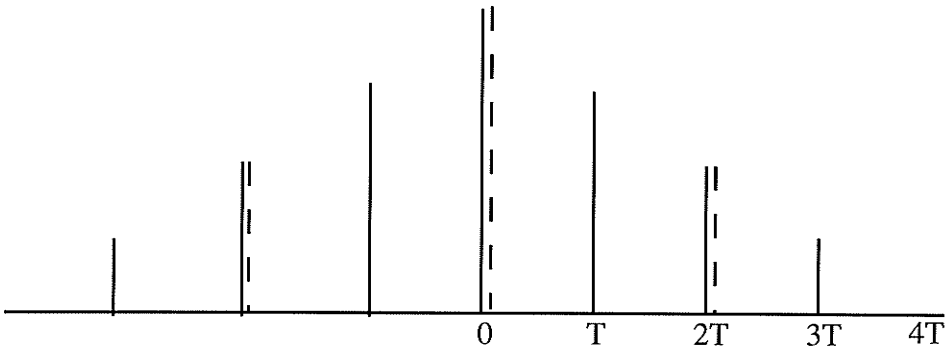
0
T
2T
3T
4T
sampled autocorrelation function for coded channel given
sampled autocorrelation function for uncoded channel where code rate is 1/2

Figure 3.8

for the uncoded case. However if the code rate is b/n then it is not possible to find out an exact uncoded response from the coded response given since the samples do not coincide.

Several examples are given next which consider codes of different rates for different channels. The signaling rate is increased to account for the encoder output, i.e., the source rate is kept constant.

(**A**) Code rate is R=1/2. Two channels are considered.

i) A single pole truncated channel of different ISI lengths.

ii) A raised cosine impulse response channel of different ISI lengths.

The coding gains for the two cases are given in Table 3.1 and 3.2. From the tables it can be seen that there is a coding gain only for the truncated single pole channel with a rate 1/2 code. For the raised cosine channel there is a loss which implies that for this kind of channel a higher rate code may be more suitable.

(**B**) R=2/3. Same channels as above are considered.

Results for distances are given in Tables 3.3 & 3.4. The tables show there is a coding gain for both truncated single pole channels and one of the half cosine channels in this case.

As seen from the results when the length of ISI is long the coding gain is either low or there is no gain. This is not intuitive because it is generally expected that there is a coding gain when a convolutional coder is used. The loss is partly due to the factor R in the coding gain expression and also due to the increase in ISI. Therefore it is essential to take the change in ISI into account when the channel rate is increased, otherwise the

a	source rate constant	R=1/2
	L (coded)	G (dB)
4	2 (4)	3.22 (3.88)
3	2 (4)	2.68 (3.73)
2	3 (6)	1.66 (3.21)
1.5	4 (8)	0.85 (2.0)

Table 3.1. Encoder Matrix G(D) = $\begin{bmatrix} 1 & 1 & 1 \\ 1 & 0 & 1 \end{bmatrix}$ Free distance = 5
Channel impulse response is e^{-at} truncated: Gain values assuming no change in ISI are given within brackets

source rate constant	R=1/2
L (coded)	G (dB)
2 (4)	-2.7 (3.0)
5 (10)	-4.95 (-0.16)

Table 3.2. Encoder Matrix G(D) = $\begin{bmatrix} 1 & 1 & 1 \\ 1 & 0 & 1 \end{bmatrix}$ Free distance = 5
Channel impulse response $\frac{1}{2LT}\left[1 - \cos\left(\frac{2\pi}{LT}t\right)\right]$: Gain values assuming no change in ISI are given within brackets

a	source rate constant R=2/3	
	L	G (dB)
4	2 (3)	3.75
3	2 (3)	4.5
2	3 (5)	3.75
1.5	4 (6)	3.75

Table 3.3. Encoder Matrix $G(D) = \begin{bmatrix} 1\,1\,1\,1\,0\,1 \\ 1\,1\,0\,1\,0\,1 \\ 0\,1\,1\,1\,0\,0 \end{bmatrix}$ Free distance = 5

Channel impulse response is e^{-at} truncated

source rate constant R= 2/3	
L	G (dB)
2 (3)	1.72
5 (8)	-3.56

Table 3.4. Encoder Matrix $G(D) = \begin{bmatrix} 1\,1\,1\,1\,0\,1 \\ 1\,1\,0\,1\,0\,1 \\ 0\,1\,1\,1\,0\,0 \end{bmatrix}$ Free distance = 5

Channel impulse response $\frac{1}{2LT}\left[1 - \cos\left(\frac{2\pi}{LT}t\right)\right]$

gain calculated assuming the ISI remains unchanged is not realistic, i.e., if (3.5) is used without accounting for the increase of ISI the gain would be higher in general. Using a higher rate code is one method of not increasing the ISI substantially although to obtain a significant amount of gain a long constraint length code which has a larger d_{free} may be necessary.

In the search for the best coder of a given rate it is important to keep in mind that the ISI used is that due to the increased channel rate.

3.3 Catastrophic Encoders:

Convolutional codes in general are divided into two main categories: catastrophic codes and noncatastrophic codes. In [6, 11, 20] properties of convolutional codes are described in detail. As the name implies catastrophic codes can produce an infinite number of decoding errors due to a finite number of channel errors. Massey and Sain [22] found the conditions for a code to be noncatastrophic. The channel they considered was a memoryless one. ISI channels, however have memory. Here it is shown that for finite memory channels the combined encoder and ISI trellis is still catastrophic whenever a catastrophic encoder is used. Note that for infinite ISI channels this may not be a problem depending on the impulse response.

Lemma:

The combined encoder and ISI trellis is catastrophic if the encoder used is catastrophic.

proof:

For a convolutional code to be noncatastrophic its generator polynomial matrix $\mathbf{G}(D)$ has determinants $\Delta_\ell(D)$, $\ell = 1,2,\ldots, \binom{n}{k}$ that satisfy

$$\mathrm{GCD}\left[\Delta_{\ell}(D)\ \ell=1,\ldots,\binom{n}{k}\right]=D^{a} \tag{3.8}$$

for some a [22].

When this condition is not met the trellis will have output sequences with finite weight for an input sequence(s) of infinite weight. This is illustrated in Figure 3.9 for a code of rate 1/2. Without loss of generality assume the length of ISI is 3. The paths in the ISI channel are shown in Figure 3.10. For the paths shown in the combined trellis the Euclidean distance does not increase after several intervals although the input sequences have an infinite weight. This would be same even if the ISI length is longer which implies that the combined trellis is catastrophic as well.

QED.

The above argument is also valid for the rate b/n codes as well. The reason is that for a catastrophic code after the first few intervals, there exists convolutional code output sequences that are the same. Thus in the ISI trellis the Euclidean distance does not increase. Hence the resulting ISI trellis is also catastrophic. Therefore only noncatastrophic codes have to be considered for the use in ISI channels. For wideband(infinite) channels the best convolutional code for a given rate and constraint length is usually considered to be one with the best free Hamming distance. Questions arise as to what would happen when the encoder and the ISI channel are combined; whether the best code still gives the best coded distance for any channel, what are the properties of the channel which gives the best distance; is it a maximum distance channel without coding? Some properties of the coded distance are discussed next to gain some insight into the above questions.

Encoder Matrix $G(D) = \begin{bmatrix} 1 & 1 & 0 \\ 0 & 1 & 1 \end{bmatrix}$

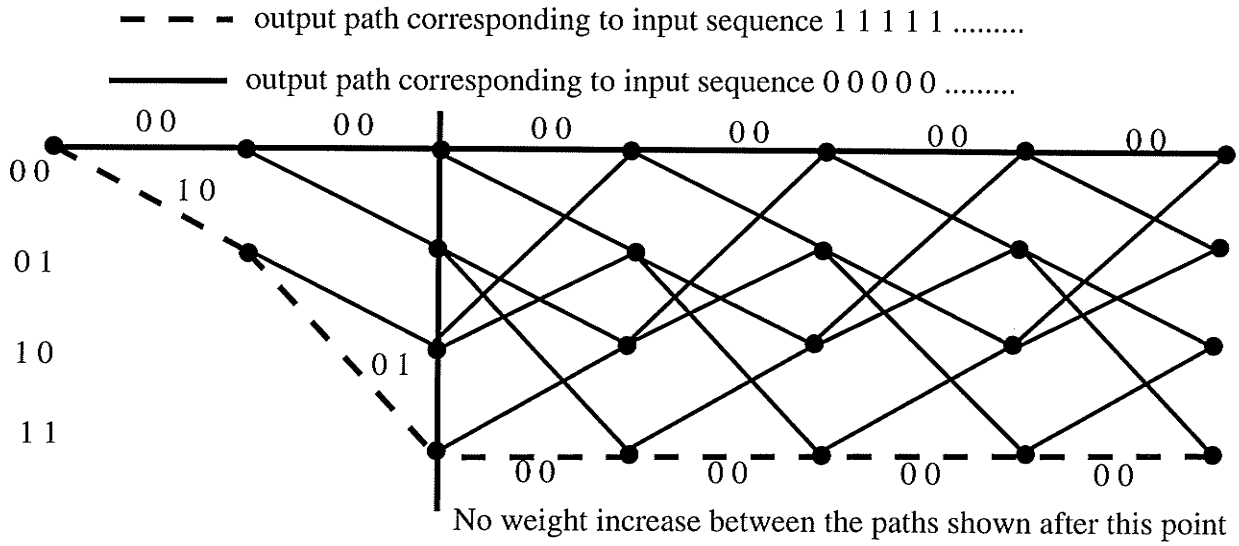

Figure 3.9. Trellis for a R=1/2 catastrophic code

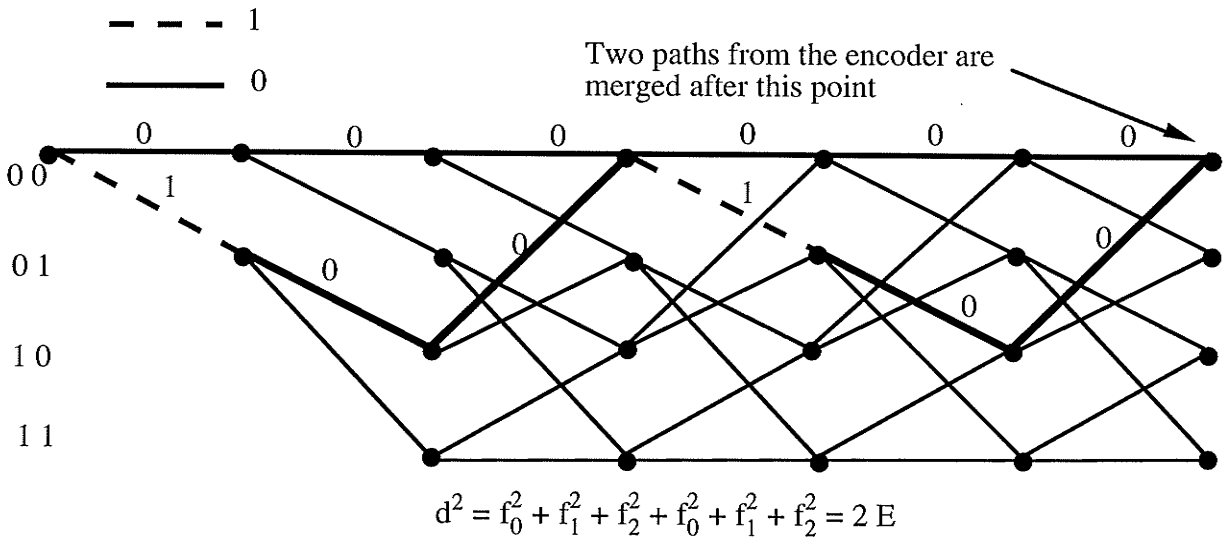

$$d^2 = f_0^2 + f_1^2 + f_2^2 + f_0^2 + f_1^2 + f_2^2 = 2E$$

Figure 3.10. ISI trellis for L=3 with paths from the encoder of Figure 3.9

3.4 Bounds for coded distance:

The channel response here is that of the coded channel where the rate increase due to the encoder is taken into consideration i.e., that the source rate is constant. With an encoder the output sequences form only part of the paths in the ISI trellis. Therefore the ISI trellis can be considered to be pruned to follow the paths that are allowed by the encoder. This is illustrated in Figure 3.11. Thus the coded ISI trellis is a pruned version of the original trellis and hence the coded distance is always larger than or equal to the minimum distance without coding. This can be stated as an upper bound.

$$(d^2_{min})_{uncoded} \leq (d^2_{min})_{coded} \tag{3.9}$$

To calculate the Euclidean distance, error sequences from the encoder need to be generated. This can be done by considering either the error events in the encoder trellis diagram or in general using a pair state diagram for the encoder to find all the possible error paths. Obviously not all the error paths are essential to find the minimum distance of the coded ISI trellis. The error sequences which have a Hamming weight equal to or close to the Hamming weight of the free distance of the convolutional encoder are more important since they have a better chance of giving the coded minimum distance.

As an example consider the encoder given in Figure 3.12. The set of error sequences with Hamming weight equal to the free distance of the code is given in Table 3.5 along with an expression for Euclidean distance for a channel of ISI length two. As seen from the table, for several sets of paths the squared distanceis of the form $d_{free}E \pm \gamma$ (E = channel energy). In general the squared coded distance is found to be less than $d_{free}.E$ or slightly higher. Thus based on the above discussion the following proposition is made for the

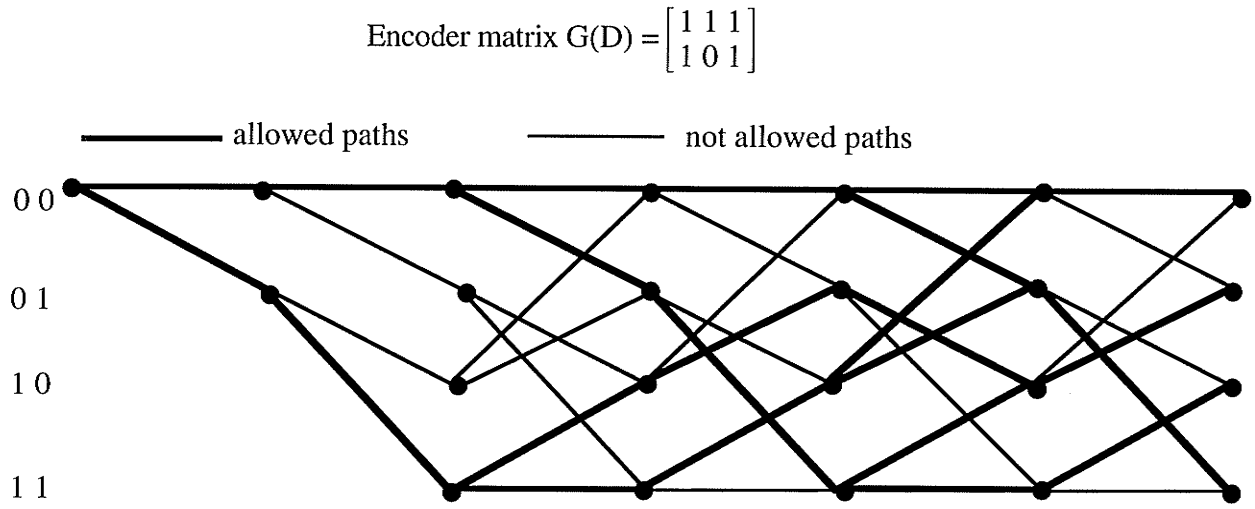

Figure 3.11. Paths allowed in the ISI trellis of L=3

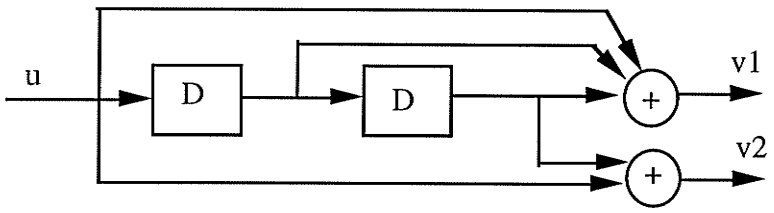

Figure 3.12. Encoder of the constraint length 2 best convolutional code

No.	Eror sequence	n_1	n_2	n_3
1	1 1 1 0 1 1	3	2	3
2	1 1 1 0 1 -1	1	2	1
3	1 1 1 0 -1 1	1	0	1
4	1 1 1 0 -1 -1	3	0	3
5	1 1 -1 0 1 1	1	-2	1
6	1 1 -1 0 1 -1	-1	-2	-1
7	1 1 -1 0 -1 1	-1	0	-1
8	1 1 -1 0 -1 -1	1	0	1
9	1 -1 1 0 1 1	-1	2	-1
10	1 -1 1 0 1 -1	-3	2	-3
11	1 -1 1 0 -1 1	-3	0	-3
12	1 -1 1 0 -1 -1	-1	0	-1
13	1 -1 -1 0 1 1	1	-2	1
14	1 -1 -1 0 1 -1	-1	-2	-1
15	1 -1 -1 0 -1 1	-1	0	-1
16	1 -1 -1 0 -1 -1	1	0	1

Table 3.5. Error sequences of shortest length. The Euclidean distance for each error sequence is $d^2 = 5E + n_1.(2f_0f_1) + n_2.(2f_0f_2) + n_3.(2f_1f_2)$ where n_1,n_2,n_3 are integers.

coded channel configuration given in Figure 3.3.

Proposition 3.1:

$$(d^2_{min})_{coded} \leq \left[(d_{free})_{cc} + \sigma\right]E \; ; \; \sigma \leq 1 \text{ usually.} \qquad (3.10)$$

where $(d_{free})_{cc}$ is the free Hamming distance of the convolutional code.

From this it can be inferred that the convolutional code with the best free distance would give the best coded distance. The specific channel or channels with this property are still to be found. To get the highest minimum distance upperbounded by the Hamming weight of the error sequence, the distance spread among the error sequences must be small. It is clear that for non maximum distance channels there are several paths with smaller distance. The reason is that the length of error events which determine the minimum distance can be up to 2(L-1) and for non maximum distance channels it is possible to have squared distances close to E (channel energy) for some of these paths. If they didn't have these paths then they would become maximum distance channels. But a good maximum distance channel with its small spread of distance would have squared distances close to (L-1)E for these paths. Therefore when an encoder is placed the maximum distance channels usually give the best coded distance. For the non maximum distance channels it is possible for the coder to pick up a path with less distance as there are usually several such paths and at least one path with smaller distance. It is also possible for a non maximum distance channel to give a better coded distance than some maximum distance channels. Still this distance is usually not the best coded distance possible for a given ISI length and for a given constraint length of the encoder. Based on the above discussion the following proposition is stated.

Proposition 3.2:

The channels that have best coded distances are in the set of maximum distance channels without coding.

3.5 Search for Good Codes:

Certain properties of the convolutionally coded ISI channels have been discussed up to now. Here a search is carried out to find out the best convolutional encoder of given constraint length and rate for a given ISI channel. In other words to match the code with the channel. It is impossible to obtain an analytical solution since there is no analytical method even to find the convolutional code with maximum free distance, hence the search. Some properties such as symmetry are used to limit the search.

Another issue is the coefficients of the ISI channel. Although a fixed energy constraint can be imposed, within that an infinite number of combinations may be possible. Hence the search has to be limited to certain set of channels. In literature the class of magnetic recording channels has been studied in detail. Here the search is carried out to find the best encoder for L=2 ISI channels and for some L=3 ISI channels.

3.5.1 A search method for a given channel:

The objective here is to find the best convolutional encoder of given constraint length and rate for a given ISI channel. A set of non catastrophic encoders are selected which usually is a subset of all the encoders possible satisfying the requirements given above. Of the total number of possible encoders, the ones with a Hamming weight in the set of

$$\left[(d_{free})_{best\ CC},(d_{free})_{best\ CC} - \gamma\right] \tag{3.11}$$

are selected for distance calculation. γ is chosen to include codes which could possibly give a better distance even though their free distances are less. In addition to this, symmetries in the encoders are used in order to reduce the amount of search. The symmetry exploited here is based on the following.

Assume there are two encoders G(D) and G'(D) of rate 1/n, constraint length v. If

$$g'_j(i) = g_{(n+1-j)}(v - i), \quad 1 \le j \le n, \; 0 \le i \le v \tag{3.12}$$

then the Euclidean distance from these two encoders when combined with an ISI channel will be the same. Aulin et al showed this for the CPM case [21]. Here a similar argument is made for the ISI channels.

proof:

Assume $\mathbf{u} = (\cdots,0,0,u_0,u_1,\cdots,u_k,\cdots)$ and $\mathbf{u}' = (\cdots,0,0,u'_0,u'_1,\cdots,u'_k,\cdots)$ are input sequences to the convolutional encoders G(D) and G'(D) respectively. If the condition given in (3.12) is satisfied and $u'_j = u_{k-j}$, the output sequences from the encoders v_j and v'_j where j=1,2,...,n are related by

$$v'_{ji} = v_{(n+1-j)(k+v-i)} \tag{3.13}$$

Thus the output sequence $\mathbf{v}'$ from the encoder G'(D) is a time reversed form of the output $\mathbf{v}$ from G(D). Therefore when the ISI trellis is considered output sequences from G'(D) make state merges which are only time reversed if G(D) is considered. Thus the Euclidean distances corresponding to these two encoders will be the same.

QED.

In the following L=2 and L=3 coded ISI channels are considered. Longer ISI lengths can also be considered, the limitation here being the complexity of the distance calculating algorithms and hence the time involved. By the same token long constraint convolutional codes also add to the complexity. Thus short constraint length codes of memory up to five are searched. For the L=2 channel first a formula is derived to show the general form of the distance curve. Search results are given next .

3.5.2 L=2 channels:

(Channel response is for the coded case)

The channel : $f_0 = \cos \alpha \quad f_1 = \sin \alpha$

Consider the v = 2 , R = 1/2 , $d_{free} = 5$ encoder given by [1 1 1, 1 0 1]. It produces the following error sequences of Hamming weight 5

a) 1 1 1 0 1 1 0 b) 1 -1 1 0 -1 1 0

$$d_a^2 = 5(f_0^2 + f_1^2) + 6f_0f_1 = 5 + 6f_0f_1 \qquad d_b^2 = 5(f_0^2 + f_1^2) - 6f_0f_1 = 5 - 6f_0f_1 \qquad (3.14)$$

Thus $d_{min}^2 \leq 5$ for with this coder achieving equality for the no ISI case. In general regardless of the encoder,

$$d_{Euc}^2 = d_{free} \pm nf_0f_1 \qquad (3.15)$$

here n is an integer multiple of 2 due to the expansion of squares.

But $$f_0f_1 = \sin \alpha.\cos \alpha = \frac{1}{2}\sin 2\alpha. \qquad (3.16)$$

therefore if $n = 2n_0$ then

$$d^2_{Euc} = d_{free} \pm n_0 \sin 2\alpha \qquad (3.17)$$

where n_0 is the adjacent pairs of 1's in the error sequence.

If error sequences other than the above are considered, one has

$$d^2_{min} = (d_H \pm n_0 \sin 2\alpha)_{min} \qquad (3.18)$$

where the minimum is taken over the set of possible candidates for the minimum Euclidean distance.

Some of the results of the search are given in Figures 3.13 - 3.16 for rate 1/2, 2/3 and 1/3 encoders. The rest are in Appendix B. The channel response is that of the coded channel. The corresponding uncoded channel is therefore an ISI free channel for rate 1/2 and 1/3 cases and a channel with one interference term for rate 2/3 codes. Convolutional codes of constraint lengths up to 5 are considered.

The following notation is used in the Figures.

R : code rate;

K : encoder constraint length , CC : Convolutional codes ;

L : Channel impulse response duration ;

Encoders are specified in terms of generator polynomial coefficients

R = 1/2 $[\mathbf{g}^{(1)}\ \mathbf{g}^{(2)}]$; R=1/3 $[\mathbf{g}^{(1)}\ \mathbf{g}^{(2)}\ \mathbf{g}^{(3)}]$

R = 2/3 Feed Back Encoders $[\mathbf{h}^{(2)}\ \mathbf{h}^{(1)}\ \mathbf{h}^{(0)}]$

All angles are given in degrees.

Coding gain = 10 Log $\left[\frac{Rd^2_{min}(coded)}{d^2_{min}(uncoded)}\right]$ dB, here $d^2_{min}(coded)$ takes the increase of ISI into account.

From the results the following observations may be made:

1) All the curves are parts of sinusoids and symmetric about the angle 45 degrees.

This can be explained using (3.18). Further from 90^0 - 180^0 the graphs are the same. Also at 45^0 the coding gain is always the lowest regardless of the encoder except for the case shown in Figure 3.15. The probable reason in this case is that the candidates for minimum distance are of the form

$$d^2_{min} = (d_H + n_0 \sin 2\alpha)_{min} \qquad (3.19)$$

and hence the distance curve has a maximum at $\alpha = 45^0$.

2) Highest coding gain is always at zero degrees, which is the ISI free situation.

Thus the presence of ISI degrades the gain here whereas without coding there is no loss in performance for L=2 channels.

3) Approximately between 30 - 50 degrees the encoder with the best d_{free} *does not give the highest coding gain for some constraint lengths.*

(see Figures 3.13, 3.14, 3.15 and 3.16) The encoder with the best d_{free} therefore, does not necessarily give the best performance for any ISI channel. This encoder always gives the best coding gain in the region close to the ISI free situation.

4) *It is also seen that for the cases considered here the upperbound given in proposition 3.1*

$$(d^2_{min})_{coded} \leq \left[(d_{free})_{cc} + \sigma\right]E \qquad (3.20)$$

holds with σ equal to zero except for the case shown in Figure 3.15 where σ is one.

The ISI free case usually achieves equality. Even for the case in Figure 3.15 the upperbound given by the encoder with best d_{free} holds with σ equal to zero.

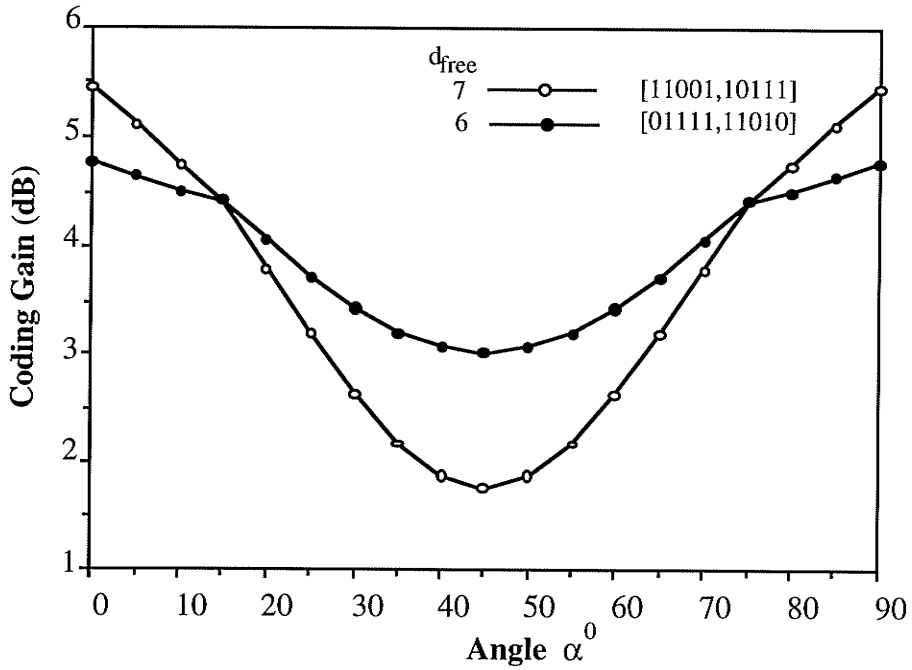

Figure 3.13. Coding gain with K=4, R=1/2 CC for L=2 ISI channel

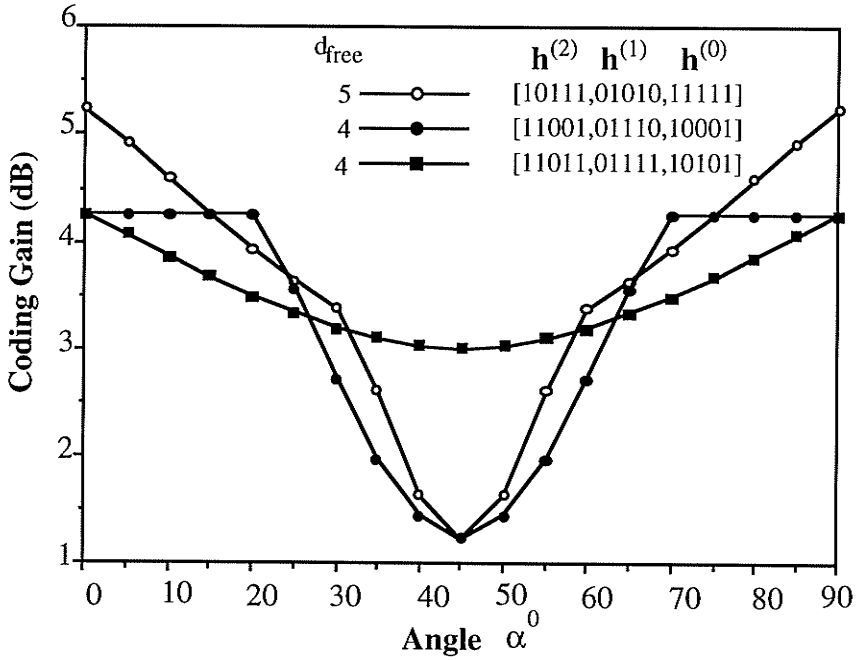

Figure 3.14. Coding gain with K=4, R=2/3 CC for L=2 ISI channel

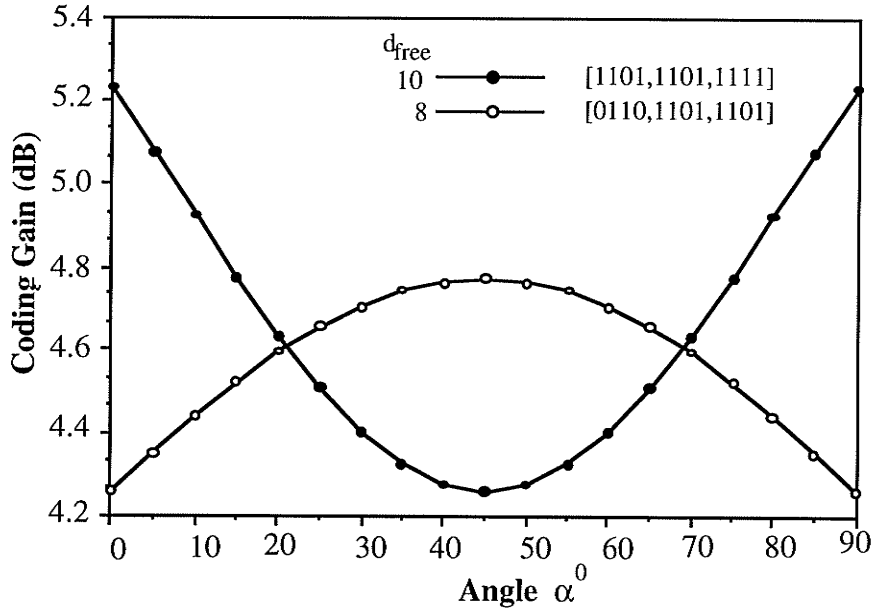

Figure 3.15. Coding gain with K=3, R=1/3 for L=2 ISI channel

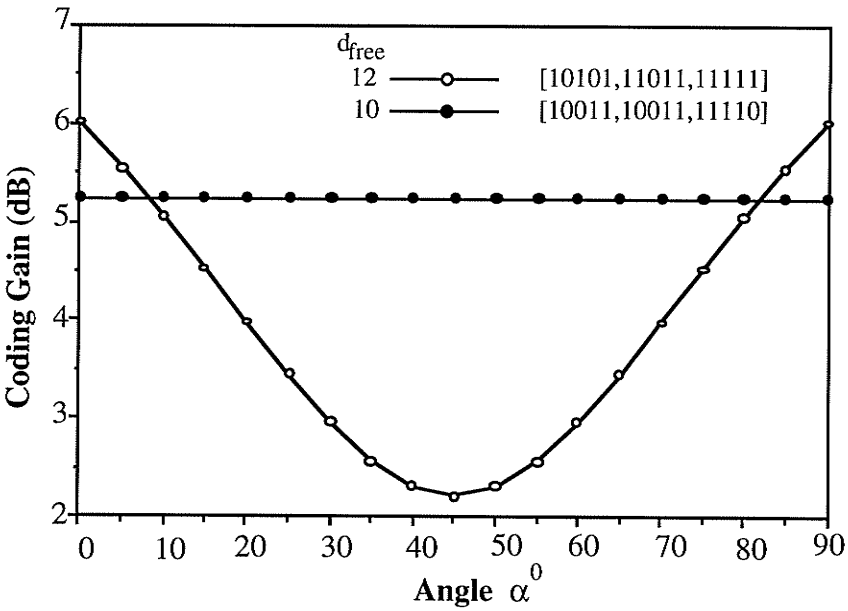

Figure 3.16. Coding gain with K=4, R=1/3 CC for L=2 ISI channel

3.5.3 L=3 channels:

The channel coefficients are expressed as

$$f_0 = \sqrt{E}\sin\alpha \qquad f_1 = \sqrt{E}\cos\alpha.\sin\beta \qquad f_2 = \sqrt{E}\cos\alpha.\cos\beta$$

so that the channel energy is fixed at E. Maximum distance regions for the channel considered here are as follows. Angles are given in degrees.

$\alpha = 10$; $\beta = 0$ to 25 ; 70 to 290 ; 335 to 360

$\alpha = 30$; $\beta = 0$ to 25 ; 85 to 275 ; 335 to 360

$\alpha = 60$; $\beta = 0$ to 360

The worst ISI channels are at $\alpha = 30^0$, $\beta = 55^0$ and $\beta = 315^0$.

Here rate 1/2 convolutional codes of constraint lengths up to 4 are considered. The corresponding uncoded channel for rate 1/2 codes is a L=1.5, a maximum distance ISI channel.

For this channel $d^2_{min}(\text{uncoded}) = 8.$

Since $$\frac{d^2_{min}(\text{uncoded})}{R} = 2d^2_{min}(\text{uncoded}) = 16$$

the $$\text{Coding gain} = \frac{d^2_{min}(\text{coded})}{16}.$$

Some of the results are given in Figures 3.17 and 3.18, the rest are in Appendix B. Squared Euclidean distance is plotted against the variation of angle β for a fixed value of angle α.

The following observations can be made:

1) As seen from all the graphs here, the encoder with the best d_{free} *does not necessarily give the best performance for all values of* β.

As an example consider the case shown in Figure 3.17. For β in range of 20^0 to 60^0 the code with $d_{free} = 5$ gives a smaller coded distance than those with $d_{free} = 4$. Many other examples can be seen by examining the Figures.

2) The highest coded distances are always given by the encoders with the highest d_{free} *values.*

Again this is the situation for all the cases considered here. Thus if the channel response can be modified, to obtain the largest coding gain the encoder with the best d_{free} may be used.

3) The highest coded distances are obtained by the maximum distance channels.

Consider Figure 3.17. The highest coded distance of approximately 38 is given by angles $\alpha = 10^0$ and $\beta = 100^0$. Channels in this region belong to the set of maximum distance channels. All figures give the same observation.

4) For some ranges of β *the coded distance is lower than 16 implying that for these cases there is no coding gain.*

Consider Figure 3.17. One of the regions in which the above happens is $\beta = 25^0$ to 60^0. The channels in this region are non maximum distance channels. The same holds for Figure 3.18 as well. Thus it can be argued that maximum distance channels give better coded distance in general. Another thing is that, as seen above, coding doesn't always improve the error performance. To obtain a gain for these channels an encoder with a large d_{free} and hence one with longer constraint length would probably be required.

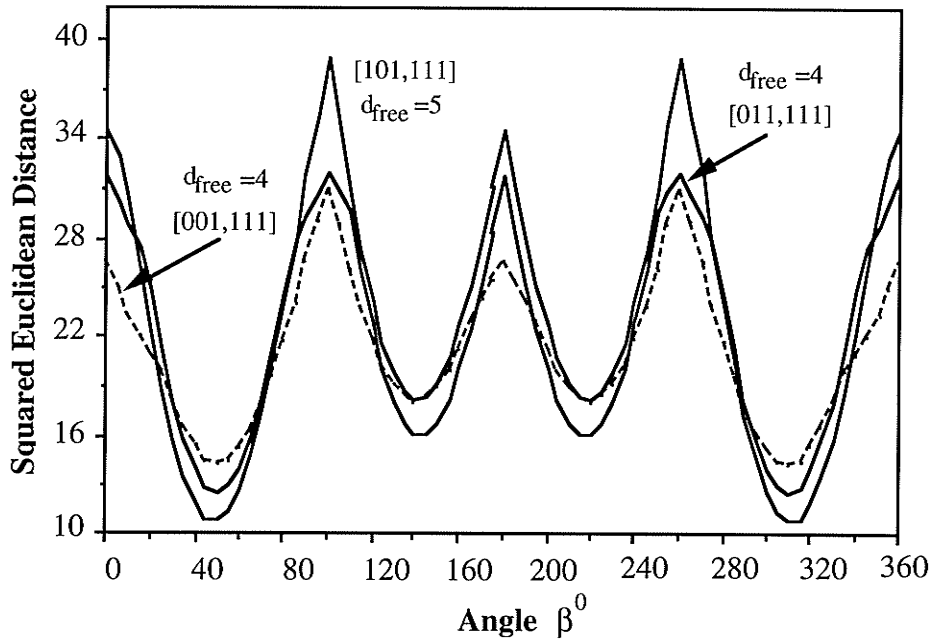

Figure 3.17. Coded distance with K=2, R=1/2 CC for L=3 ISI at Angle α=10

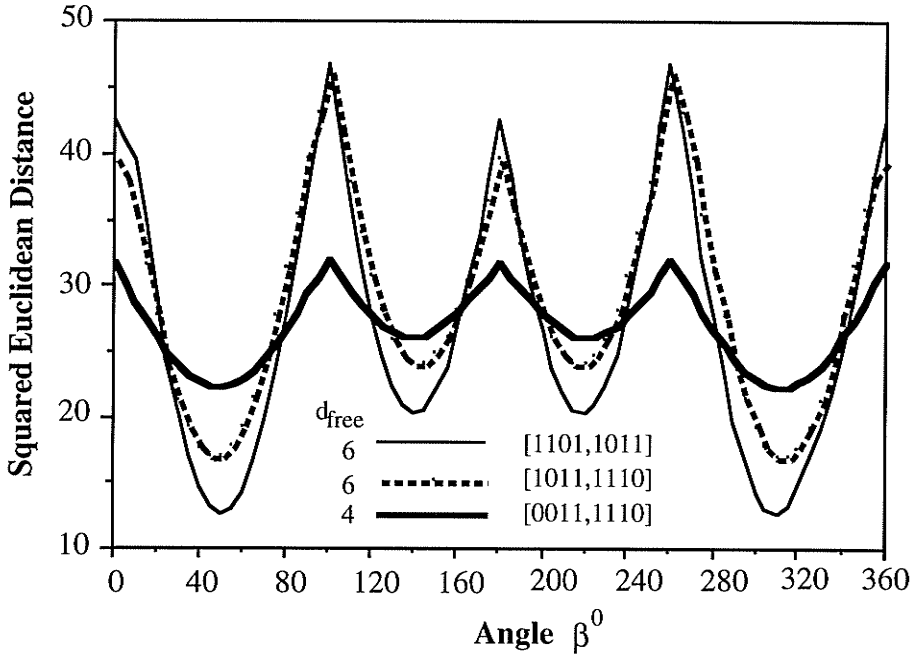

Figure 3.18. Coded distance with K=3, R=1/2 CC for L=3 ISI at Angle α=10

In conclusion, properties of ISI channels with convolutional encoded inputs have been considered in this chapter. Construction of the error state diagram or the pair state diagram for the channel/coder cascade is the first step in determining the coded Euclidean distance. Catastrophic convolutional coders produce catastrophic ISI trellises and therefore should be avoided. Without coding there is a unique upperbound, the channel energy, for the minimum Euclidean distance for ISI channels. Once coding is considered this upperbound is no longer valid, instead an upperbound related to both the free distance of the code and the channel energy is conjectured. Search results indicate that the encoder with the best free distance does not always give the best coded distance when combined with an ISI channel. On the other hand it usually gives the best coded distance possible for a given ISI length and a given constraint length of the coder. Another observation is that for the cases considered in the search, a particular encoder is usually best over a range of channel coefficients. Thus if the channel coefficients change by a small amount, the best encoder would still be the same. This is a good property specially because all channels change their characteristics over time.

Chapter 4
Trellis Coded Modulation for ISI

Trellis coded modulation (TCM) is generally used to achieve bandwidth efficiency while obtaining a higher noise margin [34]. Therefore an alternative to using a convolutional encoder for ISI channels is to use TCM techniques. A study of TCM schemes in general can be found in [5]. TCM signals usually have a quadrature component and an inphase component and these are modulated by a carrier. Hence the channel in this case is a bandpass channel. For the work presented here the equivalent baseband channel is considered. Unlike the convolutional code case where GF(2) operations are involved, here only Euclidean space is present. Hence, in loose terms, some form of continuity is preserved when TCM and ISI is combined.

The main objective is to discuss the properties of the TCM coded channels and find the best encoders for several ISI channels along the same lines as described in chapter 3. A brief survey of some of the work in this area is given first followed by a description of the communication system used. Calculation of Euclidean distance for the TCM coded trellis and methods to simplify the trellis structure are considered next. Finally a search for good TCM encoders is carried out for several ISI channels. A comparison of their coding gain against another alternative scheme is made to obtain insight into the application of coded modulation for ISI channels. Analogies drawn from the application of convolutional codes are discussed as well.

4.1 Background:

Wolf and Ungerboeck [37] discussed the application of trellis codes based on the set partitioning idea developed in [34]. The channel considered was a (1 - D) channel.

All possible noiseless channel outputs of a certain length were grouped into a number of sets. Using these sets a trellis code was found. By using longer lengths of channel outputs larger values of d^2_{min} can be obtained. Several other papers considered the same channel model with TCM [14,18,31].

Performance bounds and distance spectra for certain trellis codes in ISI are given in [30]. There it is shown that if quasiregular TCM codes are used for ISI channels the complexity for distance calculations is reduced. Larsson [19] uses this idea to find the worst case ISI channels for certain TCM schemes. Chevillat [10] describes decoding the trellis encoded signal in the presence of ISI using reduced state sequence detection(RSSD). Wong and McLane [40] considered the error performance of trellis codes for a class of equalized channels. Extensions from these results are worthwhile to investigate since it should provide more insight to the problem of matched TCM codes to ISI channels.

4.1.1 Communication system:

A block diagram of a bandlimited channel with a TCM encoder is shown in Figure 4.1. Here the channel can be thought of as the baseband equivalent of the band pass channel for the carrier modulated signals. In general it is a complex channel. Signals can be represented by a sequence of complex numbers (x) from the encoder sent to the channel. The channel output depends on the state of the encoder and the present information input, usually a binary vector.

The output of the channel, using the discrete equivalent system can be given by

$$y_k = \sum_{i=0}^{v} f_i x_{k-i} \quad ; \quad x_i \text{ 's are complex.} \qquad (4.1)$$

where v is the length of ISI and f_i's are coefficients of the discrete channel response.

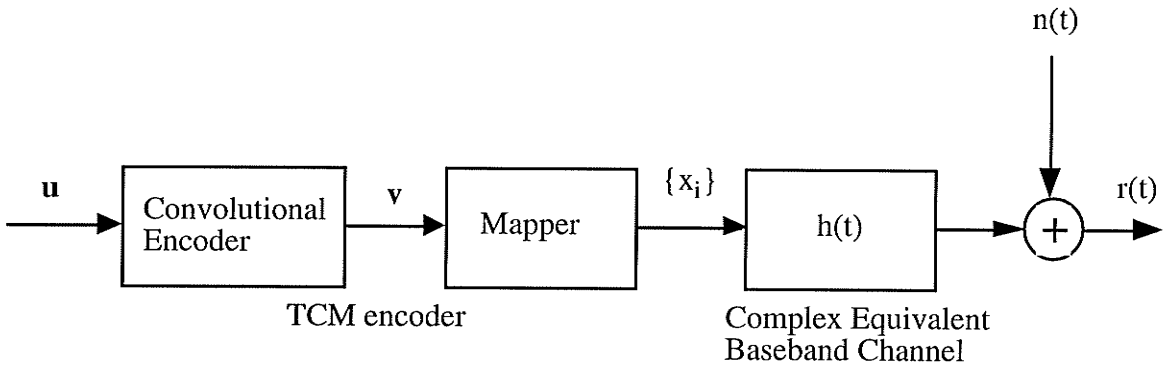

Figure 4.1. Transmitter side of a TCM system

$$x_k = g(\mathbf{u}_k, \mathbf{S}_k) \tag{4.2}$$

where $\mathbf{u}_k$ is the input vector and $\mathbf{S}_k$ is the encoder state vector. g(.) is the mapping from the binary output of the encoder to the complex channel signal.

Two typical encoders and the corresponding channel signal alphabets are shown in Figure 4.2. A definition for coding gain is given below which will be used throughout this chapter. It is the same as that given in [15].

Definition:

The asymptotic coding gain $$G \equiv \frac{(d^2_{min}/ P_{av}) \text{ coded}}{(d^2_{min}/ P_{av}) \text{ uncoded}} \tag{4.3}$$

where is d^2_{min} is the overall minimum distance and P_{av} is the average transmitted power. The reason for dividing by P_{av} is that with TCM the signal set is usually expanded. This results in a larger P_{av} thus requiring normalization to compare the coded and uncoded cases fairly. For PSK schemes P_{av}, the average transmitted power does not change whereas for other schemes such as PAM, P_{av} of the uncoded and coded signal sets are different.

When the constraint length of the convolutional coder in TCM is large the number of states in the combined coded trellis becomes very large. Thus the computational complexity of the distance calculating algorithms becomes much higher. To avoid this to a certain degree some properties of the encoder can be used. It is shown [19,30] that if the coded trellis is quasiregular then the complexity of the distance calculation can be reduced by a significant amount. The next section discusses quasiregularity as applied to various signal sets.

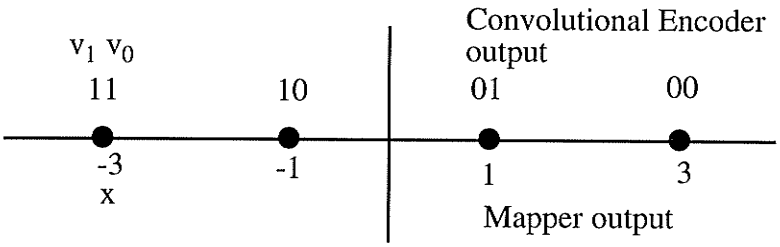

Figure 4.2(a). 4-PAM Mapping

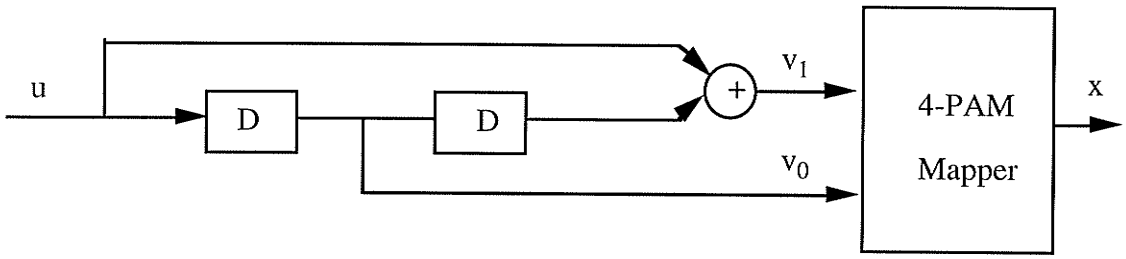

Figure 4.2(b). Four state, 4-AM convolutional encoder and mapper

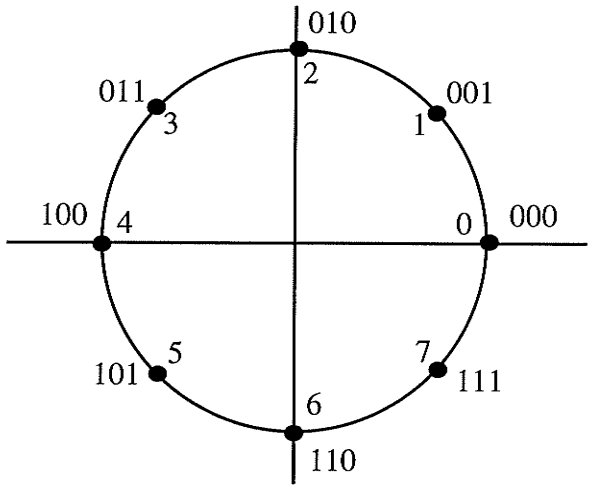

Figure 4.2(c). 8-PSK signal set

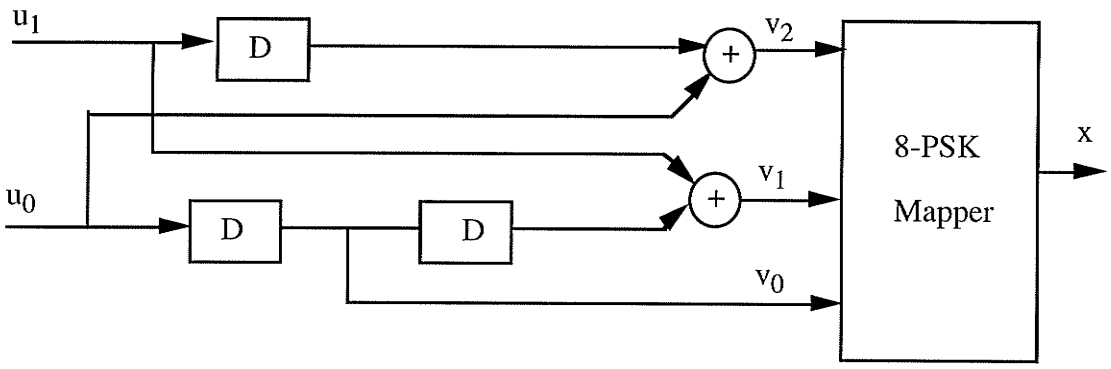

Figure 4.2(d). Ungerboeck encoder for 8-PSK, eight state

4.2 Quasiregularity in TCM encoders:

To calculate the minimum Euclidean distance for a TCM encoder combined with an ISI channel, all pairs of input sequences have to be considered in general. In other words a state pair diagram for the encoder has to be used. Hence the computational complexity of the distance calculation depends on the square of the number of states of the encoder. However by confining the encoders to have a special configuration the distance evaluation can be simplified considerably.

Recently Schlegel [30] introduced the concept of quasiregularity as applied to ISI channels using an Ungerboeck type PSK encoder as an example. A similar approach to PAM and QAM coders in ISI using the same convolutional coder configuration is considered here. Finally the reduction of complexity in the coded trellis using quasiregularity is discussed [19].

4.2.1 Set partition of PAM Encoders with Feedback Convolutional Coders:

The signal mapping for a 4 - PAM trellis code is given in Figure 4.3 and the configuration of the encoder is given in Figure 4.4. All the trellis states S are equivalent to one of two states which can be represented by the contents of the last delay cell S^1. If $S^1 = 0$ then $S \equiv 0$ and if $S^1 = 1$ then $S \equiv 1$. When $S^1 = 0$ the signals marked " A " are possible and when $S^1 = 1$ signals marked " B" are possible. The output from the convolutional encoder can be represented by $v_r = \left(u_r , S_r^1\right)$ due to the feedback representation. Hence the difference symbols can be given by $\mathbf{e} \equiv (e_u , e_S)$. Consider the distance polynomial defined by

$$P_{S,\mathbf{e}}(X) = \sum_{u} p(u)\, X^{\mu(v,\hat{v})} \qquad (4.4)$$

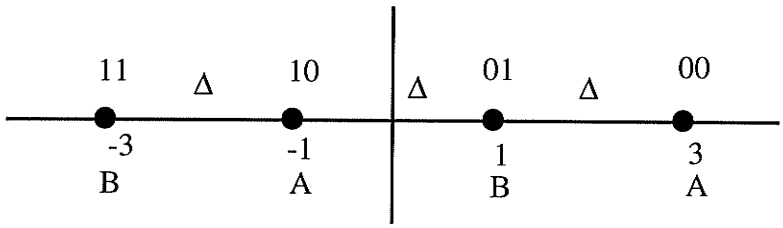

Figure 4.3(a). Signal mapping for 4 - PAM

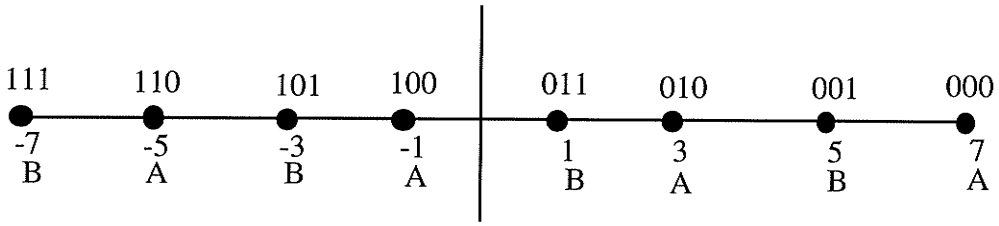

Figure 4.3(b). Signal mapping for 8 - PAM

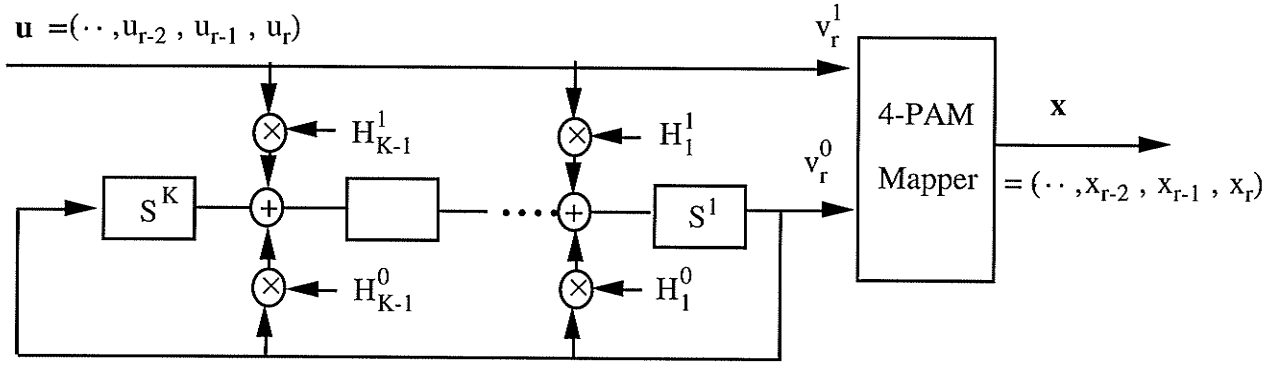

Figure 4.4. PAM Encoder Feedback Realization

where $\mu(v , \widehat{v})$ represents the difference signal and p(u) is the probability of the input signal u. $P_{S , e}(X)$ is a list of all the distances $\mu(v , \widehat{v})$ that can be generated when the correct path is in S, the incorrect path is in state $\widehat{S}$ and the two branch labels differ by **e**. Here the ISI channel is not taken into consideration. For the example given in Figure 4.3(a) $P_{S , e}(X)$ can be expressed as follows.

$$P_{(0 , 0)}(X) = X^{0} \tag{4.5}$$

$$P_{(0 , 1)}(X) = \frac{1}{2} X^{\Delta} + \frac{1}{2} X^{-\Delta} \tag{4.6}$$

$$P_{(1 , 0)}(X) = \frac{1}{2} X^{2\Delta} + \frac{1}{2} X^{-2\Delta} \tag{4.7}$$

$$P_{(1 , 1)}(X) = \frac{1}{4} X^{\Delta} + \frac{1}{4} X^{-\Delta} + \frac{1}{4} X^{3\Delta} + \frac{1}{4} X^{-3\Delta} \tag{4.8}$$

Note in the above equations S is not included since the right hand side is independent of whether $S^1 = 0$ or 1. Thus for this type of PAM encoders the distance polynomials do not depend on the equivalent state of S. In general if the sequence of equivalent states along a path does not have memory, i.e. there are "no" sequences of equivalent states 0 , 1 that cannot be traced by any path through the trellis, then the difference symbols can be generated using the encoder error state diagram. This means that the coder is quasiregular. Thus it is not necessary to consider a state pair diagram to calculate the difference symbols which are required to calculate the Euclidean distance in an ISI trellis. The procedure given above can be generalized in the following lemma for M - PAM encoders.

Lemma:

For an M - PAM encoder which produces a **Z** / 2**Z** partition, all sequences of equivalent states are possible, making it quasiregular, if and only if the input sequences

are independent and identically distributed.

Proof:

If it can be shown that $P_S(e_u, e_S)$ for $e_S = 0$ is independent of S then the code is quasiregular. e_S can be zero if the equivalent states are either 1, 1 or 0, 0. The equivalent state is given by the rightmost bit of the binary representation of the signal. Two signals with the same rightmost bit, have a difference that is an integer multiple of 2Δ (see Figures 4.3(a) and 4.3(b)) since the signals are represented in binary format (from right to left). For a given difference $2n\Delta$ (n - integer) the modulo sum of any two states e_u for $e_S = 0$ is the same. Thus $P_S(e_u, 0)$ is independent of S. Hence the code is quasiregular. On the other hand if the code is quasiregular then all $P_S(e_u, e_S)$ are independent of S and this implies that input sequences are independent as S is dependent on the input as well.

4.2.2 Set partition of QAM Encoders with Feedback Convolutional Coders:

Consider the signal mapping given in Figure 4.5 and the encoder type shown in Figure 4.6. Using the same notation as before $P_S(e_u, e_S)$ for two of the states are given below.

$$P_{0\,(001\,,\,0)}(X) = \frac{1}{2}X^{\Delta_1} + \frac{1}{2}X^{-\Delta_1} \qquad (4.9)$$

$$P_{1\,(001\,,\,0)}(X) = \frac{1}{2}X^{\Delta_2} + \frac{1}{2}X^{-\Delta_2} \qquad (4.10)$$

It is seen from the above equations that the distance polynomials $P_S(001\,,\,0)$ depend on the equivalent state of S ($\Delta_1 \neq \Delta_2$), i.e. for these cases the possible distances depend on whether the correct path passes through a state $S \equiv 0$ or $S \equiv 1$. Hence QAM encoders of the type given in Figure 4.6 are not quasiregular with respect to Δ_r, the difference

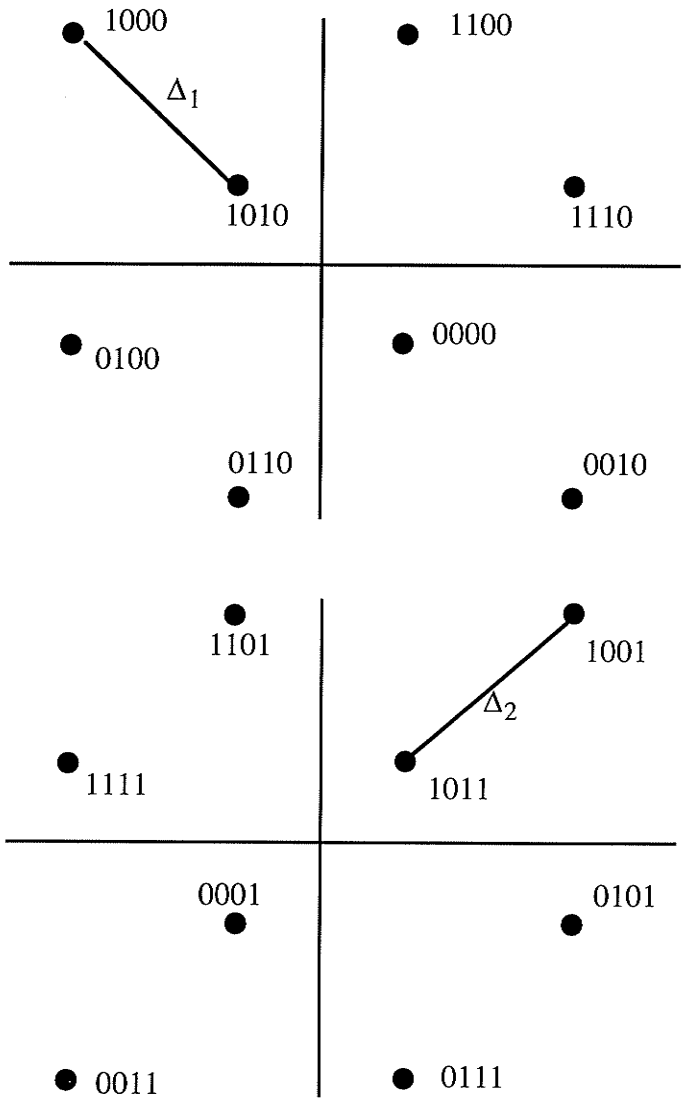

Figure 4.5. Signal mapping for QAM

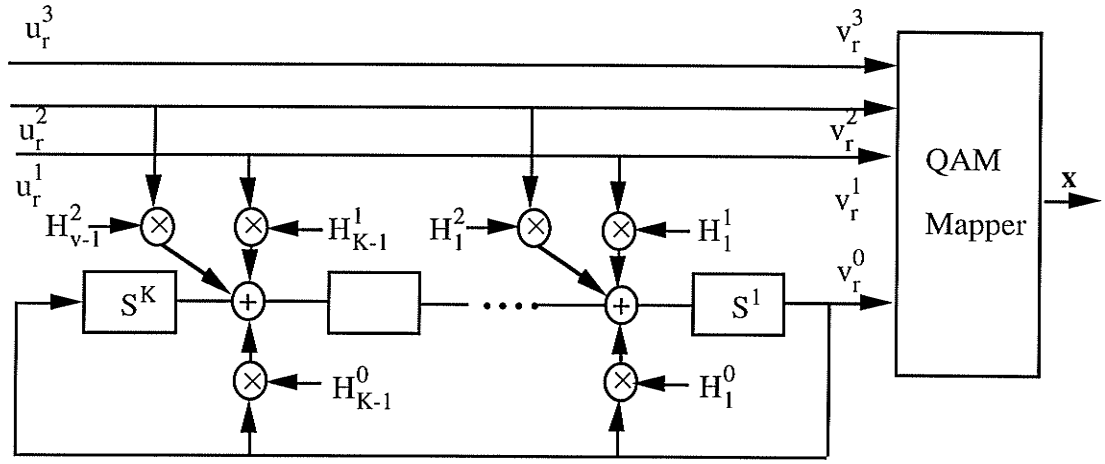

Figure 4.6. QAM Encoder Feed Back realization

symbol. To combine the two equations the equivalent states should be equiprobable. This is the same situation encountered in the case of PSK encoders [30]. Therefore the same conditions on the encoder can be imposed to make it quasiregular. i.e. to be quasiregular all equivalent states have to be possible and occur with equal probability. The conditions can be stated in the following lemma similar to the one given for PSK encoders in [30].

Lemma:

If at least one of the connections H_1^1 , H_1^2 is present in the feedback realization of the encoder then the resulting code is quasiregular. Usually for QAM coders at least one input is uncoded. Thus one of the remaining connections H_1^1 , H_1^2 must be present for the quasiregularity.

Proof:

If $H_1^1 = 1$ and $H_1^2 = 0$, the last delay cell which determines the equivalent state toggles half the time depending on whether $u_r^1 = 0$ or 1. Similarly with $H_1^1 = 0$ and $H_1^2 = 1$ the delay cell toggles with $u_r^2 = 0$ or 1. When $H_1^1 = 1$ and $H_1^2 = 1$ their binary sum $H_1^1 \oplus H_1^2$ will be 0 or 1 with equal probability and hence the equivalent state is equiprobable. On the other hand if $H_1^1 = 0$ and $H_1^2 = 0$ the equivalent state depends entirely on the preceding state.

4.2.3 Simplification of the trellis structure using quasiregular encoders:

From Chapter 2, for an ISI channel of memory v the Euclidean distance in terms of the difference symbols can be given by

$$d_n^2(\varepsilon) = d_{n-1}^2(\varepsilon) + \delta_n^2(\varepsilon_n, \varepsilon_{n-1}, \cdots, \varepsilon_{n-v}) \qquad (4.11)$$

where

$$\delta_n^2 = \sum_{i=0}^{v} \left| f_i \, \varepsilon_{n-i} \right|^2 \qquad (4.12)$$

$(\varepsilon_{n-1}, \cdots, \varepsilon_{n-v})$ defines the difference state.

Since there is an encoder in front, to generate the difference symbols it is usually necessary to consider all sequences of encoder state pairs $(\xi_n , \hat{\xi}_n)$. Thus the joint encoder and channel error state can be considered as

$$\Delta\sigma = (\xi_n , \hat{\xi}_n , \varepsilon_{n-1}, \cdots, \varepsilon_{n-v}) \qquad (4.13)$$

But for a quasiregular code instead of $(\xi_n , \hat{\xi}_n)$, the encoder error state diagram $(\Delta\xi_n)$ can be used.

Therefore $$\Delta\sigma = (\Delta\xi_n, \varepsilon_{n-1}, \cdots, \varepsilon_{n-v}) \qquad (4.14)$$

and the number of error states grow linearly with respect to S_c, the number of states in the encoder. The encoder error state diagram for the encoder of Figure 4.7 is given in Figure 4.8.

For the uncoded case there is no encoder , that means that input is directly mapped to a channel signal. Then the channel signals are independent and equiprobable. The ISI trellis has all possible channel sequences determined by the signal alphabet. Once the encoder is placed, out of all these possibilities only certain paths are allowed. The new trellis can be considered as a pruned version of the original trellis similar to the situation described in chapter 3. The next section discusses the calculation of Euclidean distance using the pruned trellis for a channel with one ISI term.

4.3 Calculation of Euclidean distance in the coded ISI trellis:

The TCM schemes considered here are either one or two dimensional schemes.

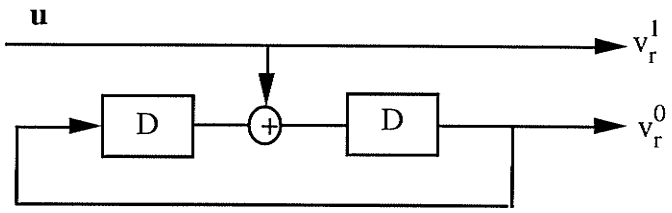

Figure 4.7. Four state PAM encoder

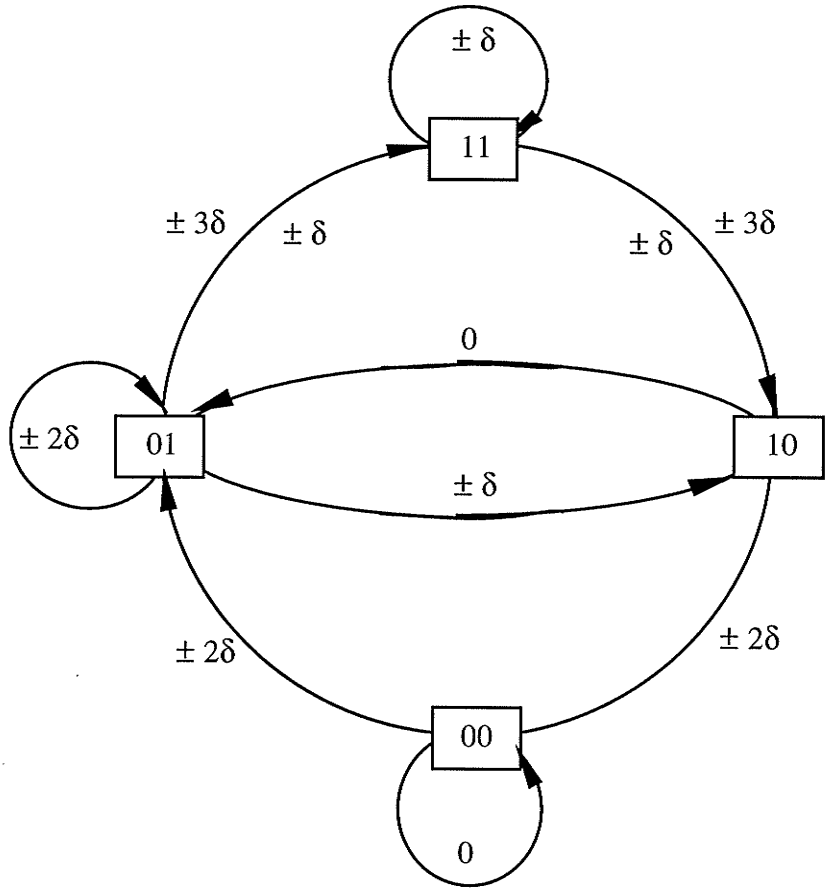

Figure 4.8. Encoder error state diagram

Consider an ISI channel of length one. i.e. L=2. The channel output from the equivalent discrete system is given by

$$y_k = f_0 x_k + f_1 x_{k-1} \tag{4.15}$$

where $$f_0 = a_1 + jb_1 \ , \ f_1 = a_2 + jb_2. \tag{4.16}$$

The difference output signal is then

$$y_k - \hat{y}_k = f_0(x_k - \hat{x}_k) + f_1(x_{k-1} - \hat{x}_{k-1}) \tag{4.17}$$

$$= (a_1+jb_1)(p_1+jq_1) + (a_2+jb_2)(p_2+jq_2) \tag{4.18}$$

where (p_1+jq_1) and (p_2+jq_2) are channel difference symbols.

$$|y_k - \hat{y}_k|^2 = (a_1^2+b_1^2)(p_1^2+q_1^2) + (a_2^2+ b_2^2)(p_2^2+q_2^2)$$

$$+ 2(a_1a_2+b_1b_2)(p_1p_2+q_1q_2) + 2(a_1b_2-b_1a_2)(q_1p_2-p_1q_2) \tag{4.19}$$

Now if, $a_1 = r \sin\alpha\sin\beta \quad b_1 = r \sin\alpha\cos\beta$ (4.20)

$a_2 = r \cos\alpha\sin\theta \quad b_2 = r \cos\alpha\cos\theta$ and $r = \sqrt{E}$ (4.21)

to satisfy the channel energy constraint, then

$$|y_k - \hat{y}_k|^2 = r^2\sin^2\alpha(p_1^2+q_1^2) + r^2\cos^2\alpha(p_2^2+q_2^2) + r^2\sin2\alpha\cos\gamma(p_1p_2+q_1q_2)$$

$$+ r^2\sin2\alpha\sin\gamma(q_1p_2-p_1q_2) \tag{4.22}$$

where $\gamma = \beta - \theta$. For real channels $\beta = \theta = \pi/2$. (4.23)

To obtain the channel difference symbols the encoder state diagram has to be used. For a valid error sequence in the ISI trellis, two sequences must start from one state of

the encoder state diagram and subsequently merge into an encoder state after several error symbols. That means it should also be an error sequence in the encoder state diagram.

As an example consider an error event (ε_1 , ε_2 , ε_3) of length 3 in the encoder state diagram . The corresponding error event in the ISI trellis is (ε_1 , ε_2 , ε_3, 0).

$$\text{Let } \varepsilon_1 = p_1 + jq_1 \ , \ \varepsilon_2 = p_2 + jq_2 \ , \ \varepsilon_3 = p_3 + jq_3. \tag{4.24}$$

Using the equation (4.22) repeatedly, it can be shown that

$$d^2 = \sum_{i=1}^{3} (p_i^2+q_i^2) +[p_2(p_1+p_3)+q_2(q_1+q_3)]\sin 2\alpha\cos\gamma+[q_2(p_1-p_3)-p_2(q_1-q_3)]\sin 2\alpha\sin\gamma \tag{4.25}$$

Equations of this form can be obtained for longer ISI lengths in a similar manner. The increase in the number of terms however makes them difficult to analyze.

For a real channel $\gamma = 0$. Therefore

$$(d^2)\text{ real} = \sum_{i=1}^{3} (p_i^2+q_i^2) +[p_2(p_1+p_3)+q_2(q_1+q_3)]\sin 2\alpha \tag{4.26}$$

Thus depending on the difference symbols

$$(d^2)\text{real} = \sum_{i=1}^{3} (p_i^2+q_i^2) \pm |[p_2(p_1+p_3)+q_2(q_1+q_3)]|\sin 2\alpha \tag{4.27}$$

Longer error events will also have the same general form for this channel. For the encoder trellis shown in Figure 4.9 the two shortest error events are indicated. One is a parallel path which governs the minimum distance for the no ISI case. From the trellis diagram the following distances can be obtained.

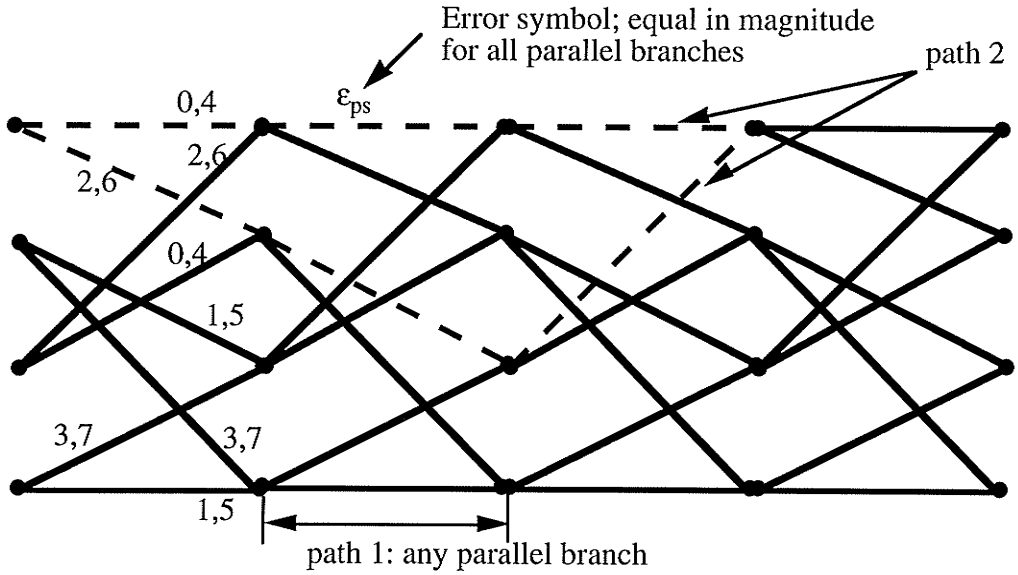

Figure 4.9. Encoder trellis diagram for the 8-PSK signal alphabet shown in Fig. 4.2(c) with signal labels

$$d_1^2 = 4 \tag{4.28}$$

$$d_2^2 = (6 - \sqrt{2}) \pm 2\sin 2\alpha \tag{4.29}$$

The minimum distance of the combined encoder and channel is governed by the distances given above. As can be seen it is upperbounded by the ISI free minimum distance d_1^2. For encoder trellises with parallel branches the following lemma can be stated.

Lemma:

If there are parallel branches in the encoder trellis then let the difference symbol with the smallest magnitude in a parallel branch be denoted by ε_{ps}. Then the minimum distance of the combined encoder and the ISI channel satisfies the following inequality regardless of the length of ISI.

$$d_{min}^2 \leq |\varepsilon_{ps}|^2 \left(\sum_{i=0}^{v} |f_i|^2 \right) \tag{4.30}$$

Proof:

After error symbol ε_{ps}, it is possible to have a sequence of '0' error symbols in the TCM trellis. i.e., ε_{ps},0,0,...,0 which defines a merged error event in the ISI trellis. The distance for this error event is given by the right hand side of the above equation. This is illustrated in Figure 4.10.

QED.

From the above discussion it can be seen that the coded distance for a real channel of ISI length one satisfies the following relationship.

$$d_{\text{coded-ISI}}^2 = d_{\text{coded-No ISI}}^2 + A\sin 2\alpha \tag{4.31}$$

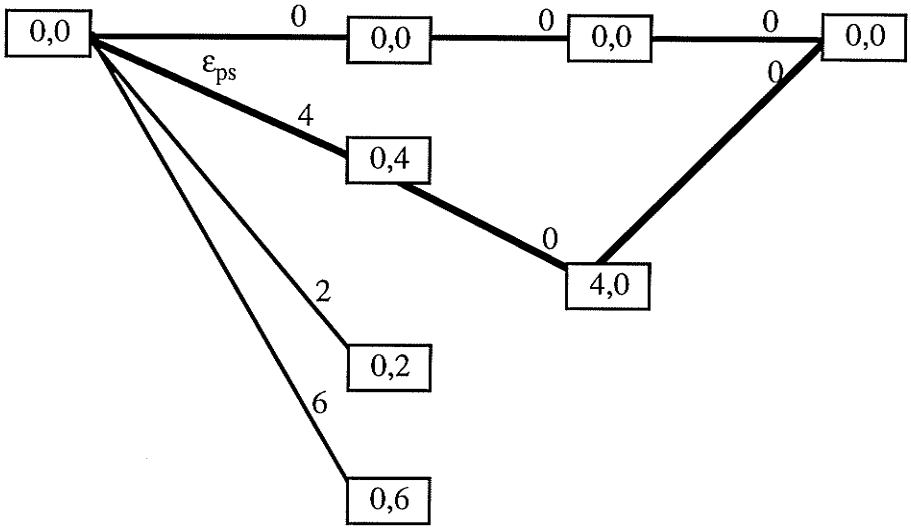

Figure 4.10. ISI trellis diagram for the trellis encoded signals showing an error event due to a parallel branch

where A is a real constant and A = 0 for parallel branches regardless of the ISI in channel.

For the minimum distance path in the encoder trellis this usually turns out to be

$$d^2_{\text{coded-ISI}} = (d^2_{\text{min}})_{\text{coded-No ISI}} \pm A\sin 2\alpha. \tag{4.32}$$

Therefore for these ISI channels

$$(d^2_{\text{min}})_{\text{coded-ISI}} \leq (d^2_{\text{min}})_{\text{coded-No ISI}}. \tag{4.33}$$

Circumstances under which the relationship in (4.33) holds, must be investigated further, specially for longer ISI lengths.

4.4 Search for TCM encoders matched to the ISI channel

Using quasiregular encoders, a search for the best encoder has been carried out for different TCM schemes (PAM, PSK & QAM). The ISI channel considered is a real-valued L=2 channel. A longer ISI length can also be used with a resultant increase in the computational complexity as indicated in (4.14). TCM coders of constraint lengths up to 6 were considered. The source code for the search was written in FORTRAN and implemented on SUN SPARC computers. Encoders are given in terms of coefficients $[\mathbf{H}^m, \ldots, \mathbf{H}^0]$, m represents the number of coded inputs. Algorithms for converting convolutional codes from feedback to feedforward form and vice versa are given in [25]. A typical encoder is given in Figure 4.11. Some of the results are given in Figures 4.12 - 4.15 with the coding gain as defined in section 4.1. The rest of the results are in Appendix B.

Notation for Figures:

The channel : $f_0 = \cos \alpha$ $f_1 = \sin \alpha$

K : constraint length of the encoder

L : length of channel impulse response

All angles are given in degrees.

The following observations may be made.

1) As shown in section 4.3 all the curves are parts of sinusoids and symmetric about the angle 45^0.

Always at 45^0 the coding gain is the lowest regardless of the encoder.

2) Highest coding gain is always at zero degrees, which in essence is the ISI free situation.

Thus the presence of ISI degrades the gain here as it did in the case of convolutional coding. For the coder given in Figure 4.15 the coding gain is constant regardless of the ISI because for these two cases the minimum distance is governed by the parallel paths in the encoder.

3) Approximately between 30 - 60 degrees the encoder with the best Euclidean distance for ISI free case does not give the highest coding gain.

(see Figures 4.12, 4.13, 4.14, 4.15) Thus the encoder with the best d^2_{EUC} without ISI does not necessarily give the best performance for any ISI channel.

The above observations are essentially the same as those seen with convolutional codes for the same ISI length.

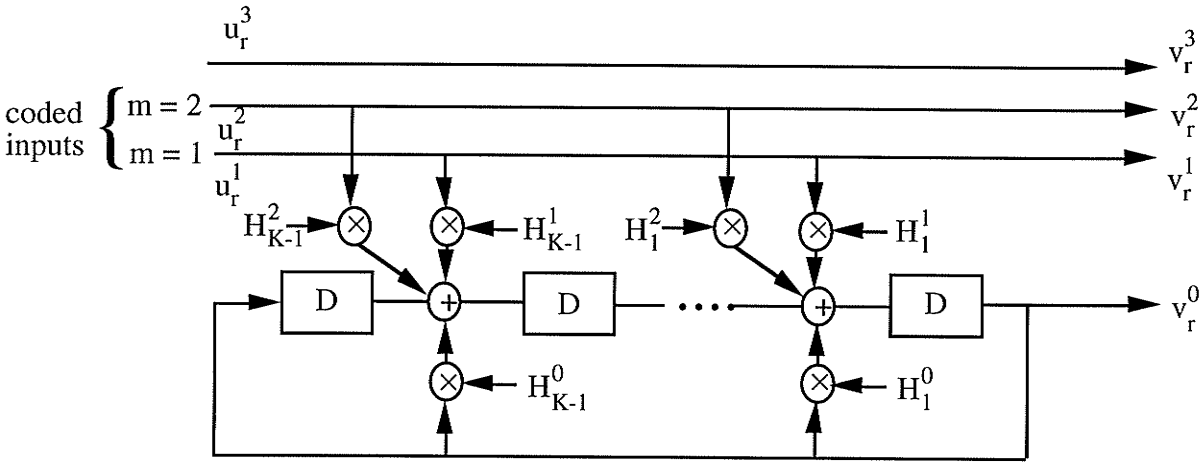

Figure 4.11. A typical convolutional encoder used in different TCM schemes

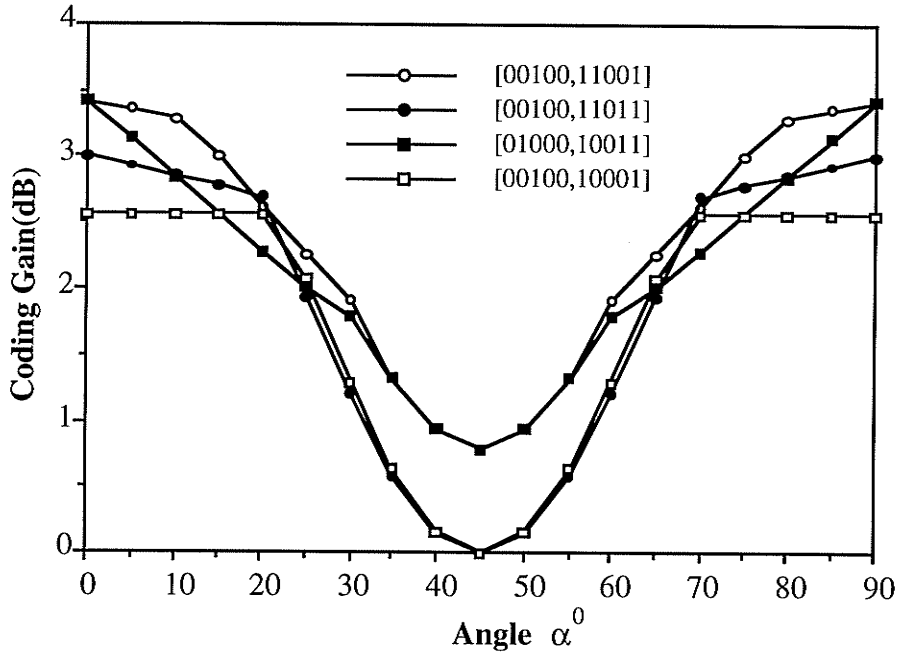

Figure 4.12. Coding gain with K=4, 4 PAM for L=2 ISI channel

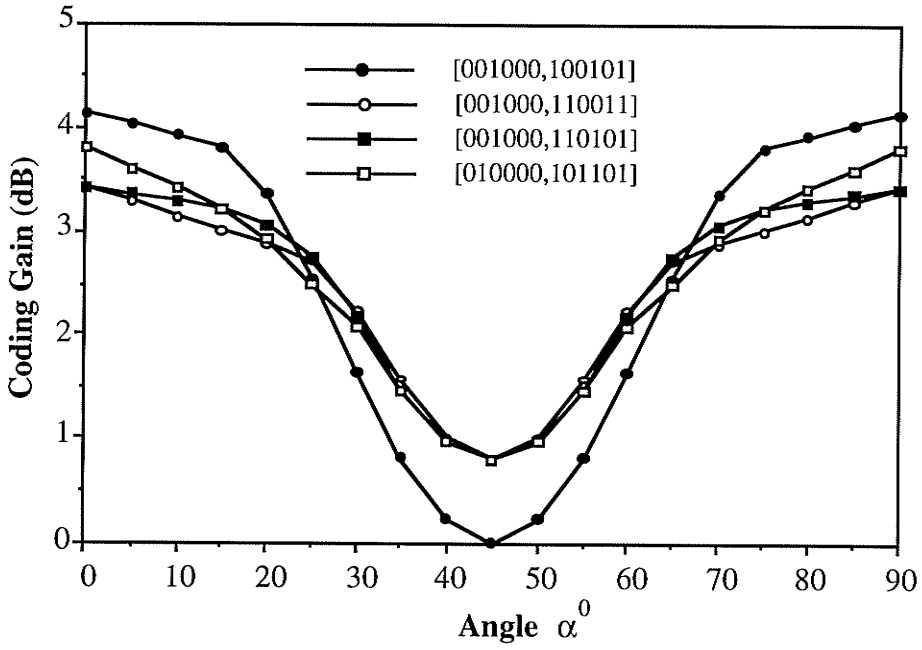

Figure 4.13. Coding gain with K=5, 4 PAM for L=2 ISI channel

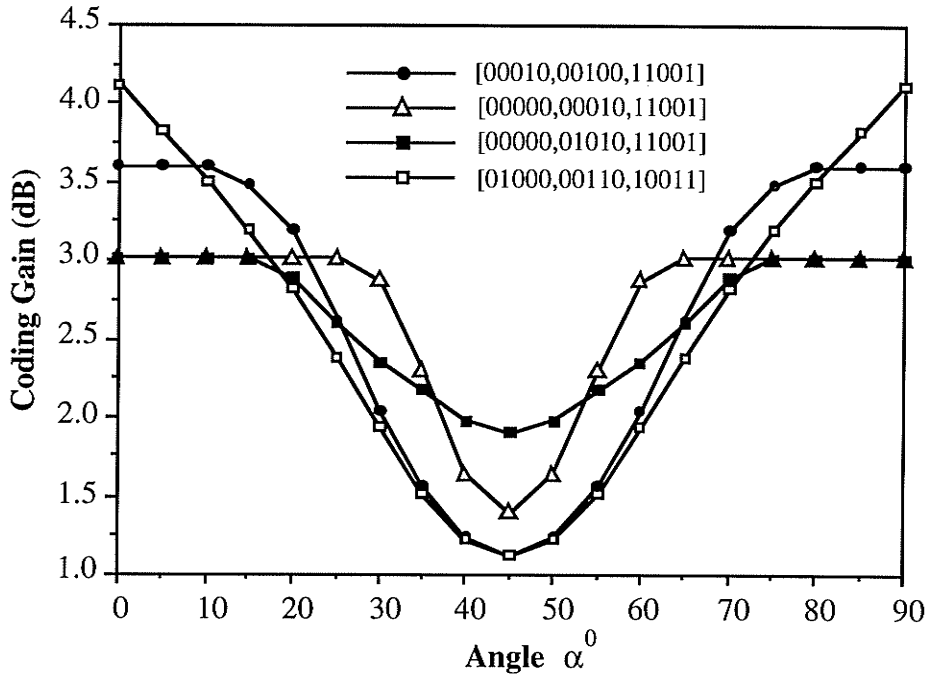

Figure 4.14. Coding gain with K=4, 8 PSK for L=2 ISI channel

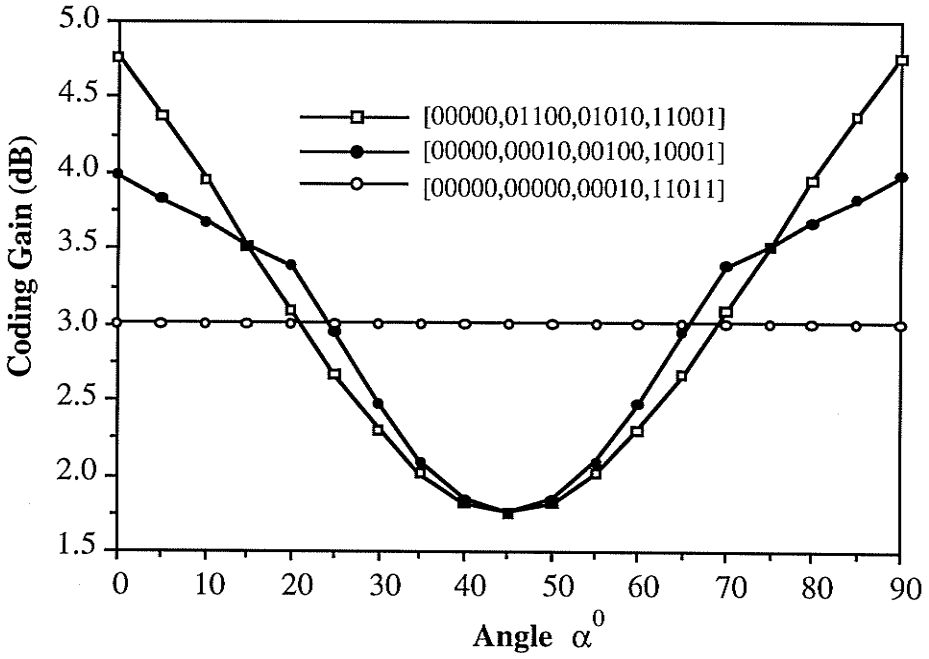

Figure 4.15. Coding gain with K=4, 16 QAM for L=2 ISI channel

As an alternative to using TCM, ring convolutional codes can be used where the ring is based on the integer modulo operation. In the next section the application of these codes for ISI channels is discussed briefly.

4.5 Ring Convolutional Codes for Coded Modulation:

Recently several authors considered using ring convolutional encoders modulo p (p>2, usually a multiple of 2) , instead of binary convolutional codes for coded modulation schemes, specially for phase modulation [3,23,24,41]. One advantage is that the relevant encoder can directly work with the modulation input non binary signal set thus avoiding the necessity to use a binary to M-ary signal mapper such as the one used in TCM schemes. Basically the convolutional coded modulation scheme maps m+1 information bits onto an expanded channels signal set which is fed to the ring convolutional encoder. As in the case of binary convolutional codes the channel rate has to be increased which results in more ISI. The transmitter side of the communication system is shown in Figure 4.16. It has been proven that systematic encoders of ring convolutional codes are always non catastrophic [23]. Therefore in the following it is assumed that the encoder is systematic.

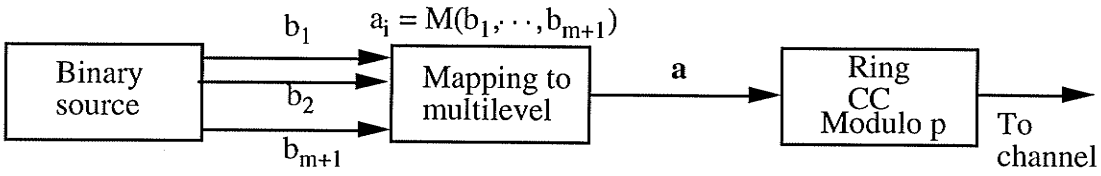

Figure 4.16. Transmitter of the ring convolutional coded scheme

First consider the following example to compare TCM and ring convolutional codes for the no ISI or wideband case.

Assume that an ISI free channel (channel energy E=2) combined with

i) the best TCM coder of constraint length K=4 or

ii) one of the mod 4 systematic convolutional encoders of K=2 and rate R=1/2 which has the largest Euclidean distance. Encoder is [1 0 0, 2 2 1].

The encoders have the same number of states for comparison. The signal alphabet used is 4 PAM (-3,-1,1,3). From Ungerboeck's paper [34]

$$G_{\frac{8PAMTCM}{4PAM\ Uncoded}} = 4.2\ dB$$

For the ring coder since it operates in 4 PAM alphabet (Channel energy E=2 Joules)

$$G_{\frac{Mod4CC}{4PAM\ Uncoded}} = 10Log\left[\frac{d^2_{Mod4}\cdot R}{d^2_{4PAM}}\right] = 10Log\left[\frac{64\ .\ 1/2}{8}\right] = 10Log[4] = 6.02\ dB$$

Therefore a gain of approximately 1.8 dB over TCM can be obtained if mod 4 ring convolutional coders are used. Even with ISI present, a higher gain than with TCM can be expected. Thus it is worthwhile to investigate the use of mod p (p>2) convolutional encoders in the presence of ISI at least as a comparison to TCM schemes which are usually designed for channels with no ISI.

Search results for constraint length K=2 encoders are shown in Figure 4.17. The channel considered is a L=2 ISI channel with the same coefficients as used in section 4.4. The channel response is that of the coded channel , again similar to binary convolutional codes. It is seen that in the regions of 0^0 - 25^0 and 65^0 - 90^0 ring convolutional codes perform better than TCM codes with the same number of encoder states. Longer constraint lengths involve searches with a long time duration due to large number of encoder combinations possible, especially with a large alphabet.

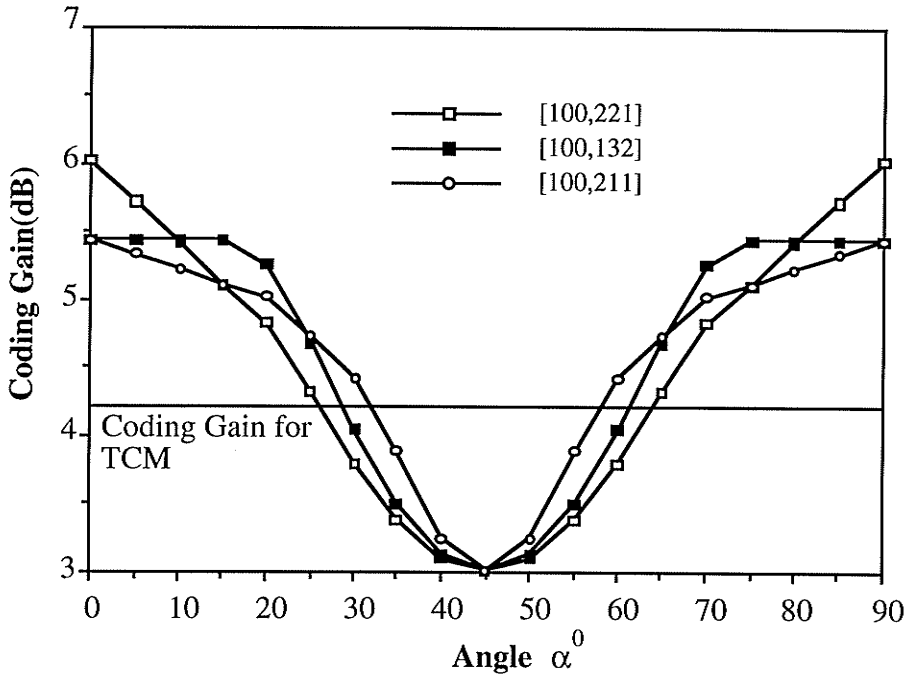

Figure 4.17. Coding gain with K=2, Mod 4 CC for L=2 ISI channel

To conclude, application of trellis coded modulation (TCM) for ISI channels has been studied in this chapter. The concept of quasiregularity has been used to reduce the computational complexity of the distance calculating algorithms. Most of the properties considered here have similarities with those in the case of convolutional codes. A main difference is that the ISI here remains unchanged due to there being only a single output from the TCM coder. Also TCM is used for non binary signaling schemes whereas convolutional codes are used for binary signaling schemes.

Ring convolutional codes also considered briefly in this chapter have the same effect on ISI as binary convolutional codes but with the added advantage of being able to work directly in the modulation alphabet. Compared with TCM it is seen (L=2 coded channel) that ring convolutional codes perform better in several cases including the ISI free situation. Therefore further investigation is warranted in the application of ring convolutional codes. From the Euclidean distance point of view all types of codes seem to behave in a similar pattern particularly with respect to the conclusions drawn for the best encoders.

Chapter 5
Conclusions and Suggestions for Further Study

5.1 Conclusions

The properties of the Euclidean distance between two received signal sequences in a finite length ISI channel have been studied in this thesis. Application of convolutional encoders and trellis coded modulation for these types of channels have also been investigated.

A theorem has been proven to show the existence of the maximum distance channels for any finite length of interference. Channel energy has been used as a constraint throughout the thesis. Certain properties have been established for the worst case channels since it is important to have an idea about the worst performance to be expected at the receiver. It has been shown that if the worst distance decreases with the length of interference then the zeros of those channels lie on the unit circle. Conversely to the worst distance case it has been shown that for a given length of interference, there is a maximum distance region defined by certain regions of channel coefficients subject to the energy constraint . Using a prefilter to modify the channel impulse response appropriately one can obtain a maximum distance channel. Since this is done at the transmitter noise enhancement is not a problem. However if one chooses to use an equalizer at the receiver to obtain a maximum distance channel then noise enhancement becomes an issue. Therefore the objective is to select a proper maximum distance channel which maximizes the output signal to noise ratio.

Alternatively convolutional codes can be used to increase the minimum Euclidean distance. A search has been carried out for L=2 channels and certain L=3 channels for convolutional codes of different rates and constraint lengths. The objective was to find out the best encoders for given ISI channels. With the convolutional encoder generally

it is required to transmit data at a higher speed which produces more interference terms. It has been seen from the results for several ISI channels that moderate coding gains can be obtained if the channel and the encoder are properly matched. Further it has been observed that if the channel is a maximum distance one then the resulting coded distance is usually higher than that for a non maximum distance channel. Another thing to note is the fact that convolutional codes with the best Hamming distance sometimes give poor coded distance compared to other encoders with less Hamming distance. However usually the best Hamming distance encoders produce the highest coded distances for a given length of interference. Further while the uncoded distance for any L=2 channel is the same, with an encoder present the coded distance usually changes from channel to channel. The results confirm the propositions given in chapter 3 regarding the bound on coded distance and the best coded channels.

Trellis coded modulation (TCM) has been investigated with respect to several modulation alphabets for bandlimited channels as the coding technique for non binary signaling schemes. The Euclidean distance is found for the best encoders for given modulation schemes where the channel considered has one interference term. For PSK and QAM schemes quasiregular encoders have been used to simplify the distance calculation procedure using a computer program. The results from the search indicate that similar to the Hamming distance in convolutional encoders, a TCM encoder with the best Euclidean distance do not always give the highest coding gain when combined with an ISI channel.

A main difference between convolutional coders and TCM is that the original ISI before coding remains unchanged in the case of TCM due to the fact that there is only one output from the TCM coder. With convolutional codes, however, the ISI increases with the increase of the channel rate due to the multiple outputs from the encoder. Also TCM is used in general for non binary signaling schemes whereas convolutional codes

are applied in binary cases. A maximum gain of approximately 1 dB can be obtained from the convolutional codes over the TCM schemes for the same constraint length of the encoder. The number of states in the decoder trellis for ISI with TCM is much higher due to non binary signaling schemes. Finally instead of binary convolutional encoders, ring convolutional encoders which work in the modulation alphabet have been considered. For a 4 - PAM system a maximum gain of 2 dB can be obtained over the conventional TCM (see Fig. 4.17).

5.2 Suggestions for Further Study:

The following problems are suggested for further investigation.

1) Location of zeros for the worst ISI channels. In the thesis it has been shown that if the worst distance decreases with the length of interference then the roots will lie on the unit circle. It remains to be shown that the worst distance decreases with the length of interference.

2) Performance of equalized maximum distance channels. If the channel is not a maximum distance channel then using an equalizer at the receiver the channel response can be modified to a maximum distance one. The selection of the proper maximum distance channel plays an important role in reducing the noise enhancement as there are many maximum distance channels to choose from. Thus it may be worthwhile to find a method to select a suitable maximum distance channel instead of going through all the maximum distance channels to see whether any gain can be obtained in this manner.

3) Analytical expressions for the coded distance with convolutional coders have been given in the two propositions in chapter 3. A challenging problem is to prove that the encoders with the best Hamming distance give the best coded distance for a given length of interference. Another is to prove that the highest coded distance is always obtained by maximum distance ISI channels.

4) More thorough investigation about ring convolutional codes in ISI channels. Up to now it has been seen that some amount of gain over TCM schemes can be obtained for some specific constraint length. From these results it seems promising to study these codes further for the application in ISI channels. A potential difficulty is the amount of time required for a search involving longer constraint lengths.

APPENDIX A

Existence of maximum distance channels for complex alphabets(QAM):

Starting with (2.93), the equation for complex alphabets can be given as

$$\Delta_{L-1} = \left|f_{L-2}\delta_{m-L+1} + f_{L-1}\varepsilon_{m-L}\right|^2 - \left|f_{L-1}\varepsilon_{m-L}\right|^2$$

Now assume the channel to be real; the purpose is to select the channel coefficients so that the channel is a maximum distance one.

Also let $\delta_{m-L+1} = a_{m-L+1} + jb_{m-L+1}$ and $\varepsilon_{m-L} = c_{m-L} + jd_{m-L}$

Therefore

$$\Delta_{L-1} = f_{L-2}^2(a_{m-L+1}^2 + b_{m-L+1}^2) + 2f_{L-2}f_{L-1}(a_{m-L+1}c_{m-L} + b_{m-L+1}d_{m-L}) \quad \text{A.1}$$

Thus if $f_i > 0$, for Δ_{L-1} to be greater than zero

$$f_{L-2} \geq -2\, f_{L-1}\left[\frac{a_{m-L+1}c_{m-L} + b_{m-L+1}d_{m-L}}{a_{m-L+1}^2 + b_{m-L+1}^2}\right]_{\text{minimum}}$$

If for the given complex alphabet for all error symbols

$$\sigma_m = \left[\frac{a_{m-L+1}c_{m-L} + b_{m-L+1}d_{m-L}}{a_{m-L+1}^2 + b_{m-L+1}^2}\right]_{\text{maximum}}$$

then

$$f_{L-2} \geq 2\, f_{L-1}\sigma_m$$

similarly $f_{L-3} \geq 2\, \sigma_m(f_{L-2} + f_{L-1})$

This procedure can be continued for other coefficients as well.

In general $f_i \geq 2\,\sigma_m(f_{i+1} + f_{i+2} + \cdots + f_{L-1})$, i=0,1, ...,L-2

Therefore the existence of a maximum distance channel is proved based on the argument made in section 2.3.2.

For M - PAM:

From A.1 for real δ and ε

$$\Delta_{L-1} = f_{L-2}^2 \delta_{m-L+1}^2 + 2 f_{L-2} f_{L-1} \delta_{m-L+1} \varepsilon_{m-L}$$

for the maximum difference

$\delta_{m-L+1} = 2$ and $\varepsilon_{m-L} = -(2M - 2)$; largest difference symbol

Therefore $f_{L-2} \geq (2M - 2)\, f_{L-1}$

In general the condition is

$$f_i \geq (2M-2)\,(f_{i+1} + f_{i+2} + \cdots + f_{L-1}) \ , \ i = 0,1,...,L-2$$

Once this is satisfied the channel is a maximum distance channel.

APPENDIX B

Additional results from chapters 3 and 4 are given here.

Notation for Figures:

R : code rate;

K : encoder constraint length , CC : Convolutional codes ;

L : Channel impulse response duration ;

Encoders are specified in terms of generator polynomial coefficients for

$$R = 1/2 \ [\mathbf{g}^{(1)}\,\mathbf{g}^{(2)}] \ ; R=1/3 \ [\mathbf{g}^{(1)}\,\mathbf{g}^{(2)}\,\mathbf{g}^{(3)}].$$

Feed Back Encoders $[\mathbf{h}^{(2)}\,\mathbf{h}^{(1)}\,\mathbf{h}^{(0)}]$ are given for R = 2/3 CC and the same format is followed for the encoders in Figures B.11 to B.17. All angles are given in degrees.

Also for Figures B.7 to B.10

$$\text{Coding gain} = \frac{d^2_{min}(\text{coded})}{16}$$

Figures B.1 to B.10 show search results for chapter 3 and the rest, from B.11 to B.17 give results for chapter 4.

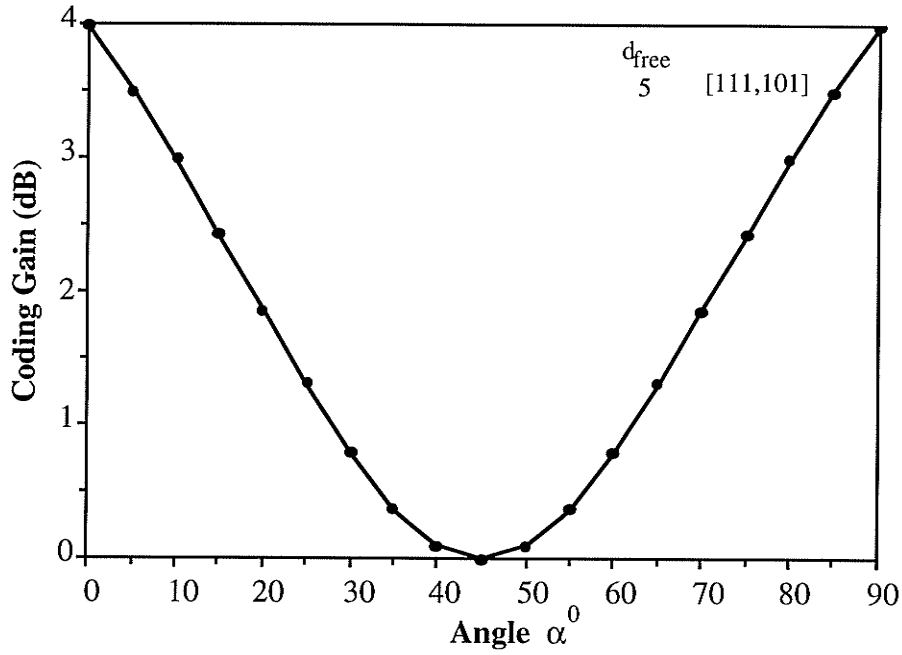

Figure B.1. Coding gain with K=2, R=1/2 CC for L=2 ISI channel

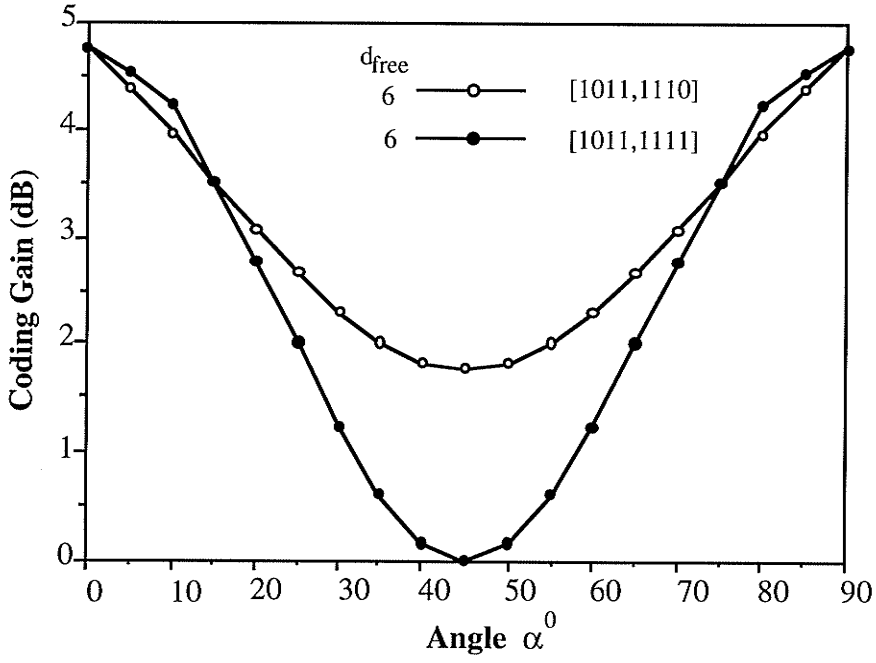

Figure B.2. Coding gain with K=3, R=1/2 CC for L=2 ISI channel

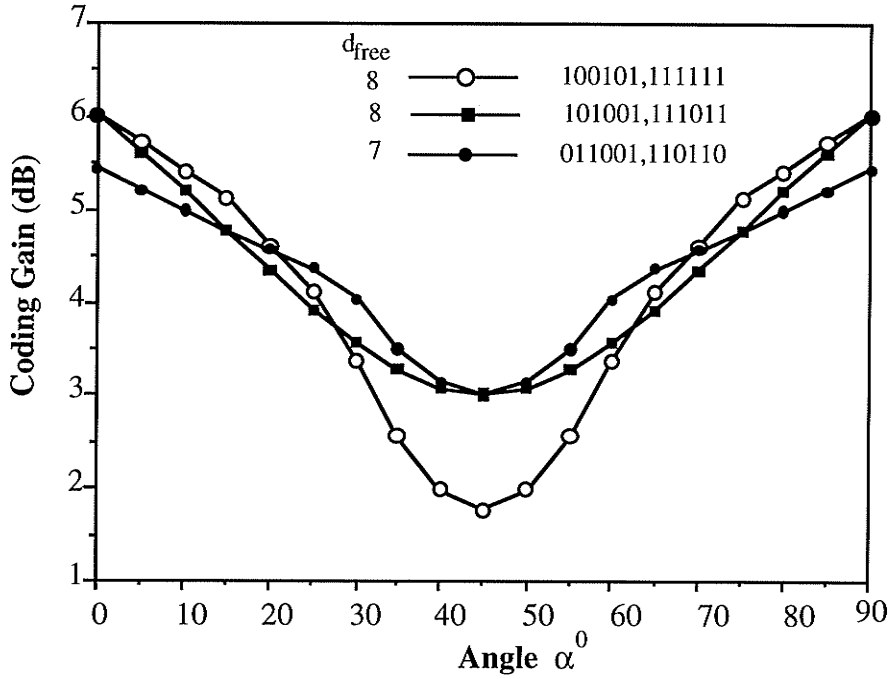

Figure B.3. Coding gain with K=5, R=1/2 CC for L=2 ISI channel

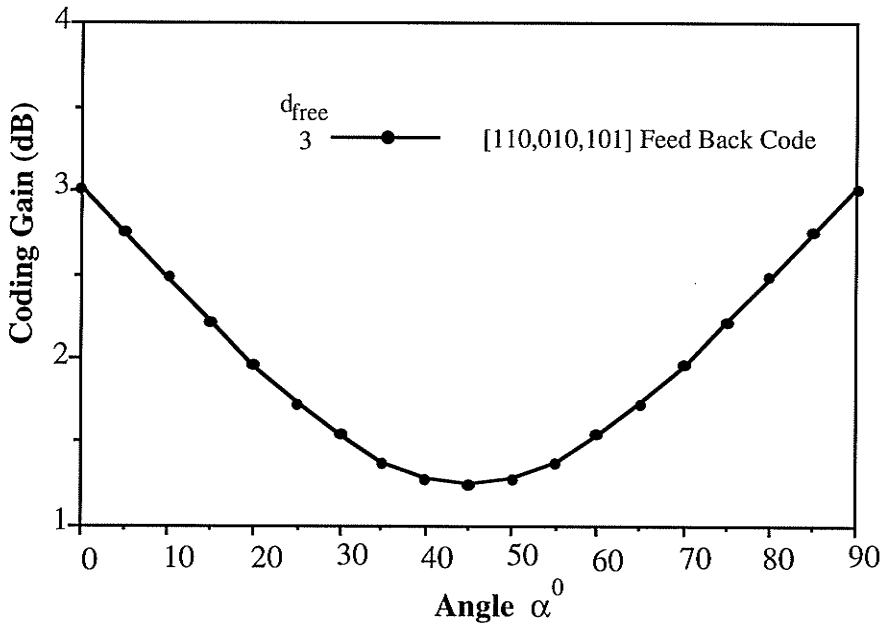

Figure B.4. Coding gain with K=2, R=2/3 CC for L=2 ISI channel

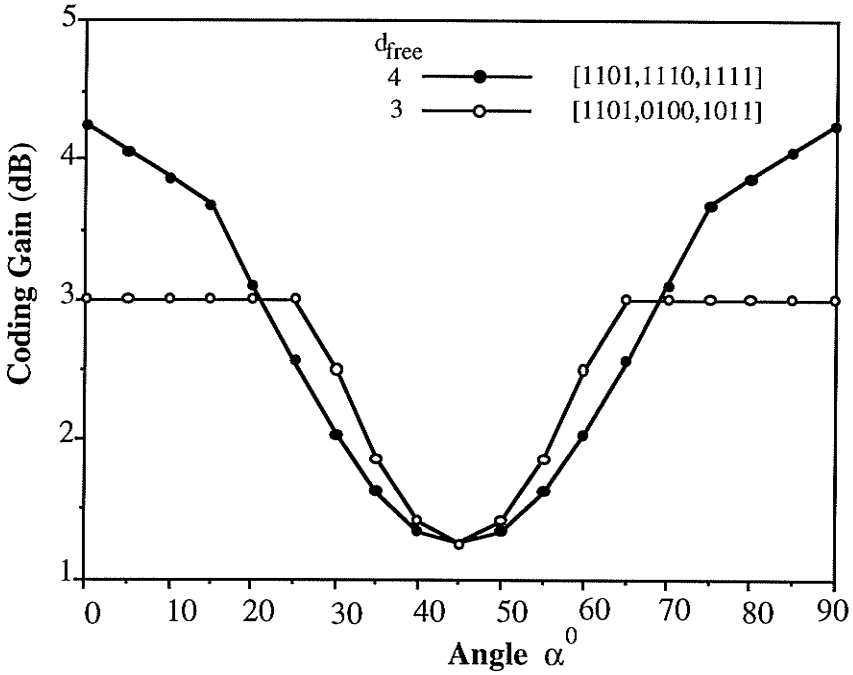

Figure B.5. Coding gain with K=3, R = 2/3 CC for L=2 ISI channel

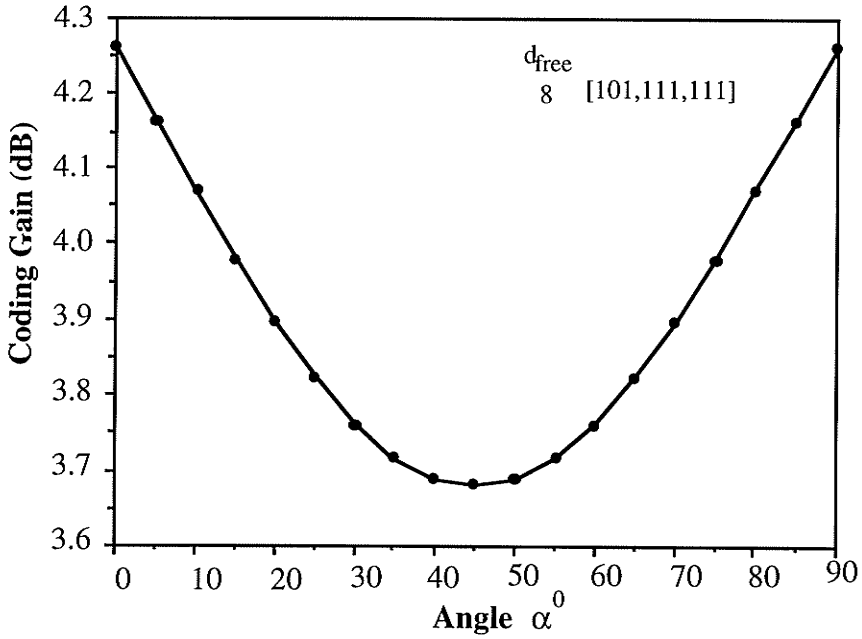

Figure B.6. Coding gain with K=2, R=1/3 CC for L=2 ISI channel

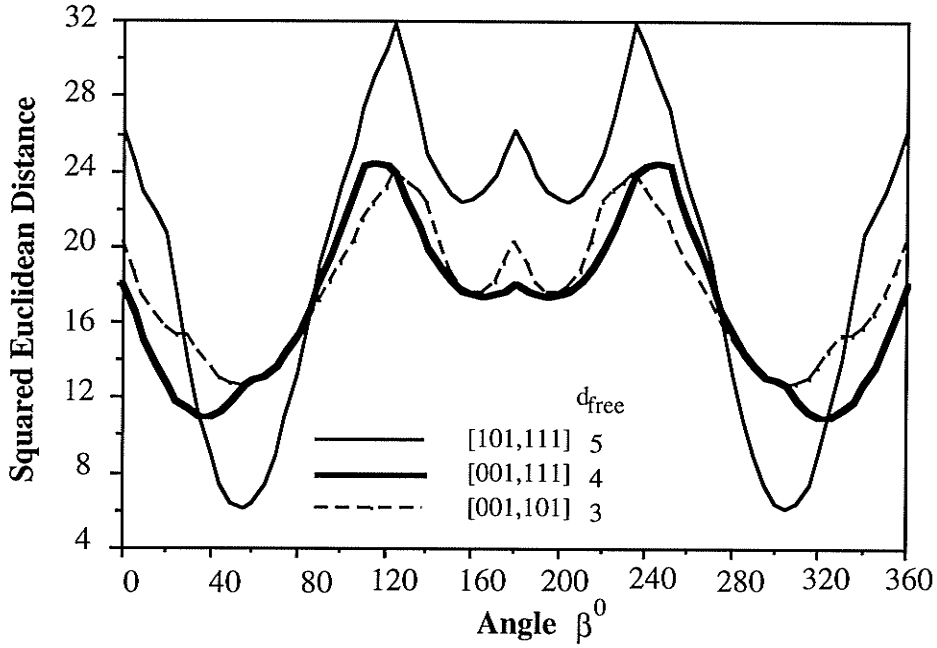

Figure B.7. Coded distance with K=2, R=1/2 CC for L=3 ISI at Angle α=30

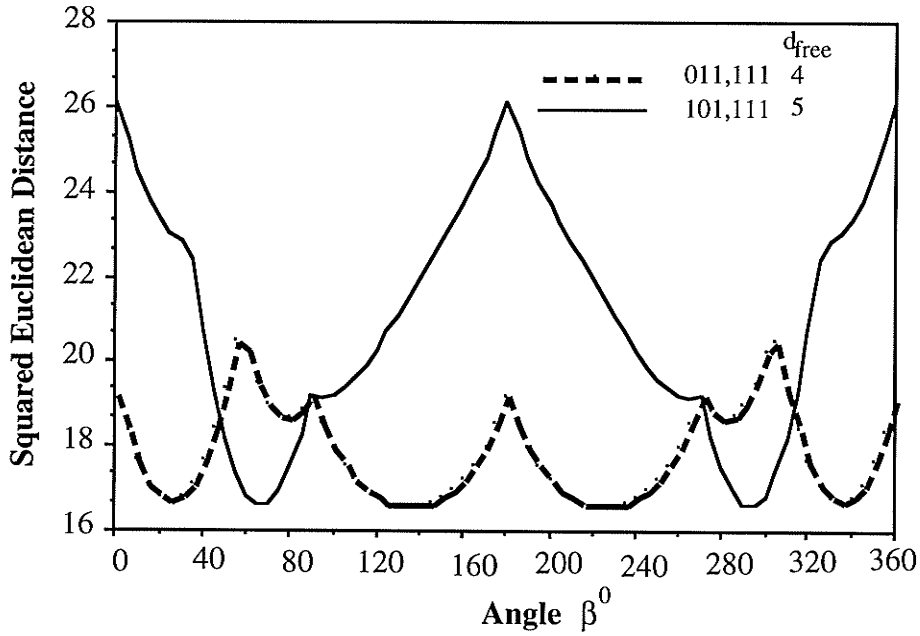

Figure B.8. Coded distance with K=2, R=1/2 CC for L=3 ISI at Angle α=60

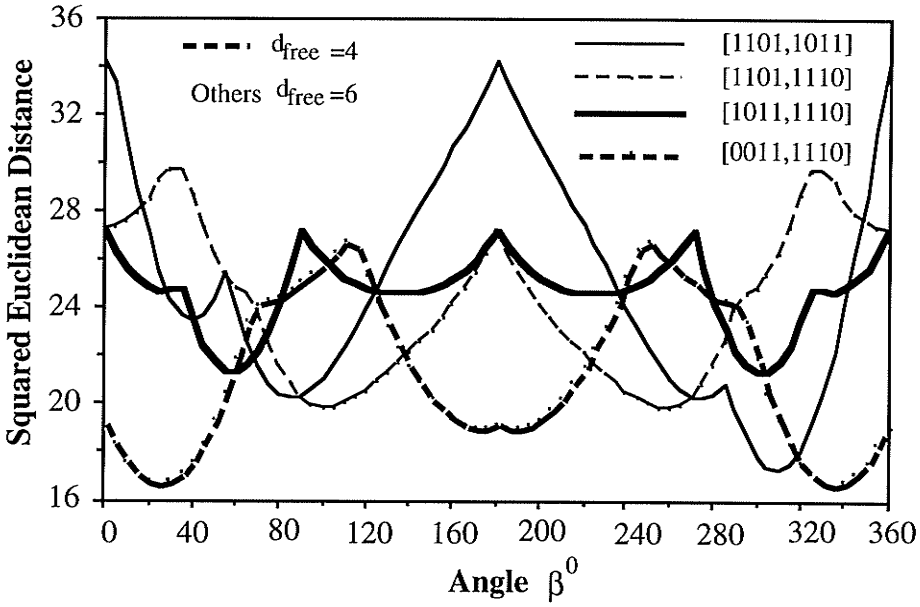

Figure B.9. Coded distance with K=3, R=1/2 CC for L=3 ISI at Angle α=60

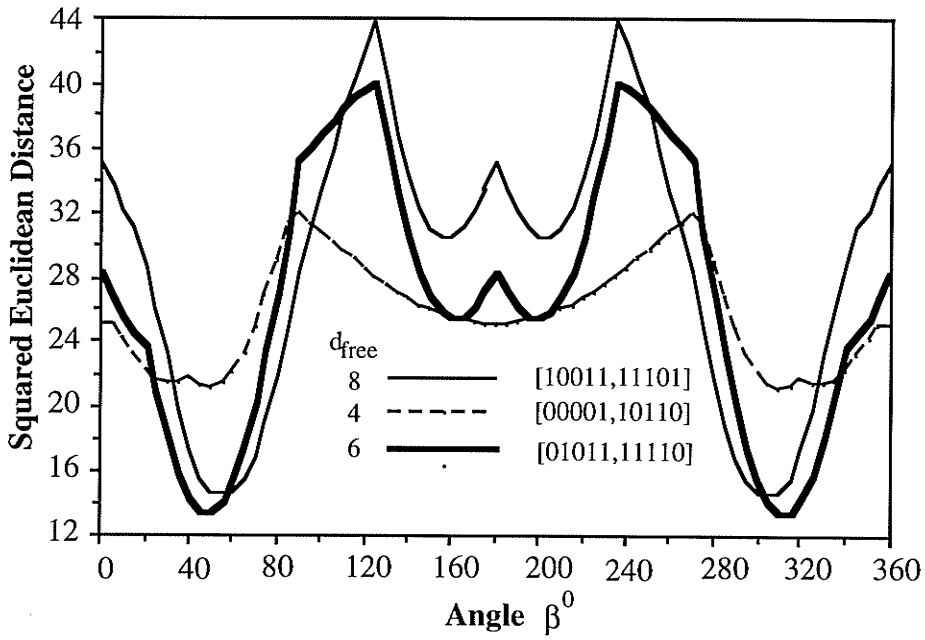

Figure B.10. Coded distance with K=4, R=1/2 CC for L=3 ISI at Angle α=30

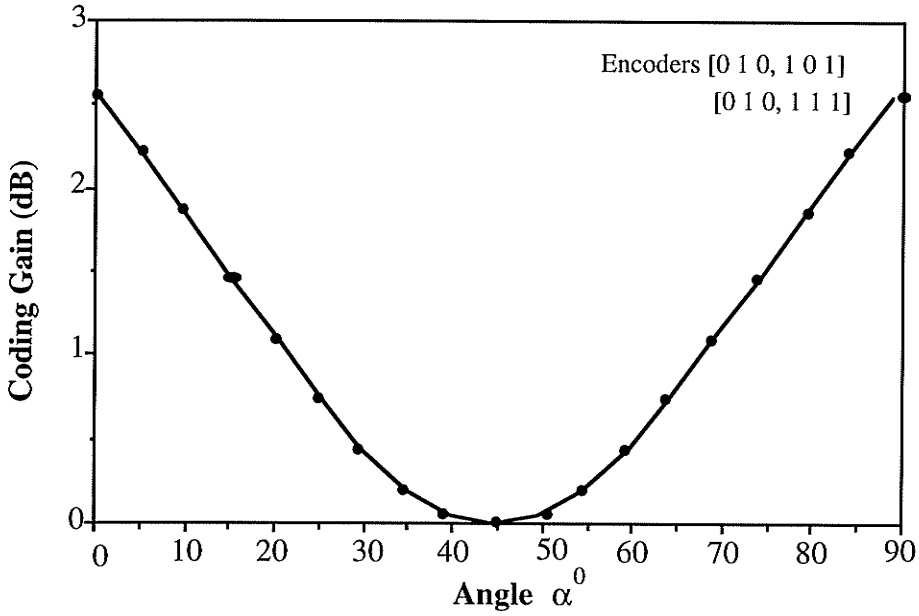

Figure B.11. Coding gain with K=2, 4 PAM for L=2 ISI channel

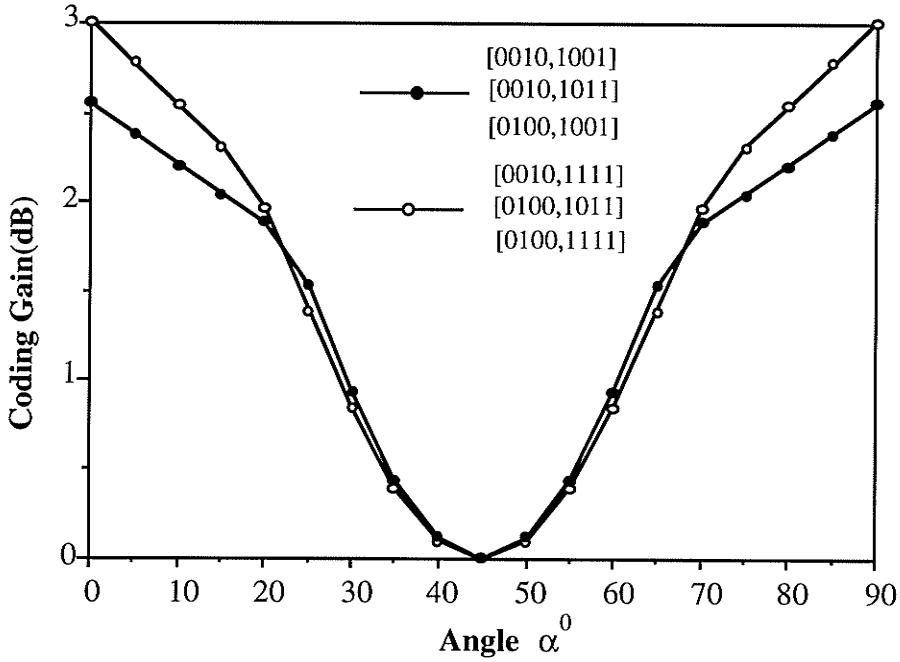

Figure B.12. Coding gain with K=3, 4 PAM for L=2 ISI channel

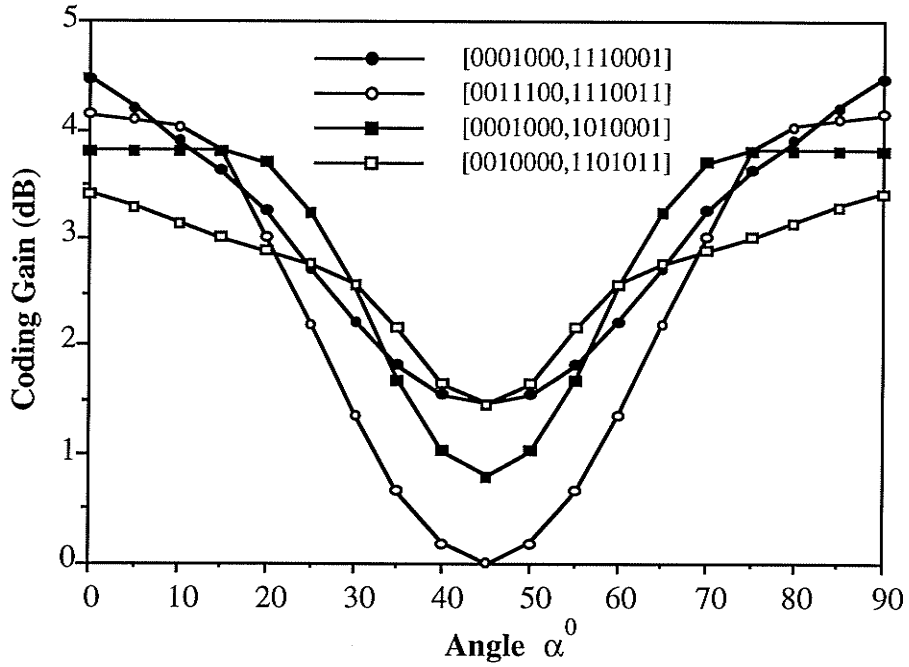

Figure B.13. Coding gain with K=6, 4 PAM for L=2 ISI channel

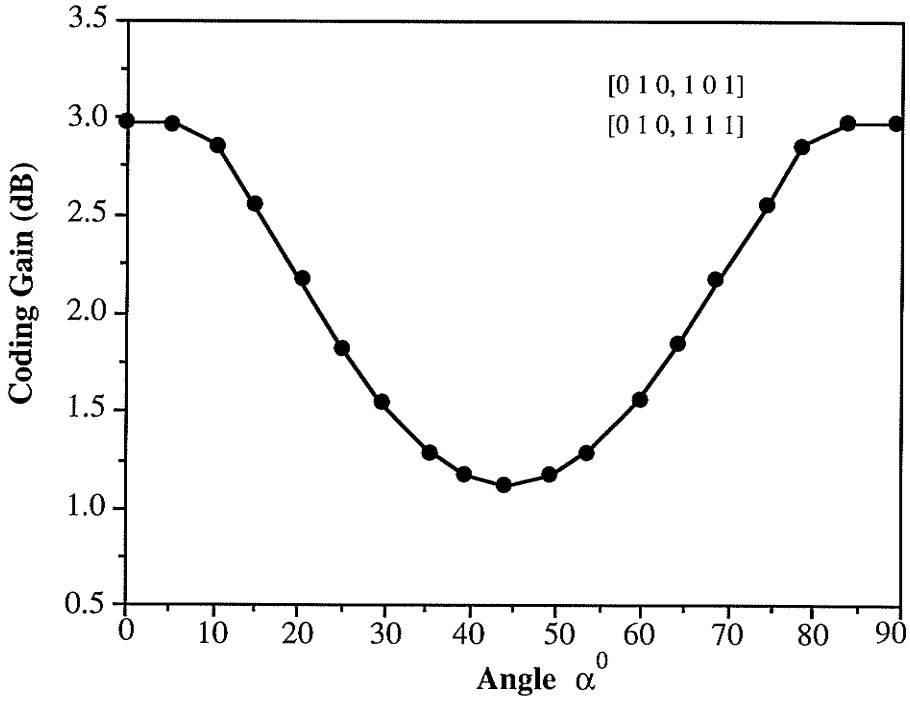

Figure B.14. Coding gain with K=2, 8 PSK for L=2 ISI channel

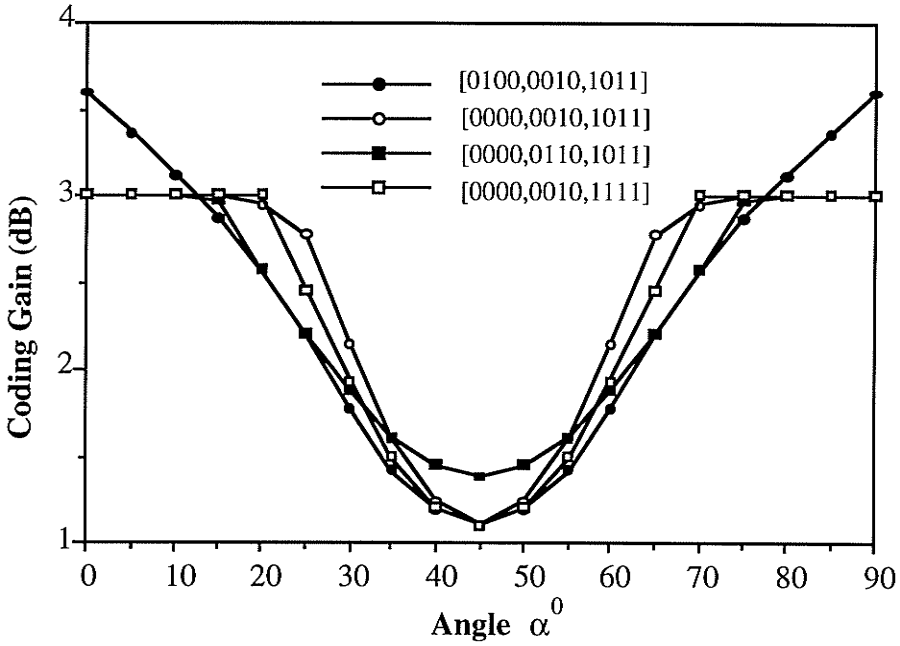

Figure B.15. Coding gain with K=3, 8 PSK for L=2 ISI channel

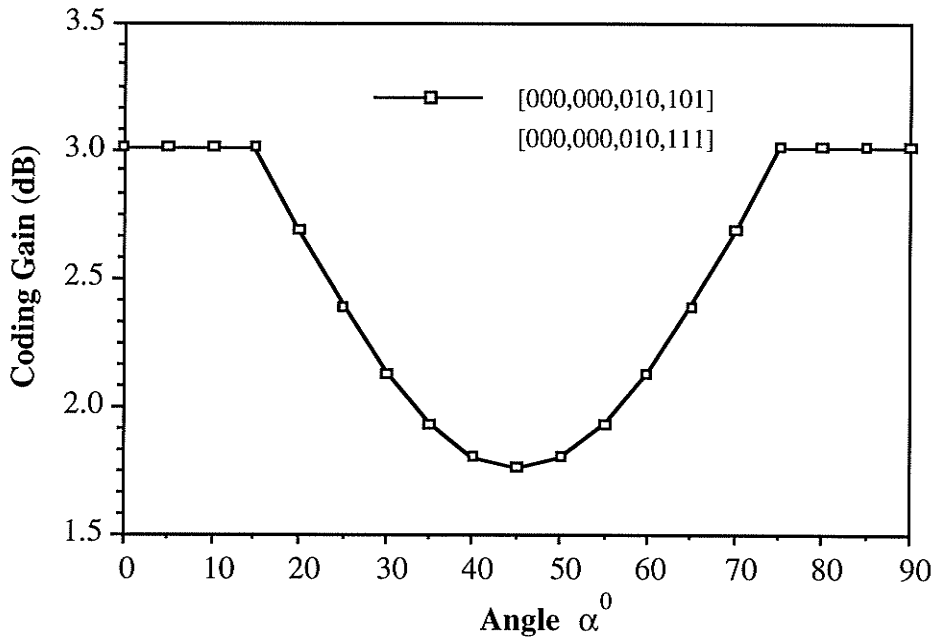

Figure B.16. Coding gain with K=2, 16 QAM for L=2 ISI channel

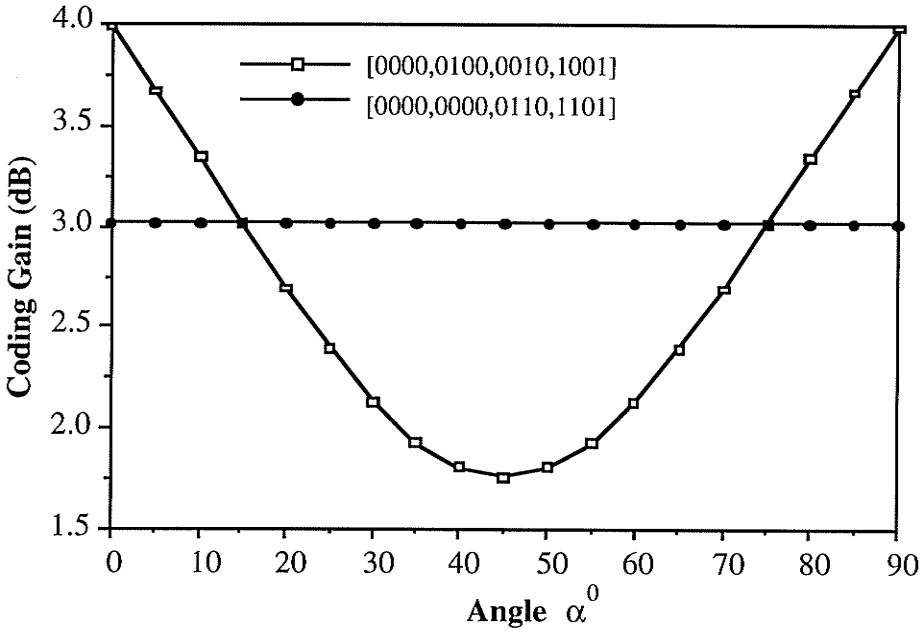

Figure B.17. Coding gain with K=3, 16 QAM for L=2 ISI channel

REFERENCES

[1] R. R. Anderson and G. J. Foschini, "The Minimum Distance for MLSE Digital Data Systems of Limited Complexity", IEEE Trans. on Information Theory, Vol. IT-21, No. 5, pp. 544 - 551, Sept. 1975.

[2] K. Balachandran, Design and Performance Analysis of Constant-Envelope and Non-Constant-Envelope Digital Phase Modulation Schemes, Communications, Information and Voice Processing Report Series, TR92-1, Rensselaer Polytechnic Institute, Troy, NY 12180, February 1992.

[3] R.Baldini, P.G.Farell, "Coded modulation based on rings of integers modulo-q:Part 2-Convolutional codes", IEE Proc. Commun.,Vol 141, No. 3, pp.137-142, June 1994.

[4] J.W.M. Bergmans, "Effect of Binary Modulation Codes with Rate R = 1 / N on Equivalent Discrete-Time Models for Channels with Intersymbol Interference", IEEE Trans. on Information theory, Vol. 38, No. 5, pp. 1587-1592, Sept. 1992.

[5] E. Biglieri, D. Divsalar, P. J. McLane, M.K. Simon, Introduction to Trellis-Coded Modulation with Applications, Macmillan, 1991.

[6] R. Blahut, Theory and Practice of Error Control Codes, Addison Wesley, 1984.

[7] A. R. Calderbank, C. Heegard, and T. A. Lee, "Binary Convolutional Codes with

Application to Magnetic Recording", IEEE Trans. Information Theory, Vol. IT-32, pp. 797-815, Nov. 1986.

[8] A. Cantoni and P. Butler, "Properties of the Eigenvectors of Persymmetric Matrices with Applications to Communications Theory", IEEE Trans. on Comm., Vol. Com-24, No. 8, pp. 804 - 809, Aug. 1974.

[9] C. J. Carlisle, D. P. Taylor, M. Shafi, W. K. Kennedy, "Performance Bounds for Trellis-Coded Modulation on Time Dispersive Channels", GLOBECOM '91, Vol. 2, pp. 1176-1181, December 1991.

[10] P. R. Chevillat, E. Eleftheriou, "Decoding of Trellis-Encoded Signals in the Presence of Intersymbol Interference and Noise", IEEE Trans. on Comm., Vol. 37, No. 7, pp. 669-676, July 1989.

[11] G. D. Forney, "Convolutional Codes I: Algebraic Structure", IEEE Trans. Information Theory, Vol IT-16, No. 6, pp. 720 - 738, Nov. 1970.

[12] G. D. Forney, Jr., "Maximum-Likelihood sequence Estimation of Digital Sequences in the Presence of Intersymbol Interference", IEEE Trans. on Information Theory, vol. IT-18, pp. 363-378, May 1972.

[13] Francis R. Magee, Jr. and J. G. Proakis, " An Estimate of the Upper Bound on Error Probability for Maximum-Likelihood Sequence Estimation on Channels Having a Finite-Duration Pulse Response", IEEE Trans. on Information Theory, Vol. IT-19, pp. 699 - 702, Sept. 1973.

[14] R. Haeb, "A Modified Trellis Coding Technique for Partial-Response Channels", IEEE Trans. on Comm., Vol. 40, pp. 513-520, March 1992.

[15] P. K. M. Ho, P. J. McLane, "Spectrum, Distance, and Receiver Complexity of Encoded Continuous Phase Modulation", IEEE Trans. on Information Theory, Vol. IT-34, pp. 1021-1032, Sept. 1988.

[16] K. J. Hole, "Punctured Convolutional Codes for the 1 - D Partial-Response Channel", IEEE Trans. on Information Theory, Vol. 37, Iss. 3, pt. 2, pp. 808-817, May 1991.

[17] E. Horowitz and S. Shani, Fundamentals of Data Structures, Pitman, 1976.

[18] J. W. Ketchum, "Performance of Trellis Codes for M-ary Partial Response", GLOBECOM '87, pp. 43.7.1 - 43.7.5

[19] T. Larsson, A State-Space Partitioning Approach to Trellis Decoding, Technical Report No. 222, School of Electrical and Computer Eng., Chalmers University of Technology, Sweden, 1991.

[20] S. Lin, D. J. Costello, Error Control Coding, Prentice Hall, 1983.

[21] G. Lindell, C. E. Sundberg and T. Aulin, "Minimum Euclidean Distance for Combinations if Short Rate 1/2 Convolutional Codes and CPFSK Modulation", IEEE Trans. Information Theory, Vol. IT-30, No. 3, pp. 509-519, May 1984.

[22] J.L. Massey and M.K. Sain, "Inverses of Linear Sequential Circuits", IEE Trans. Comput., C-17, pp. 330-337, April 1968.

[23] J.L.Massey, T.Mittelholzer, "Systematicity and rotational invariance of convolutional codes over rings", in Proc. 2nd Int. Workshop Algebraic Combinatorial Coding Theory, pp. 154-159, Sept. 1990.

[24] J.L.Massey, T.Mittelholzer, T.Riedel and M. Vollenweider, " Ring convolutional codes for phase modulation", in proc.IEE Int. Symp. on Information theory, p. 176, Jan 1990.

[25] J. -E. Porath, "Algorithms for Converting Convolutional Codes from Feedback to Feedforward form and Vice Versa", IEE Electronic Letters, July 1989.

[26] J.G. Proakis, Digital Communications, McGraw-Hill, 1983.

[27] S. A. Raghavan, J. K. Wolf and L. B. Milstein, "On the Performance Evaluation of ISI Channels", IEEE Trans. Information Theory, Vol. IT-39, No. 3, pp. 957 - 965, May 1993.

[28] B. E. Rimoldi, "Design of Coded CPFSK Modulation Systems for Bandwidth and Energy Efficiency", IEEE Trans. on Comm., Vol. 37, No. 9, pp. 897-905, March 1988.

[29] A. Said, Design of Optimal Signals for Bandwidth-Efficient Linear Coded Modulation,

Report TR 94-1,Dept. of Electrical, Computer and Systems Engineering, Rensselaer Polytechnic Institute, Feb. 1994.

[30] C. Schlegel, "Evaluating Distance Spectra and Performance Bounds of Trellis Codes on Channels with Intersymbol Interference", IEEE Trans. on Information Theory, Vol. 37, No. 3, pp. 627-634, May 1991.

[31] K.A. Schouhamer Immink, "Coding Techniques for Partial-Response Channels", IEEE Trans. on Commm., Vol.36, No. 10, pp.1163-1165, Oct. 1988.

[32] Staffan A. Fredricsson, "Optimum Transmitting Filter in Digital PAM Systems with a Viterbi Detector", IEEE Trans. on Information Theory, Vol. IT-20, No.4, pp. 479 - 489, July 1974.

[33] N. O. Ucan, U. Aygolu, E. Panayirci, "Decoding of Quadrature Partial Response Trellis Coded Signals (QPR-TCM) in the Presence of Intersymbol Interference and Noise", Applied Algebra, Algebraic Algorithms and Error-Correction Codes 9th international symposium, AAECC-9 proceedings, pp. 434-445, Oct. 1991.

[34] G. Ungerboeck, "Channel Coding with Multilevel/Phase Signals", IEEE Trans. Information Theory, Vol. IT-28, pp. 55-67, Jan. 1982.

[35] A. J. Viterbi and J. K. Omura, Principles of Digital Communication and Coding, pp. 284-286, McGraw-Hill, 1979.

[36] J. H. Wilkinson, The Algebraic Eigenvalue Problem, Oxford University Press 1965.

[37] J. K. Wolf, G. Ungerboeck, "Trellis Coding for Partial-Response Channels", IEEE Trans. on Communications, Vol. COM-34, No.8, pp.765-773, Aug. 1986.

[38] J. K. Wolf, E. Zehavi, A. J. Viterbi, Combined Maximum Likelihood of Decoding for Coded Partial-Response Channels", NTIS Final report on phase I, Rept. no. NSF / ISI - 87041, 1987.

[39] C. C. W. Wong and J. B. Anderson, "Optimal Short Impulse Response Channels for an MLSE Receiver", Proc. IEEE 1979, pp. 25.3.1 - 25.3.5

[40] L. -N.,Wong and P. J. McLane, "Performance of Trellis Codes for a Class of Equalized ISI Channels", IEEE Trans. on Comm., Vol. 36, No.12, pp. 1330 - 1336, Dec. 1988.

[41] R.H.-H.Yang, D.P.Taylor, "Trellis-Coded Continuous-Phase Frequency-Shift Keying with Ring Convolutional Codes", IEEE Trans. Information Theory, Vol 40, No. 4, pp. 1057-1067, July 1994.